UNIVERSITY OF CALIFORNIA,
IRVINE

Microfluidic Generation of Monodisperse, Cell-Sized Multisomes and Vesicles from Storable Double Emulsion Templates

submitted in partial satisfaction of the requirements
for the degree of

DOCTOR OF PHILOSOPHY

In Biomedical Engineering

by

Derek Vallejo

<div align="right">

Dissertation Committee
Professor Abraham Lee, Chair
Assistant Professor Jered Haun
Professor Philip Felgner

</div>

2016

The dissertation of Derek Vallejo is approved
and is acceptable in quality and form for
publication on microfilm and in digital formats

DEDICATION

To my wife,

Debora Chin,

and my parents,

Randi and Roberto Vallejo

who have supported, believed, stood by, and brought out the very best in me

I wouldn't be where I am without them

TABLE OF CONTENTS

LIST OF FIGURES

Chapter 1

Chapter 2

Chapter 3

Chapter 4

Chapter 5

LIST OF TABLES

Chapter 3

LIST OF EQUATIONS

Chapter 1

Chapter 2

Chapter 3

ACKNOWLEDGEMENTS

CURRICULUM VITAE

DEREK HUNTER VALLEJO

EDUCATION

Ph. D., Biomedical Engineering
University of California at Irvine, July 2016
Dissertation Title: *Microfluidic Generation of Monodisperse, Cell-Sized Multisomes and Vesicles from Storable Double Emulsion Templates*

M.S., Biomedical Engineering
University of California at Irvine, December 2012

B.S., Bioengineering: Pre-Medical
University of California at Irvine, June 2010

PROFESSIONAL CERTIFICATIONS

Engineer-in-Training (Certificate No. EIT 155511)
Pomona, CA, May 2015

PATENTS

D. Vallejo, C. Rapier, A. P. Lee, "On Demand Vesicle Formation from Vesicle Precursors Suitable for Long-Term Storage", U.S. Provisional Application No.: 14/964,381. December, 2015

RESEARCH EXPERIENCE

Graduate Student Researcher
Biomolecular Microsystems and Nanotransducers Lab, UC Irvine (September 2010-Present)
Advisor: Professor Abraham Lee

Primary Project (Thesis)
- Developed device for microfluidic generation of double emulsion templates, which can be converted into giant unilamellar vesicles (GUVs) or cell-sized single compartment multisomes at any time.
- Overcomes the limitations of bulk productions methods, and the double emulsions can be stored in solution for over a year.
- The GUVs were functionalized for use as artificial antigen presenting cells (aAPCs) and to promote beta-cell insulin secretion.

Secondary Projects
- Microfluidic design and optimization for single cell encapsulation in hydrogel microparticles.
- GUV production for drug delivery via acoustic tweezers.
- Development of a portable microfluidic Qdot protein microarray for rapid disease diagnoses.

Research Grant/Technical Writing, Budgeting, and Administrative Functions
- DARPA BAA ($3.5M)
- NIH R21 ($200k)
- NSF EAGER ($300k)

Alliances for Graduate Education and the Professoriate (AGEP)
Biomolecular Microsystems and Nanotransducers Lab, UC Irvine (June – August, 2010)
Advisor: Professor Abraham Lee

- 8-weeks research project with faculty advisor. Results presented at a research symposium following the conclusion of the program.
- Impact: Optimization and development of a microfluidic device for production of fibrin hydrogel micro-beads to encapsulate neural stem cells in a single generation step for therapeutic applications.

SKILLS
Software:
General: Microsoft Office (Word, PowerPoint, Excel)
Drafting and Design: AutoCAD, SolidWorks, Adobe Illustrator
Simulation/Modeling: CFD-ACE, COMSOL
Image Analysis: ImageJ
Programing Languages: Matlab, LabVIEW, C++, R

Laboratory
Engineering: Class 1000 Cleanroom Training, Soft Lithography, Basic Circuit Design
Analysis: Fluorescence Spectrophotometer, Hemocytometer, Tensiometer
Imaging: Cryo-TEM, Fluorescence Microscopy
Cell Biology: Cell Culture, Cytotoxicity Assays

WORK EXPERIENCE
Pathology Tissue Technician
Kaiser Permanente/Aerotek, Los Angeles, CA (Summer, Winter 2007-2009)
- Assisted pathologists with the description and dissection of surgical pathology specimens for histological processing.
- Used CoPath software to accession pathological specimens, assign pathology numbers, review tissue forms for accuracy and completeness, and prepare specimen cassettes with the proper pathology numbers and information.
- Assisted in the cutting of frozen sections for follow up staining on slides using the H&E method. Also proficient in the Diff-Quik and Wright-Giemsa staining methods.

Intern – Malaria Drug Development
GNF Novartis, La Jolla, CA (January-June, 2009)
Industry Advisor: Dr. Kelli Kuhen
Academic Advisor: Dr. Thomas Hermann
- Responsible for production of media and reagents for malaria cultures.

- Preparation and maintenance of infected red blood cell cultures.
- Participated in anti-malarial drug discovery assays and screening.

SCHOLASTIC ACHIEVEMENTS
- GRC Carl Storm Underrepresented Minority Fellowship (2015)
- UC Systemwide Bioengineering Symposium Travel Grant (2012)
- Alliance for Graduate Education and the Professoriate Competitive Edge Fellowship, National Science Foundation (37 awards, 2010)
- Graduated *Cum Laude* from USCD (2010)
- Earl Warren College Provost's Honors (11 quarters, 2006-2010)

TEACHIN EXPERIENCE
Teaching Assistant, University of California, Irvine
- BME 110C – Biomechanics (Spring, 2015)
- BME 60B – Engineering Analysis/Design: Data Analysis (Winter, 2015)
- BME 147/295 – Microfluidics and Lab-on-a-Chip (Winter, 2012)

PUBLICATIONS
A. Jain, O. Taghavian, **D. Vallejo**, E. Dotsey, D. Schwartz, F. G. Bell, et al., "Evaluation of Quantum dot immunofluorescence and a digital CMOS imaging system as an alternative to conventional organic fluorescence dyes and laser scanning for quantifying protein microarrays," Proteomics, February 2016.

BOOK CHAPTERS (*equal contribution)
G. Kamalakshakurup*, C. Rapier*, **D. Vallejo***, S.-H. Lee*, and A. P. Lee, "Microfluidic Micro/Nano Droplets: Technology and its Applications," in Springer Handbook of Nanotechnology, B. Bhushan, Ed., 4th ed: Springer Verlag, 2017. (in preparation)

D. Vallejo, S-H. Lee, A. P. Lee, "Functionalized Vesicles by Microfluidic Device," in Biosensors and Biodetection: Methods and Protocols, A. Rasooly, Prickril, B., Ed., 2nd ed New York, N. Y.: Springer Science+Business Media, LLC, 2016. (accepted)

CONFERENCE PRESENTATIONS (*equal contribution)
D. Vallejo, S-H. Lee, A. P. Lee, "Generation of Multisomes and Giant Unilamellar Vesicles from Storable Double Emulsion Templates," μTAS 2016 20th International Conference on Miniaturized Systems for Chemistry and Life Sciences, Dublin, Ireland, October 2016. (Poster)

N. Garg*, D. Boyle*, **D. Vallejo***, N. Flohn, I. Nanayakkara, A. Teng, J. Pablo, X. Liang, D. Camerini, A. P. Lee, "Integrated On-Chip Microfluidic Immunoassay for Rapid Biomarker Detection," Humanitarian Technology 2016: Science, Systems and Global Impact, Boston, Massachusetts, June 2016. (Oral & Paper in HumTech2016 Proceedings published by Elsevier)

D. Vallejo, S-H. Lee, C. Rapier, A. P. Lee, "Microfluidic Generation of Double Emulsion Templates Suitable for Long-Term Storage and On-Demand Conversion into Giant Unilamellar Vesicles," Microfluidics, Physics & Chemistry of, Gordon Research Conference, West Dover, Vermont, June 2015. (Oral & Poster, 8 students chosen from over 70 applicants)

D. Vallejo, A. P. Lee, "Microfluidic Cell-Sized Vesicles for Use as Artificial Antigen Presenting Cells," EMBS Micro and Nanotechnology in Medicine Conference, Oahu, Hawaii, December 2014. (Poster)

D. Vallejo, A. P. Lee, "Microfluidic Generation of Cell-like Liposomes," 2014 BMES Annual Meeting, San Antonio, Texas, October 2014. (Poster)

S-H. Lee, **D. Vallejo**, G. L. Damhorst, R. Bashir, and A.P. Lee, "Controllable Microfluidic Synthesis Of High Ionic Solution Encapsulated Liposomes For Diagnostic Applications," 14th Annual UC Systemwide Bioengineering Symposium, Irvine, CA, June 2014. (Poster)

D. Vallejo, R. Lin, A.P. Lee, "The Preparation Of Fibrin Hydrogel Microbeads Encapsulating Neural Stem Cells Within A Microfluidic Device", Alliance for Graduate Education and the Professoriate (AGEP) Competitive Edge Research Symposium, Irvine, CA, August 2010. (Oral)

COURSEWORK

Graduate
Cell and Tissue Engineering, Quantitative Physiology (Sensory and Motor Systems and Organ Transport Systems), Microsystem Technologies for Biomolecular Assays, Medical Techniques II (Medical Imaging), Seminars in Biomedical Engineering

Undergraduate
Bioengineering Statics & Dynamics, Continuum Mechanics, Biomechanics, Genetics, Linear Circuits, Structural Biochemistry, Metabolic Biochemistry, Principles of Bioinstrumentation Design, Cellular Neurobiology, Principles of Biomaterials Design, C/C++ Programming

ABSTRACT OF THE DISSERTATION

Microfluidic Generation of Monodisperse, Cell-Sized Multisomes and Vesicles from Storable Double Emulsion Templates

By

Derek Vallejo

Doctor of Philosophy in Biomedical Engineering

University of California, Irvine, 2016

Professor Abraham Lee, Chair

Giant unilamellar vesicles (GUVs) show great potential as biosensors and artificial cells and have been utilized extensively as cellular models for studies on dynamic membrane properties, mechanical measurements, phospholipid domain formation, and membrane protein integration. Macroscale methods to make GUVs are widespread, but suffer from polydispersity, multilamellarity, and low encapsulation efficiency. While the control of droplet production provided by microfluidic technologies have been able to overcome many of these limitations, widespread usage of GUVs outside of research settings has been hindered by their fragility and short shelf life, rendering them difficult to ship and commercialize. A similar structure, known collectively as multisomes, can be suitable for the same applications as GUVs, but their potential has been undervalued and they also suffer similar storage limitations as GUVs. In order for GUVs and multisomes to realize their vast potential, it is paramount that they can be produced in bulk, and stored for a reasonable amount of time without structural degradation.

Numerous microfluidic methods to produce GUVs employ water-in-oil-in-water (W/O/W) double emulsion templates that quickly convert into lipid vesicles via dewetting and/or solvent extraction. These methods generally use harsh, volatile solvents in the sheath (oil) phase

that can potentially harm both cells and encapsulated biological materials. Furthermore, the immediate removal of the solvent to form GUVs limits their useful lifetime. Nearly all the work to improve GUV shelf life has been focused on modifying their storage conditions after production, which can be damaging.

In this work, we present a method to circumvent the storage limitations and fragility of GUVs and multisomes. Double emulsions templates are produced utilizing a single junction co-focusing microfluidic device to ensure monodispersity, and are composed of only biocompatible surfactants and fatty acids. The design allows for double emulsions to be produced with diameters ranging from 9-50µm and generation rates up to 3 kHz by simply varying the fluid flow rates. The templates can be stored for up to a year and converted into multisomes or GUVs on demand within minutes by a simple solution change that alters the spreading coefficients of the system. We have also uncovered the interfacial parameters that control the stability of double emulsions for storage, and their subsequent dewetting to form multisomes or GUVs. Furthermore, multisomes were surface functionalized to demonstrate their applicability as artificial cells. In particular, they were surface modified to promote insulin secretion in pancreatic B cells through surface interactions with neuroligin-2. Ultimately, we envision that these multisomes and GUVs can be utilized as blank templates for a variety of applications, including drug delivery vehicles, artificial antigen presenting cells, and biosensors.

Chapter 1 - Introduction

1.1 Microfluidics

Microfluidics is a broad field that encompasses the utilization and manipulation of small fluid volumes (picoliter to femtoliter) for a variety of scientific and engineering applications. Examples include molecular analysis and detection systems, biological assays, gas chromatography, capillary electrophoresis, protein crystallization, functionalized microparticles, point-of-care diagnosis, personalized medicine, and high-throughput screening [1]. The use of miniscule reagent volumes means results can be produced in mere seconds, while not sacrificing detection or resolution, and saving substantially in cost (Fig. 1.1) when compared to conventional assay techniques. As a result, interest in the field has increased immensely in the last two decades.
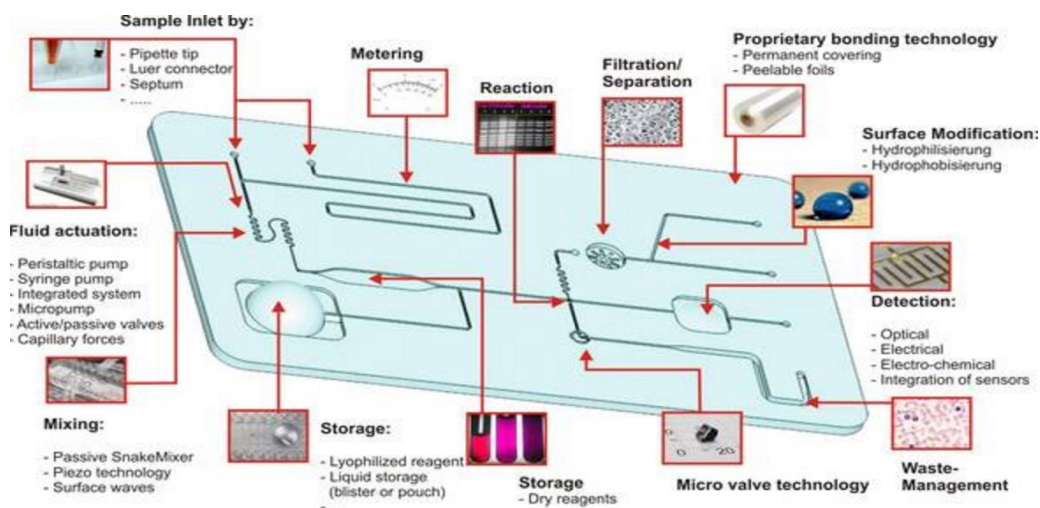
Figure 1.1. Illustration of conventional assay sample preparation, manipulation, and detection incorporated within a microfluidic device.

Microfluidics originally emerged as an alternative to traditional, expensive, and bulky laboratory techniques. Costly reagents could be used in even smaller quantities, meaning that reactions time were shortened, translating to high resolution and sensitive detection. Academic growth of microfluidic technology grew tremendously in the 1990s when the U.S. government

$$\rho\left(\frac{\partial \mathbf{u}}{\partial t} + \mathbf{u}\cdot\nabla\mathbf{u}\right) = \nabla\cdot\overleftrightarrow{\boldsymbol{\sigma}} + \mathbf{f} = -\nabla p + \eta\nabla^2\mathbf{u} + \mathbf{f}$$

Equation 1.1. Naiver-Stokes Equation

$$\rho\frac{\partial \mathbf{u}}{\partial t} = \nabla\cdot\boldsymbol{\sigma} + \mathbf{f} = -\nabla p + \eta\nabla^2\mathbf{u} + \mathbf{f}$$

Equation 1.2. Stokes Equation

$$\frac{\partial \rho}{\partial t} + \nabla\cdot(\rho\mathbf{u}) = 0$$

Equation 1.3. Continuity Equation

$$\frac{\rho U_0 L_0}{\eta}$$

Equation 1.4. Reynold's Number

$$\frac{\eta U_0}{\gamma}$$

Equation 1.5. Capillary Number

realized that chemical and biological materials could serve as dangerous agents of war. The U.S. Department of Defense saw an oppurtunity in microfluidic technology to serve as portable detection systems for biological and chemical threats, and in turn, developed a series of programs to stimulate microfluidic research in academic instituions.

With the realization that the size of microfluidic analysis devices allowed a level of portability and cost reduction not achievable with traditional equipment, the scientific and medical community began developing interest in disease diagnosis and monitoring outside of traditional facilities and in the field, meaning remote regions of the world the did not have the resources or infrastructure to sustain modern facilities could now be open to scientific analysis. The implications were enormous, especially for disease diagnosis and prevention. While most infectious diseases such as malaria, typhoid, dysentry, etc have been eradicated from developed countries (infectious diseases in general only account for approximately 5% of deaths in first world countries) nearly 80% of the deaths in developing countries are still due to infectious diseases because efficient disease monitoring and prevention systems are not in place. With the advent of microfluidic technologies, there has been an increased focus on developing miniaturized, simple, and low power diagnostic tools that can be used in the field to expand access to healthcare globally.

To understand why manipulating fluids at the micro-level has had such an impact on microanalytical techniques, it is necessary to be familiar with the underlying physics and fluid mechanics. For a Newtonian fluid, the velocity field obeys the Navier-Stokes equation (1.1) where ρ is the fluid density, $\mathbf{u}$ is the flow velocity, p is the pressure, η is the fluid viscosity, and $\mathbf{f}$ represents the sum of the body forces. This equation is essentially the continuum version of Newton's 2nd Law ($\mathbf{F}=m\mathbf{a}$), on a per unit volume basis. For incompressible fluids, such as liquids, the equation can be simplified to the Stokes equation (1.2). Solving the Stokes equation requires that conservation of mass be maintained, which is represented by the continuity equation (1.3). Solving the system of equations gives the velocity field of the liquid under specified boundary and initial conditions. The Stokes equation can be simplified via non-dimensionalization, giving rise to a parameter known as the Reynolds number (1.4), where U_0 is a characteristic velocity and L_0 is a characteristic length. The Reynolds number is a ratio of inertial to viscous forces, and in microfluidic systems, the Reynolds number is typically less than 1, meaning that viscous forces dominate; thus fluid behavior is atypical of what is seen on the macro-level. In this regime, fluid flow is laminar, and mixing does not occur, resulting in diffusion-controlled transport and the ability to co-flow miscible fluid phases. The insignificance of inertial forces allows for fine control over fluid flow that can be exploited to perform a wide range of processes useful for chemical separation [2], polymerase chain reaction (PCR) [3], and the creation of unique microenvironments [4-6].

1.1 Droplet Microfluidics

Droplet microfluidics, a subcategory of microfluidics, creates discrete fluid volumes with the use of immiscible fluid phases, rather than using continuous flow fluids (Fig. 1.2). When immiscible fluids are concerned, an interfacial tension γ affects the dynamics of the free surfaces. This phenomenon is described by the capillary number (1.5), which is a ratio of viscous to interfacial forces. Above a critical capillary number droplet break-up occurs. The critical

Figure 1.2. Droplet formation in a microfluidic device using flow focusing. Flow direction identified by larger arrows. Encapsulated cells identified by small arrows.

capillary number is moderately dependent on the fluids and geometries employed in the system.

Depending on the value of the capillary number, different regimes of droplet break up can be achieved, resulting in differing droplet sizes, degrees of monodispersity, and mechanisms

of droplet formation (Fig. 1.3). At lower capillary numbers, droplet formation exists in the geometry-controlled regime [7], where the minimum droplet size is limited to the same order of magnitude as the orifice. During droplet formation, the dispersed phase interface is drawn into the orifice, which forces the continuous phase liquid to flow in a narrow region around the fluid-fluid interface. To maintain the applied flow rate, the shear force from the continuous phase is higher in this narrow region, which leads to a

Figure 1.3 Regimes of droplet formation in a flow-focusing device. a) Geometry-Controlled. b) Dripping. c) Jetting. Reprinted (adapted) with permission from [8].

4

pinching of the interface that forms discrete droplets of the dispersed phase. The finger of dispersed phase liquid then retracts back to a position upstream of the orifice and this process repeats itself (Fig. 1.3a). Increasing the capillary number further pushes droplet formation into the dripping regime (Fig. 1.3b), where the droplets tend to be smaller than the orifice, and the dispersed phase finger is longer and narrower than seen in the geometry-controlled regime. Characteristic of the dripping regime is that the dispersed phase finger does not retract after droplet pinch off, but remains at a fixed location inside the orifice during the entire droplet formation process. Droplets can achieve diameters of at least one order of magnitude smaller than the orifice size in this regime [8], and production rates can approach values three orders of magnitude larger than those achievable during geometry-controlled droplet production. Continuing to increase the capillary number gives way to the jetting regime (Fig. 1.3c), where the dispersed phase finger extends beyond the orifice and resembles a jet [9]. Generally, this regime is usually not desired, as the fluid jet breaks into discrete droplets due to Rayleigh capillary instability, resulting in droplets that are less monodisperse than the former two regimes.

Utilizing micro-droplets, one also gains the ability to manipulate, transport, analyze, detect, or fuse each individual unit, allowing for a wide variety of digital-like processes to be realized [10]. The various types of droplets and particles that can be produced with droplet microfluidics range from double emulsions [11, 12], microcapsules [13], hydrogel beads [14], encapsulated cells [15], and microbubbles [16]. Potential applications are immense and have included vehicles for single cell analysis [17], drug delivery [18], therapeutics [16], imaging [19], cell-free protein synthesis [12], and the creation of artificial cell-like structures through the formation of giant unilamellar vesicles (GUVs) [20], the primary focus of this work.

1.3 GUVs

1.3.1 Introduction

GUVs are spherical structures that have an internal aqueous compartment enclosed by a lipid bilayer, with diameters in excess of 1μm. Though the primary focus of this work will be on GUVs, the naming scheme for different types of vesicles is summarized in Fig. 1.4, and further reading on such structures can be found elsewhere [21, 22]. This section will provide some background on the conventional and microfluidic methods for making GUVs, the improvements offered by microfluidics, the current limitations and opportunities for improvement in microfluidic GUV production, and finally some of their practical and therapeutic their applications as artificial cells, biosensors, and vehicles for drug delivery.
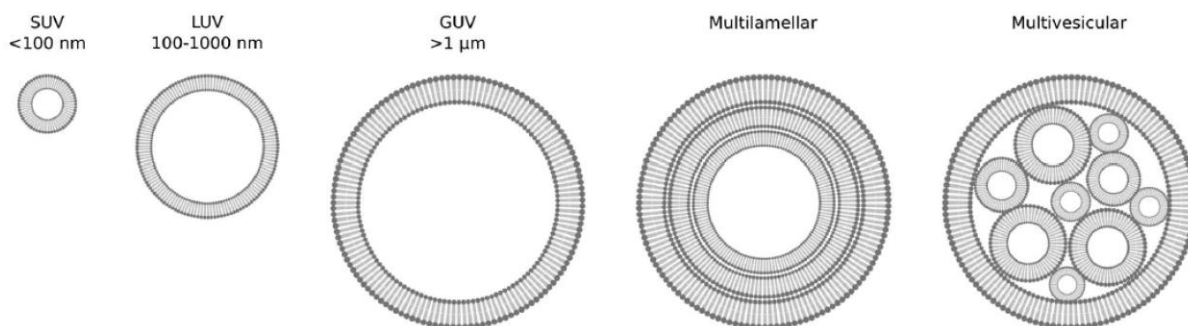
Figure 1.4. Vesicle identification system based on lamellarity and size. Reprinted (adapted) with permission from [22].

1.3.2 Methods of Formation

Conventional Methods

Bulk methods for fabricating GUVs are widespread and though they are normally quick and simple, but even with additional post-processing such as sonication or membrane extrusion, they typically form a heterogeneous population of unilamellar and multi-lamellar vesicles (Fig. 1.5). The majority of these methods also do not produce GUVs that are suitable for medical applications, as they do not allow for efficient encapsulation, and the volatile organic solvents

that are usually used in the production process have the potential to remain present in the final GUV structure, posing a health hazard. For these reasons, some have moved towards microfluidic methods for the creation of vesicles for the greater control over encapsulation, unilamellarity, and size. This section will cover some of the popular methods for forming GUVs in bulk as some of the same principles are applied to their microfluidic preparation.
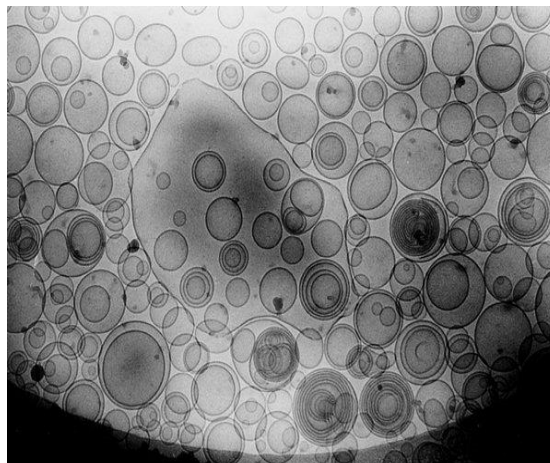
Figure 1.5. Cyro-TEM demonstrating polydispersity and multilamellarity suffered by vesicle populations produced by conventional means.

Hydration of Dry Lipid Films

Lipid film hydration, gentle hydration, spontaneous swelling, and natural swelling are all terms that are synonymous for a method of GUV production originally developed by Reeves and Dowben [23] in the 1960s. The procedure consists of the controlled hydration of dry lipids films that are usually prepared via slow evaporation of a lipid-volatile organic solvent mixture (chloroform, hexane, ether, etc) (Fig. 1.6). Evaporation of the solvent leads to deposition of the films onto the surface of the container (usually glass). Generally the method of choice for the preparation of GUVs that contain charged lipids [24], though zwitterionic phosphatidylcholines (i.e., DOPC) can also be used if the dry lipid film contains non-electrolytic monosaccharides (glucose, mannose or fructose). The neutral molecules act to increase the spacing between the lipid layers during swelling due to osmotic pressure
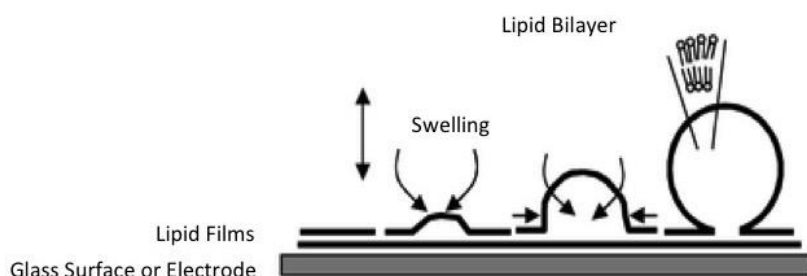
Figure 1.6. Schematic of GUV formation via dry lipid film hydration. Reprinted (adapted) with permission from [27].

7

differences promoting the movement of water to the spaces between the bilayers. For gentle hydration to successfully form GUVs, the process should take place above the phase transition temperature (T_m) for the lipid(s) included in the dried film, when they are the liquid-disordered state within the lipid bilayer [25].

Electroswelling

In 1986, Angelova et al. [26] published a report on a variation of the gentle hydration method that is now known as electroformation or electroswelling [27]. In that study, they investigated the effects of externally applied electric fields on the hydration of lipid films deposited on an electrode surface (indium tin oxide coated glass or platinum wires). They found that depending on quantity and composition of lipid used, parameters related to the applied electric field, and the hydration medium, fairly homogeneous GUVs could be formed in low ionic strength solutions. Later variations of this method did not need an organic volatile solvent and instead lipid deposition could take place via an aqueous solution that contained both preformed SUVs or LUVs [28]. Similarly, lipid deposition could also be achieved using lipid stabilized W/O emulsions in a water-immiscible volatile organic external phase [29]. Both these methods produce lipid films that are not fully dry due to the presence of aqueous solution in the preformed vesicles or emulsions. As a result of this, the latter of these methods can also be used for the encapsulation of various hydrophilic compounds, as molecules present in the aqueous phase of the performed W/O emulsions will be incorporated into the interior of the GUVs during the hydration process. In general though, both gentle hydration and electroswelling do not allow for efficient encapsulation of large (i.e., enzymes, proteins, etc.) or charged molecules during the formation process since these molecules have to penetrate through the outermost layer of the deposited lipid film, which is a very slow process for larger molecules.

With electroswelling, GUVs will not form if too many charged lipids are present, which is in contrast to the gentle hydration method where the presence of charged lipids is beneficial. GUVs formed by electroswelling also tend to show thin, long protrusions that remain connected to the electrode, which can be stable for many hours. The presence of these protrusions may or may not be desired, depending on the particular application. Another drawback to traditional electroswelling stems from the concern of partial lipid oxidation do to the film's direct contact with an electrically conductive surface. In response to this, Okumura et al. [30] developed a method whereby lipids can be deposited on a glass tube that is then held in place between two platinum wires where an electric field is applied. Some degree of size control can also be achieved from electroswelling by patterning the lipids on micropatterned electrode surfaces [31].

Lipid Stabilized W/O Emulsion Precursors

GUVs can also be formed from preformed W/O emulsions, in this case using lipids as the primary emulsifier. The two most common methods are referred to as the W/O emulsion transfer method [32, 33] or inverted emulsion method and the lipid coated ice-droplet hydration method [34]. In both methods, the initial W/O emulsions can be produced via conventional means (i.e., Couette mixer [35], etc.) or using droplet microfluidics techniques.

In the W/O emulsion transfer method (Fig. 1.7), preformed, bilayer-forming lipid stabilized W/O emulsions are poured onto a two-phase system that contains a layer of an oil-lipid mixture (intermediate phase) on top of a lower aqueous phase. Given enough incubation time, the interface between the intermediate and aqueous phase will become saturated with lipids and form a monolayer whereby the hydrophobic lipid tails are in contact with the intermediate phase and the hydrophilic lipid head groups protrude into the aqueous phase. Given the density difference between the three phases (emulsion, intermediate, and aqueous), the W/O emulsions

will generally migrate into the intermediate phase and then pass into the water phase. As the emulsions pass through the interface separating the intermediate and aqueous phases, the hydrophobic tails of the lipid monolayers surrounding each emulsion will interact with the hydrophobic ends of the lipids separating the two fluid phases, eventually forming a GUV as the emulsions completely crosses the interface. Centrifugal forces can also be utilized if the phase transfer is not spontaneous or to speed up the process. Given that this method essentially assembles a second lipid layer on a lipid coated water droplet, it was initially employed as a method to create GUVs with different (though not permanent) lipid leaflet compositions, also known as asymmetric GUVs. It is reasonable to consider that the

Figure 1.7. Schematic of W/O emulsion transfer method. Preformed W/O emulsions are dropped into a lipid-oil intermediate phase that is immiscible, and denser, than oil phase containing the emulsions. The intermediate phase is layered on top of an aqueous phase. The denser emulsions will sink through the oil layers and form a bilayer as it traverses the interface separating the intermediate and aqueous phases. Reprinted (adapted) with permission from [33].

finalized GUVs could have oil lingering in the membrane that either originates from the initial external phase of the W/O emulsions, and/or from the intermediate phase. Given that the bilayer is only a few nanometers thick, the size and monodispersity of the original W/O emulsions will be the same for the final GUV population if not effects or changes the size of the emulsions during the transfer process (i.e., oil incorporation, Ostwald ripening, coalescence, interfacial instabilities, etc.).

Another more recent method that involves the use of preformed W/O emulsions is known as the lipid-coated ice droplet hydration method (Figure 1.8). In this case, the initial W/O

emulsions are stabilized with a surfactant (or mixture of surfactants) and not bilayer forming lipids. The stability of the W/O emulsion is essential for vesicles to be formed using this method, and bilayer forming lipids are not very well suited at creating highly stable W/O emulsions. After preparation of the W/O emulsions (microfluidically or otherwise), the emulsions are frozen via transfer into liquid nitrogen. As with the overwhelming majority of vesicle formation methods, the oil phase is an organic volatile solvent, and remains in a liquid state as the water droplets freeze. With the water droplets frozen, the surfactant rich external phase is replaced with another volatile organic solvent saturated with bilayer forming lipids. Evaporation of the oil phase below the freezing temperature of water promotes the formation of dry lipid films on the surface of each frozen water droplet. Upon rehydration in an aqueous media, the frozen core melts and a giant vesicle is formed. While this method allows for very efficient encapsulation of hydrophilic

Figure 1.8. Illustration of the lipid-coated ice droplet hydration method. The aqueous interior of the W/O emulsions are first frozen and then undergo (i) replacement of the surfactant(s) with bilayer-forming lipids via external phase exchange, (ii) evaporation of external phase below 0°C and (iii) resuspension in aqueous solution above 0°C. Reprinted (adapted) with permission from [34].

compounds, the intermediate formation of lipid films before rehydration means that the resultant vesicles are overwhelmingly multilamellar, and cannot be considered GUVs.

Droplet Microfluidic Methods

The control of droplet production provided by microfluidic flow regimes has been able to overcome many of the limitations seen with conventional bulk methods of GUV formation. While sacrificing throughput, microfluidic production simultaneously allows for improved encapsulation efficiency, unilamellarity, monodispersity, and asymmetry (if desired). Barring a few exceptions, microfluidic production of GUVs is primarily based on two methodologies: forming GUVs from the microfluidic jetting of a planar lipid bilayer [36-38], or utilizing post-process solvent extraction to convert double emulsion templates into vesicles [12, 39, 40].

Jetting of a Planar Lipid Bilayer

Formation of the bilayer used for microfluidic jetting begin with the dissolution of bilayer forming lipids into a volatile oil phase that is squeezed and stretched between two aqueous fluid compartments. As the lipid-oil mixture begins to thin, the hydrophobic regions of the lipids at each interface interact and form a
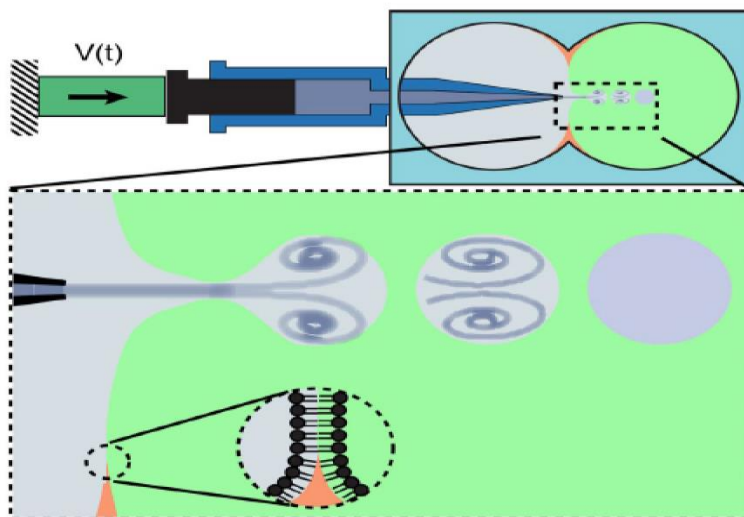
Figure 1.9. Schematic of microfluidic jetting device and close-up of GUV formation process. Reprinted (adapted) with permission from [36].

bilayer. Applying a focused pressure to one side of the bilayer forces the bilayer to expand like a bubble and eventually break off, encapsulating a portion of the adjacent fluid.

One of the first iterations of this method formed GUVs from a planar lipid membrane that was extended between two circular microfluidic compartments [36]. A piezoelectric actuated syringe fitted with a glass micro-nozzle (Fig. 1.9) was used to apply pressure to one side of the

membrane and extend it into the opposite fluid compartment. After protruding a certain distance, the membrane would collapse and reform on itself to separate from the membrane and create a GUV. The method can produce very monodisperse GUV populations and reported generation frequencies of approximately 200 Hz. Given the extent that the membrane must protrude before GUVs formed, diameters below 100μm were not reported, though some indication was given that smaller injection nozzles could lead to smaller GUV sizes. Regardless, anything above 10μm in diameter is potentially too large for in-vivo therapeutic applications and could cause an embolism. Additionally, it is likely that a small amount of the organic solvent used in the preparation of the planar bilayer may be sequestered in the GUV membrane.

In a more recent iteration, this method was extended to the high throughput production of cell-sized GUVs (~20μm reported) [37]. In this case, a planar lipid bilayer was formed at multiple microfluidic T-junctions perpendicularly lining a larger straight channel (Fig. 1.10). After filling the main channel with an aqueous solution, a hexadecane-lipid mixture was run through the device to wash out the aqueous phase, keeping a small portion sequestered in the side chambers. A second aqueous solution then washed out the oil phase, leaving behind a thin oil-lipid film at each T-junction that could be used to form a bilayer upon introducing flow in the main channel. Shear forces provided by this flow caused the oil-lipid film to protrude outside the chamber and finally be stretched and pinched by a small overhang to form a GUV.

While the methods described have the ability to produce a wide range of GUV diameters with throughput comparable to other microfluidic techniques, the supply of lipids to make the GUVs is cannot be replenished and is limited to what is present in the preformed bilayer. Also, the diameters that have been reported (100-200μm) are still at least an order of magnitude too large for in-vivo applications (1-10μm).
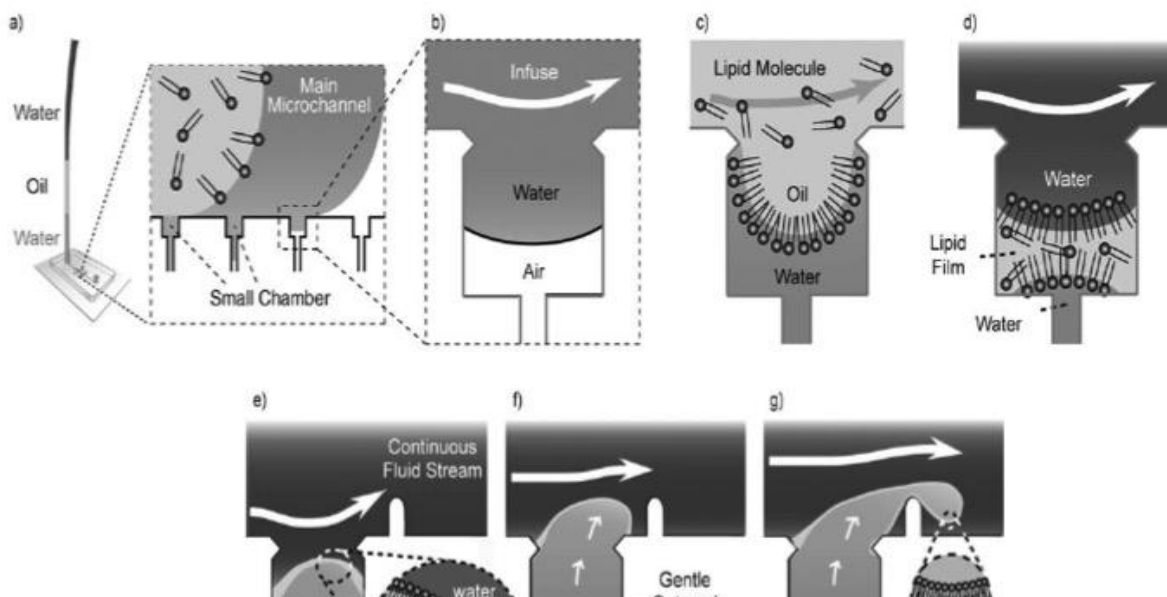
Figure 1.10. Illustration of high throughput microfluidic production of GUVs from multiple planar lipid bilayers. a) Water, oil with dissolved lipids, and water are sequentially introduced into a microfluidic channel with many smaller chambers in the walls. b)-d) Sequence of planar lipid bilayer formation. b) As first water solution fills the device, air is pushed out through the PDMS walls of the side chambers. c) Oil solution pushes out first water solution from main channel, leaving behind a pocket of water in each chamber. A lipid monolayer forms at each water-oil interface. d) The second water solution flushes out the oil, while the remaining oil forms a thin film at the entrance of each chamber. Another lipid monolayer forms at the second water-oil interface. e)-g) Sequence of GUV formation. e) Shear forces from the flow of the aqueous phase in the main channel thins the oil film covering each chamber and promotes bilayer formation from the lipid monolayers. f) Shear forces further drive the bilayer sto protrude out into the main channel. g) A small protrusion next to the chamber pinches the tail end of the bilayer, forcing it to fuse to the other end and break off to form a GUV. Reprinted (adapted) with permission from [37].

Double Emulsion Templates

Given that the ability to form droplets (microfluidically or otherwise) inherently relies on the presence of immiscible fluids, the use of water-in-oil-in-water (W/O/W) double emulsion templates have become a very popular method to create GUVs while benefiting from the fine control on droplet size and composition that is offered by droplet microfluidics [12, 39, 40]. Additionally, the ability to produce complex emulsions can be used to aid in the creation of multi-compartment GUVs to mimic the compartmentalized nature of biological cells or to separate vital components [41, 42]. Double emulsions production is accomplished by co-flowing two immiscible fluid phases in a microfluidic device: an internal aqueous phase and a surrounding immiscible sheath phase composed of an oil with dissolved lipids. Both phases can

14

be sheared together by an external aqueous phase, or sequentially, to produce a double emulsion (Fig. 1.11).
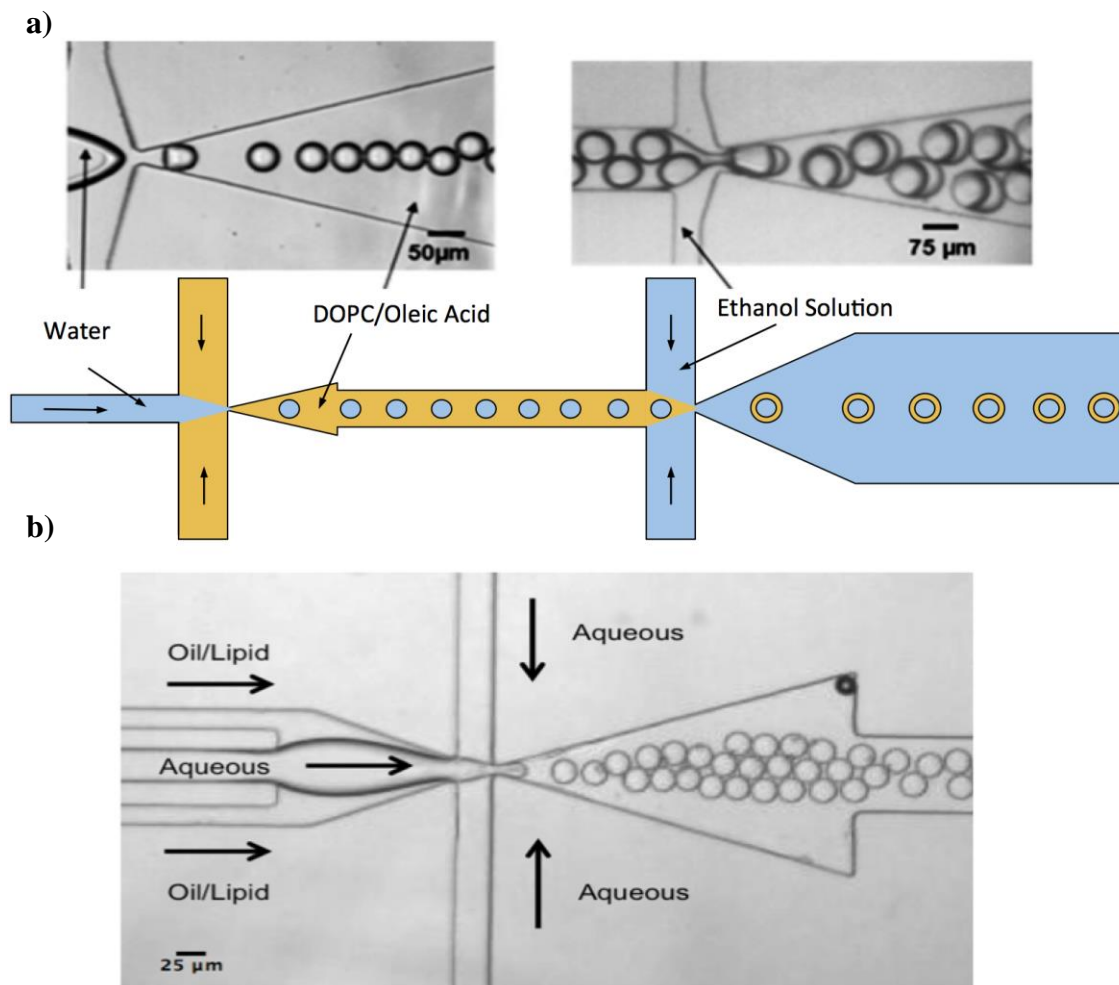
Figure 1.11. Double emulsion production in microfluidic devices. a) Microscopic image (top) and schematic of two-step production (bottom). Reprinted (adapted) with permission from [12]. b) Microscopic image of single-step production.

Nearly all reported methods for forming GUVs from double emulsion templates involve the use of one or more organic volatile solvents as the oil phase, since it can remove itself spontaneously via evaporation to form the bilayer [39, 40] and these solvents have a track record of being used in earlier methods of vesicle formation. Unfortunately, these harsh solvents can harm cells and encapsulated biological materials, as these components are encapsulated during double emulsion formation, while the solvent(s) is still present. Furthermore, theses solvents

aren't compatible with PDMS that is generally used in a laboratory environment for rapid prototyping and instead require the use of more robust materials. This generally comes in the form of glass microcapillary tubes, which are not well suited for reagent mixing and other droplet manipulation capabilities (splitting, fusion, sorting, etc.).

When a non-volatile oil phase is used to create the double emulsion templates, GUVs can also be formed by solvent extraction. Contrary to the method just described, Teh et al. [12] utilized double emulsion template where the oil phase was composed of a fatty acid-lipid mixture. The fatty acid in particular, oleic acid, is slightly soluble in alcohols, so a small percentage of ethanol in the external solution can slowly extract the oil from the bilayer, conceivably allowing a GUV form, though no conformation to the presence of a bilayer was presented. Even with the use of oleic acid as the oil phase, a volatile, non-biocompatible solvent was still necessary to promote GUV formation.

1.3.3 Artificial Cells

Due to their similar size to natural cells, GUVs have been used extensively as models for multiple studies on dynamic membrane properties, including mechanical measurements [43-46], phospholipid domain formation [40, 47], vesicle budding [48, 49], fusion [50, 51], and membrane protein integration [52-55]. They have also demonstrated success as vehicles for cell targeting and communication [56, 57], and as bioreactors for biochemical reactions and protein synthesis [12, 58-60]. Accordingly, their potential to be used as a basis for the creation of artificial cells cannot be overlooked. In the following sections, a brief introduction to the concept of the artificial cell will be followed by a summary of work that has created GUVs to mimic several important cellular functions. Given that an exhaustive review of the work covering the progress made with artificial cells is beyond the scope of this work, three specific examples will

be discussed here as they can be applied to the GUVs that are the primary focus of this thesis: reagent release (drug delivery), sensing (biosensors), and professional cell mimicry (artificial antigen presenting cells). For further reading and a more in depth review on the subject, please refer to the following reviews [61-64].

Background

Since its conception, two fields of thought have dominated the field concerning artificial cells and synthetic biology: the 'top-down' and the 'bottom-up' approaches. The top-down approach regards the simplest organisms (mycoplasmas, bacteria, viruses, etc.) as a window to establish how a fully functioning cell can be constructed from individual components and meet the simplest qualifications for life (though there exists different schools of thought as to what constitutes 'life', the general requirements include the abilities of adaptation and reproduction, and the presence of a self-sustaining metabolism) [65]. In general, this school of thought focuses on the reverse engineering of natural cells to achieve what's known as a 'minimal' or 'proto' cell. Beginning with natural cells, features deemed 'non-essential' are subtracted out via gene manipulation until only the basic functions of life are present. The ultimate goal of the bottom-up approach is to build a fully functioning cell using only basic (natural or synthetic) molecular building blocks (amino acids, lipids, nucleic acids, etc.) and then impart interesting functions via programming of the cell's genetic material. Given the infancy of this field, development has been limited to simply mimicking a few cellular functions using different types of micro-particles (vesicles, hydrogels, micro-capsules and beads, etc.). This field of though first gained headway in the 1960s, when T.M.S. Chang created what can be considered the first artificial cells by encapsulating biological reagents within capsules made from ultrathin, semi-permeable polymeric membranes [66]. Starting with these capsules as a scaffold, it was realized that cell-

like functionality can be added to create 'smart' micro-particles, with groundbreaking implications. Regardless of the method used, both fields of thought seek the same eventual objective: a completely functional, fully programmable, self-sufficient cell. Almost certainly, cooperation and knowledge gained from both schools of thought will be necessary to achieve that goal.

With the top-down approach, one is essentially "reverse engineering" a cell. This process comes in two steps: 1) Completely reduce a cell to only the minimal components necessary for it to be "alive", usually be removing unnecessary genetic sequences, and 2) Reprogram the cell to impart the intended functionality. Cells that have been reduced to the minimal requirements necessary to be considered alive are understandably termed "minimal cells". Using this metabolically active body as a platform, one can then impart functionalization by adding new gene sequences in a controlled and precise manner [67]. Since the genome is usually the only component being altered, the cell still has all the components it needs to survive, replicate, and carry out essential cellular processes, such as its organelles, lipid membrane, proteins and enzymes, cytoskeleton, etc. The limiting factors with this approach mainly stem from our still evolving understanding of the complexity of genes and gene regulatory networks [68] and the fact that we still can only mimic or alter functions found naturally; we still lack the knowledge necessary to program entirely novel functional proteins from the ground up and it is always necessary to start with a natural analog or a large screening process to "discover" novel proteins that can impart new functions [17]. Unfortunately, building a self-replicating, programmable biological system in this manner has many drawbacks since our understanding of the cell's internal workings is still developing. Even though it might seem as if the cell has been reduced to just the basic functions of life, there are still numerous unknown or unaccounted for processes

that could be occurring that may interfere with the intended function(s). This is of upmost importance when multiple new genes may be introduced, as they can interact with each other and impart unforeseen outcomes, as cells are not neatly organized like the circuit board in a computer, with many processes overlapping and influencing others (Fig. 1.12) [69]. The molecules in a cell are also free to move around randomly, increasing the chances of cross-reactions and creating problems with synthetic systems. Artificial cells created in this manner can also evolve in unpredictable ways, slightly altering the phenotype with each successive generation and possibly limiting their lifetime of usefulness. In its current state, far more knowledge needs to be gained before such cells can provide any therapeutic benefit, but the knowledge gained from this cellular "reverse engineering" will ultimately provide the necessary
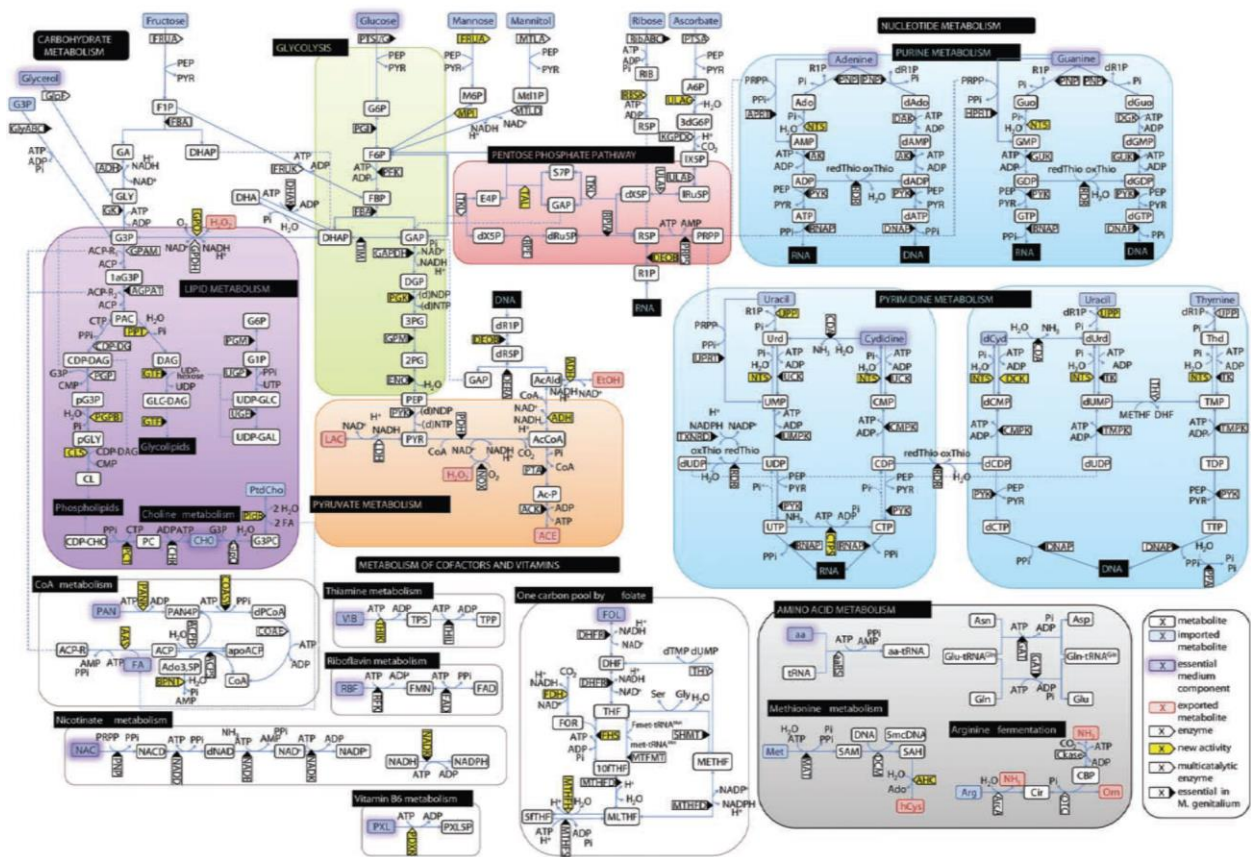
Figure 1.12. Metabolic schematic of M. pneumoniae. Reprinted (adapted) with permission from [69].

framework to build a cell from its basic building blocks, or from the "bottom-up".

Currently, there has been no report of a "true" minimal cell that has been built from is basic building blocks. The difficulty lies in the fact that a cell is not foreign man-made technology that can simply be reverse engineered. It is a complex, self-contained bioreactor that has many functions; it can reproduce, store and use energy and information, respond and adapt to its environment, and can accomplish a slew of other processes through the intricate workings of millions of chemical processes that are only beginning to be understood. The complexity of the cell has required that only one or few basic functional elements of the cell be recreated at a time.

Since the terms "minimal cell" and "artificial cell" are commonly used interchangeably, it is important to define an artificial cell as it pertains to any work presented herein. At this point in time, cell-like systems made from the bottom-up are more appropriately termed "artificial cells", as they are not yet designed to be living, but instead for some biocompatible, investigatory, or therapeutic application that requires that replication of a cellular function or process. To avoid confusion, cells that have had been reduced to the minimal components to still be considered alive should not be referred to "minimal cells", rather than "artificial cells". From this point forward, artificial cells will refer to cell-sized structures that are built from the "bottom-up", starting with some kind of cell-size spherical scaffold, capsule, emulsion, or self-enclosed membrane that can be made from synthetic or biological components, or some combination of both. From this scaffold, functionality can be imbued such that the structure mimics the outcome of at least one process or activity that any cell does naturally. These artificial cells need not be considered "alive"; they may or may not have an active metabolism, store any genetic information, or reproduce, but they are only constructed from individual components and not sculpted from a living organism. Ultimately, development an artificial cell

will lead to a greater understanding of complex genetic and biological processes that are necessary to sustain life, while also enabling the advancement of technologies that could utilize artificial cells for therapeutic and environmental purposes.

Artificial Antigen Presenting Cells

An established application of professional cell mimicry that is currently under investigation in the medical community is that of aAPCs for the purposes of immunotherapy, which aims to utilize this effective immune response to eliminate cells and pathogens associated with difficult to treat infectious diseases and cancer. However, vaccines have not been successful in all cases, and certain diseases such as malaria [70], HIV , and cancer cannot currently be vaccinated against. Furthermore, vaccines do not help once an unvaccinated individual has been exposed to the pathogen, at which point, the outcome can sometimes be fatal. Immunotherapy can be generalized into two categories: active and adoptive. Active immunotherapy involves the introduction of an inactivated antigen into a patient, such that the immune system becomes familiar with the antigen and can initiate a proper response if needed during future exposure. This process is commonly accomplished through the use of vaccines, which have been utilized for a variety of diseases over the last 200 years, since the creation of the first vaccine for smallpox in the 1790's [71].

In contrast, adoptive immunotherapy aims to treat those individuals that have already been exposed to a disease causing pathogen, and is commonly explored as a potential treatment for cancer [72]. Originally, adoptive immunotherapy was directed at collecting a patient's own dendritic cells and expanding them ex-vivo in co-culture with the antigen of interest, then releasing them back into the body to activate the immune system (Fig. 1.13) [73]. Regrettably, this process was very labor intensive, expensive, and it is difficult to isolate a significant amount
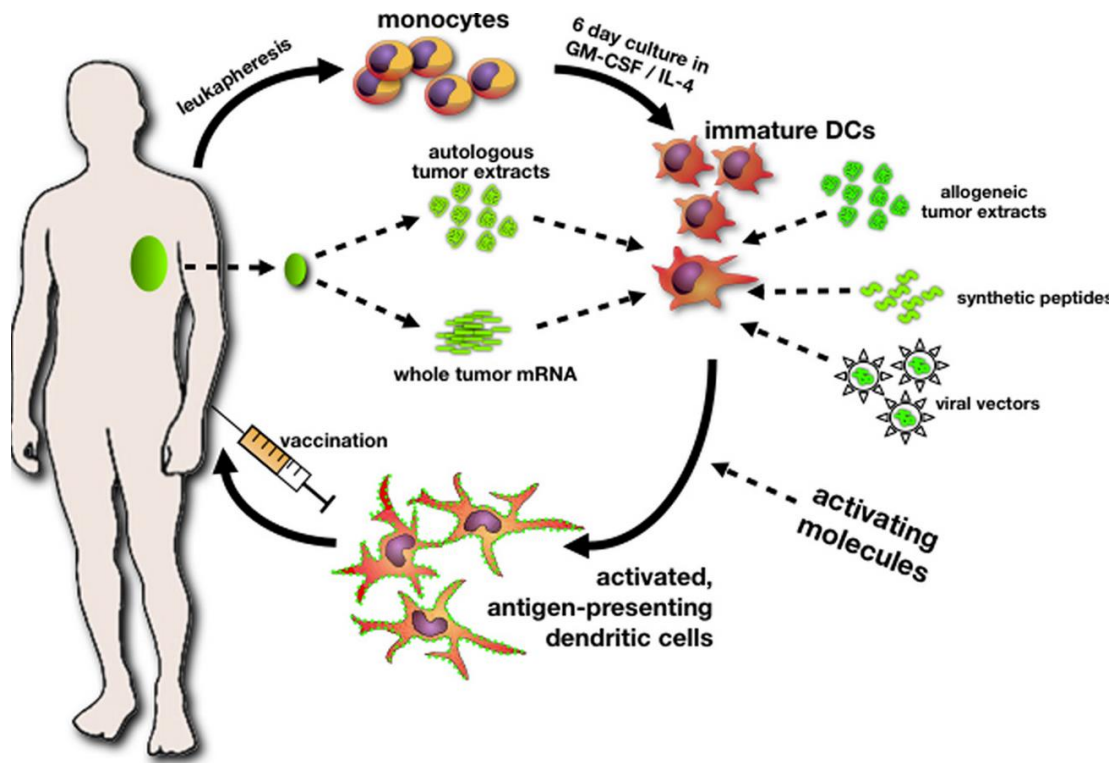
Figure 1.13. Schematic of the general workflow for ex-vivo expansion of autologous dendritic cells for cancer immunotherapy. Reprinted (adapted) with permission from [73].

of autologous dendritic cells for ex-vivo T-cell expansion. Furthermore, their effectiveness and response varies in consistency between individuals [74]. To circumvent these limitations, aAPCs have been developed to stimulate and expand autologous populations of T-cells ex-vivo, though the potential of in-vivo stimulation is gaining traction as the field evolves.

Various types of bead-based solutions have been utilized as aAPCs for the expansion of antigen-specific T-cells. Some of the first studies use latex beads that had biotinylated MHC class-I and costimulatory molecules coupled to their to the surface [75]. Similarly, HLA-A2–Ig molecules and anti-CD28 antibodies have been coupled to magnetic beads to direct T-cells at clinically relevant tumor antigens [76, 77]. By using an HLA-A2-Ig molecule, rather than a single chain MHC-peptide complex, the peptide resident in the HLA–Ig molecule can be easily exchanged with any HLA-A2-restricted antigenic peptide, negating the need for multiple

transfection steps. This allows for a single batch of HLA-A2–Ig-based aAPCs to be loaded with a variety of different antigenic peptides to expand a population of T-cells with different antigen specificities.

While these various bead-based solutions have shown success in expanding T-cell populations, only a few systems are suitable for clinical use [57]. A major limitation to bead based methods is the absence of a fluid membrane. Consequently, interactions with T-cells may be suboptimal since they are not being activated in a physiological manner. Within the body, T-cells undergo a series of transient interactions with a variety antigen-presenting cells before becoming activated against a specific antigen [78]. When encountering a specific antigen-presenting cell, a T-cell will bind to the exposed MHC complexes on the cell's surface. This interaction tends to be of low affinity and the binding time is very short. However, this is necessary to give the opportunity to trigger many T-cell receptors on the membrane, which results in stable binding between the antigen presenting cell and T cell [79]. Once activated, the T-cell rearranges its membrane and cytoskeleton to form what is known as the "immune synapse" (Figure 1.14). The synapse consists of a cluster of T-cell receptors surrounded by adhesion molecules [80]. The formation of this synapse ultimately triggers a signaling cascade that activates the T-cell and causes it to produce cytokines [79]. With this insight, it is clear that bead-based methods cannot allow for the formation of the immune synapse, whereas the ligands on the surface of a lipid bilayer can be easily rearranged for optimal immune synapse formation. This may be a perfect opportunity for vesicles, as their fluid membrane makes them optimal candidates to simulate the physiological environment of the T-cell interaction with professional antigen presenting cells. Furthermore, vesicles are potential candidates for *in vivo* T-cell activation, due to their biocompatibility and biodegradability [56]. As mentioned in section 1.3,

therapeutic amounts of monodisperse GUVs can be produced within reasonable time frames, with compete control over size and membrane composition via the utilization of microfluidic techniques.

While limited, there has been some work investigating the use of vesicles as aAPCs. In 2000, Prakken et al. published a report where MHC class II molecules were incorporated onto the bilayer surface of lipid vesicles [81]. While the aAPCs demonstrated binding to MHC-II restricted T-cells and promoted physiological clustering of T-cell receptors (TCRs) on the T-cell membrane, these vesicles were 100nm-1μm in diameter, ultimately too small to effectively induce T-cells proliferation. Moreover, they did not contain two other essential components of the immune synapse, namely the adhesion and costimulatory molecules. To further mimic the multicomponent characteristics of the immune synapse, consequent studies developed vesicles that displayed MHC class II-peptide complexes in association with costimulatory and adhesions molecules. For instance, Giannoni et al. incorporated a micro-domain of an MHC-peptide
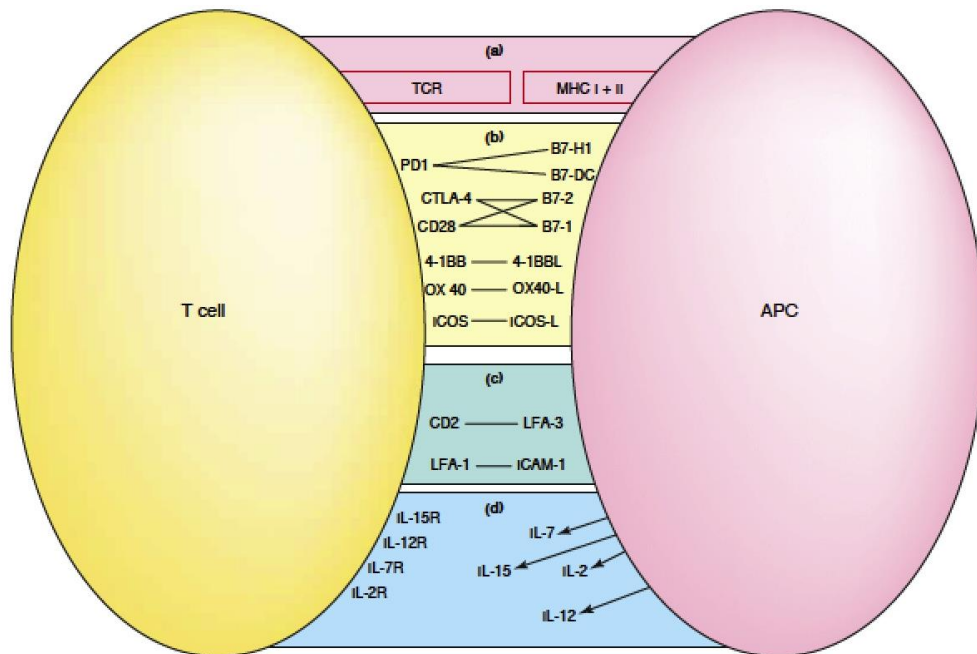
Figure 1.14. Overview of interactions between T-cell and antigen presenting cell that make-up the immune synapse. Reprinted (adapted) with permission from [74].

24

complex, a costimulatory molecule, and an adhesion molecule to simulate the structure of the immune synapse on the vesicle membrane [82]. This micro-domain consisted of a neutravidin complex that bound an MHC-II-peptide complex, the adhesion molecule anti-LFA1, and the costimulatory molecule anti-CD28 [83, 84]. The organization and pre-clustering of the three components into microdomains on the aAPC surface yielded superior T-cell activation in comparison to bead-based aAPCs and demonstrated stimulation at levels comparable to natural aAPCs. Again however, these vesicles averaged a few 100nm in diameter, and no assessment was made as to how size may influence T-cell response to aAPCs. Furthermore, the use of cholera toxin to bind the immune synapse components to the GUV surface may further limit the clinical applications of this approach.

Contrary to traditional bulk methods of vesicle and GUV formation, microfluidics offers an ideal platform for the creation of GUV based aAPCs as it provides a simple method for generating large numbers of uniform, monodisperse GUV populations where the amount of functionalized surface components can be easily controlled and homogeneously distributed. GUVs with diameters between 1-15μm-size have the potential to fill a niche as cell-sized aAPCs to mimic the function of dendritic cells. By swapping the peptide sequences displayed by these cells, it may be possible to direct T-cells to attack different types of cancer cells in a specified manner [77]. Additionally, the GUVs presented in this work establish a pathway to commercial adoption of GUVs given that they can be converted on-demand from storage templates (in bulk) and functionalized immediately prior to their intended use (i.e., patient administration, in the case of aAPCs).

Biosensors

Biosensors are analytical tools that utilize a biologically derived recognition element to detect an analyte of interest. The biological recognition element is the key to biosensor function and specificity, as the inherent advantage of a biosensor is to utilize the incredibly specific interaction of the biorecognition element with the analyte of interest, as is seen with cells. In turn, various substances and organisms can be detected in vital environmental resources (i.e., drinking water) or biological systems, with incredible specificity.

The interaction of the analyte with the bio-recognition element produces a physical or chemical change that is then converted by a transducer into an electrical signal proportional to the concentration of analyte in the sample. The biorecognition element is commonly an enzyme or protein [85], or antibody [86], but oligonucleotides [87], whole cells [88, 89], and organelles [90, 91] have also been used. In most cases, the biorecognition element is placed in direct physical contact with the transducing element [92]. The nature of the physical or chemical signal passed to the transducer can be electrochemical [93, 94], optical (fluorescent or colorimetric) [85, 95], calorimetric [96-98], or piezoelectric [99, 100], among others [101, 102]. While the biorecognition element allows for biosensors to have incredible specificity, it traditionally falls on the transducer to amplify the signal to increase the sensitivity of the system, and the degree and quality of this amplification will be dependent on the particular transducer [103].

The sensing mechanism for a biosensor can take many forms: for example, the biosensor can utilize an enzyme that will initiate a biochemical reaction in response to an analyte binding event or a protein that will undergo a conformation change when bound to the target analyte. In nature, cells sense their environment through a signaling cascade of multiple reactions that allow for highly efficient amplification via reaction cascades [104]. For this reason, there has been an

interest in using vesicles as biosensors for their ability to encapsulate biological reaction components. The very nature of the reaction can be one that involves signal amplification, such that the signal can be pre-amplified before reaching the transducer, or the vesicle can itself act as the transducer, further simplifying the system. By placing the components of the biochemical reaction within a small, confined volume, the concentration of product molecules can increase to a detectable level much more rapidly, and with much less analyte, than in a larger, bulk solutions. The use of an enzyme and a biochemical reaction scheme in a biosensor platform also means that a single molecule of analyte can initiate multiple reaction events, allowing for tremendous signal amplification and even single molecule detection. Such technology can negate the need for analyte pre-enrichment above a specific detection threshold, as is still the case with many traditional detection platforms (PCR, Elisa, etc.) [105]. Placement within a physical boundary also protects the reaction components from contamination, allows the system to be deployable into sensitive, biological environments, and provides a platform for the placement of the sensing elements. Natural cells contain the ideal physical boundary between their interiors and the external environment, the lipid bilayer, which can be functionalized to meet a variety of demands and tasks. Over the last few decades, many biosensing platforms have utilized either planar or enclosed lipid bilayers, or their synthetic, biomimetic equivalents [106, 107]. With a membrane, the biorecognition element can either be enclosed within the vesicle, embedded within the membrane itself, or conjugated to the membrane surface. The biomimetic nature of lipid vesicles also provides the ideal environment to stabilize and maintain the activity of proteins and enzymes for analyte. The ease with which vesicles can be modified and functionalized also makes them compatible with many current sensor technologies opens the possibility for multi-target sensing.

Enzymatic reaction events have been utilized in biosensor applications [108, 109], and with design of artificial organelles, such reactions have been contained within vesicles and polymersomes [110-112]. While many artificial organelles are designed with the therapeutic intent to correct cellular function or introduce novel biochemical functions into established cells, the application to biosensing cannot be overlooked. For membrane permeable analytes, the design of the biosensor is simplified, in that there is no need for any active components to be in, or conjugated to, the membrane and all the sensing and reaction components can be entirely contained within the vesicle interior, where the result of the reaction releases a fluorescent signal that can be correlated to the concentration of analyte [113]. For example, Ben-Haim et al. demonstrated that enzymatic activity could be maintained within vesicles by encapsulating trypsin and using it to cleave the membrane permeable BZiPAR (bis-(CBZ-Ile-Pro-Arg)-R110, a Rhodamine 110 peptide substrate), releasing green fluorescent Rhodamine 110 [113]. Enzymatic cascades are also possible within vesicle structures, where different vesicles can contain different steps to an enzymatic cascade reaction, leading to the plausibility of compartmentalized, sequential reaction steps within a single structure. Kuiper et al. demonstrated such a scheme by encapsulating horseradish peroxidase (HRP) and glucose oxidase (GOx) in separate polymersomes to detect glucose [110]. After GOx converts glucose to into gluconolactone and H_2O_2, the membrane permeable H_2O_2 diffuses into solution and enters polymersomes containing HRP and 2,2'-azino-bis(3-ethylbenzthiazoline-6-sulfonic acid) (ABTS), where the resultant reaction produces the ABTS radical cation (ABTS^{*+}). This reaction was also realized in a single structure with an additional extra step where membrane bound Candida Antarctica lipase B (CalB) converts 1,2,3,4-tetra-O-acetyl-b-glucopyranose (GAc4) to glucose [111]. The polymersome biosensors that contained these reaction components were formulated to be

naturally permeable to glucose so it could pass through the membrane and initiate the remainder of the reaction cascade in the interior. Channels imbedded in the membrane can also be utilized as in vesicle biosensors for electrochemical detection schemes [114], or to allow the passage of membrane impermeable analytes to internal reaction components [85, 112]. With cascade events, amplification can be achieved in this format as well.

Vesicles can also be designed to undergo structural changes in response to environmental signal as a means to indicate detection of a target analyte. Vesicles produced from polydiacetylene (PDA) lipids are very popular in this regard for use in colorimetric assays, as they will undergo a rapid color change that is visible to the naked eye in response to various environmental stimuli, including pH, temperature, and exposure to a variety of molecules, peptides, and solvents [115]. For biosensor applications, biorecognition elements can be conjugated to the PDA vesicle membrane, and binding of analytes will cause a sharp color change, the degree of which is proportional to the concentration of analyte in the sample [116-118]. Although PDA vesicles are generally very stable, their production cost is currently prohibitive to widespread commercialization and they can suffer from issue with specificity, as they are naturally responsive to a wide range of stimuli.

Other effective strategies also exist to realize amplification with the use of vesicle that makes use of their mass and surface-to-volume-ratio. For one, they can be used to encapsulate high concentrations of signaling molecules to increase the sensitivity of various types of immunoassays [119]. Antibodies specific to the analyte in question are immobilized to a surface and the vesicles can either be tagged with the analyte and compete with the free analyte in solution to bind with the immobilized antibodies (competitive immunoassay, where analyte concentration and signal output are inversely related) or the vesicles can be tagged with

antibodies and bind to the analyte-immobilized antibody complex (sandwich immunoassay, where analyte concentration and signal output are directly related). In this way, a large concentration of signaling molecules can be associated with a single binding event, and analysis can be accomplished through the localization of dye containing vesicles for colorimetric [120-122] and fluorescent [123, 124] assays, release or production of ions for electrochemical signaling [119], and the release of chemiluminescent substrates for chemiluminescence assays [125]. The extra mass and size provided by vesicles as compared to the analyte being detected is another use of vesicles for signal amplification. With surface plasma resonance (SPR) sensors, vesicles can be used in sandwich immunoassays to amplify the degree of SPR shift measured by the detector [126]. Vesicles can also enhance the sensitivity of quartz microbalances (QCM) [127, 128]. Quartz microbalances measure the mass of absorbed material based on its oscillation frequency, and this mass can be increased significantly with the attachment of a vesicle to each bound analyte on the microbalance. Theoretically, however, any nano- or micro- particle with an easily modifiable surface can accomplish the same effect as vesicles with respect to SPR and QCM.

Drug Delivery

Traditionally drug-carrying vesicles (and other particles) are usually no more than a few 100nm in diameter, as this size permits them to traverse blood vessels and enter interstitial fluids to directly deliver drug payloads to target cells [95, 129]. However, the drawback of these nano-carrier delivery systems is a low loading capacity compared to their micro-sized counterparts, as the mass of these structures is far larger than the drugs they carry ($\geq 80\%$) [130, 131]. Given that any micro-sized objects injected into the body will remain in the blood stream, GUV based drug carries show great potential for the encapsulation of chemotherapeutic drugs for the targeted

treatment of tumors [18, 132], which tend to have a leaky vasculature and can even allow penetration of larger particles relative to typical blood vessels [133].

Given that lipid vesicles are produced from biological materials, this greatly enhances their biocompatibility compared to drug carriers made from synthetic sources, and allows the implementation of physiological degradation pathways. Furthermore, there is wide variety of lipids available and each can have different properties depending if they are in the liquid ordered or disordered phase. Altering the phase of components of lipids in a bilayer membrane can introduce varying levels of order, viscosity and permeability that can all be utilized to influence how the vesicles respond to changes in the external environment. Likewise, the inclusion of biological components (i.e. enzymes, membrane proteins and pores, etc.) can further enhance their therapeutic effectiveness. Adverse effects of a drug can also be minimized by encapsulation in a vesicle or other carrier and the protection provided by these structures can also help prolong circulation times [134].

Since vesicles contain both hydrophilic and hydrophobic regions, they can acts as carriers for both hydrophobic and hydrophilic drugs. With the ability to also have functional components bound to their surface, they show great potential in terms of targeting these drugs to specific diseased cells. Vesicles can also further be instilled with cell-like functions to enhance their drug delivery and therapeutic properties. For instance, they have the potential to be programmed for the continued synthesis of drug molecules from environmental components [58], be imbued with the ability to replicate and move on their own [135], and communicate with other cells [57]. Having these capacities opens the possibility that a single treatment of drug carrying vesicles has the prospective to act on a multitude of therapeutic fronts to combat disease.

A key advantage that vesicles have over other types of drug carriers is the ease at which they can be sectioned into interconnected compartments (i.e. compartmentalized). The importance of compartmentalization can be seen in eukaryotic cells, which are naturally composed of a diverse array of discrete nano-compartments called organelles, that all play essential roles in cell homeostasis and carry out a variety of other critical cell functions. These individual compartments are highly specialized for specific tasks and are usually coupled with other organelles to form more complex units. Compartmentalization in vesicles can effectively allow a high level of control over internal chemical processes, such as multistep enzymatic reactions, or a method to keep reagents or inactive reaction components separated during storage until the proper conditions are encountered in the environment.

A common method achieve compartmentalization in vesicles has simply been to produce smaller vesicles, polymersomes, or double emulsions and then have them encapsulated into larger structures [41, 42, 136, 137]. Traditionally, this has been accomplished through the self-assembly of large vesicles that then inevitably encapsulate smaller vesicles that have already been preformed in solution [138]; but this method lacks the ability to precisely control the number of encapsulated compartments or the ratio of different compartment types in the final structure. While sacrificing throughput, these limitations can be overcome with gravity mediated phase-transfer formation of droplet interface bilayers (DIB) [139]. However, the advent of microfluidic methods has alleviated these shortcomings while also maintaining high-throughput production. An early example of microfluidic vesicle compartmentalization was demonstrated by Lorenceau et al., who produced compartmentalized polymersomes in a micro-capillary device from double emulsions templates [136]. Control of the fluid flow rates and droplet production regimes of the oil and water phases during double emulsion production allowed for multiple

aqueous drops to be encapsulated within a single oil droplet. This enables modular multipart delivery systems to be constructed, with each compartment existing in distinct biochemical environments, and optimized to perform specific tasks in a manner analogous to eukaryotic organelles. Notably, chemical cross talk between compartments has also been shown, demonstrating their use as a platform with which bench top chemistry can be performed in the interior of vesicles [3]. These developments will help facilitate the incorporation of emergent features into vesicle-based artificial cells and drug delivery vehicles.

1.4 Summary

With all the talk about the utility of GUVs for various therapeutic and industrial applications, there has yet to be wide spread adoption of them commercially. A major bottleneck is their inherent fragility and short-shelf life, where fusion and lipid hydrolysis remain to be the most common culprits of population degradation. Long-term storage of a few months to more than a year will be a requirement of any GUV kit utilized in the public domain. While freeze drying is a popular means of storage, this has not been successfully demonstrated with vesicles that are immobilized to surfaces and rehydration efficiency could potentially be a challenge [140]. In the following chapters, we report on how to create GUVs and single compartment multisomes (SCMs) from microfluidically generated double emulsion templates that are suitable for long-term storage in an aqueous environment. The GUVs and SCMs produced from these methods can be used as a basis for future artificial cell, biosensing, and drug delivery technologies and applications.

Chapter 2 – Double Emulsion Formation

2.1 Introduction

GUVs typically have a short life span in solution and begin to degrade via hydrolysis or oxidation of the lipid bilayer relatively quickly [141, 142]. Nearly all the work to improve vesicle shelf life has focused on modifying the storage conditions of the vesicles after they have been produced (such as freeze drying [142]), where the reversal of this process can be damaging to the vesicle population. To make vesicles suitable for widespread use in clinical and commercial settings, it is tantamount that they can be produced in bulk, and stored for a reasonable amount of time without degradation or alteration to their structure. In this chapter, we present a microfluidic method for the production of double emulsions that are stable for at least a year. They can be converted into GUVs or SCMs at any time by the addition of electrolytes into the solution to introduce interfacial instabilities that result in morphological changes.

2.2 Background

First described by in 1925 [143], double emulsions consist of a fluid compartment encapsulated within another immiscible fluid droplet within in a bulk fluid carrier phase (Fig. 2.1). For the purposes of this work, double emulsions will be considered distinct from Janus particles [144], multisomes [145], and multiple-compartment double emulsions [41]. Three distinct fluid phases exist to create a double emulsion, and from here on will be referred to as the external, middle, and internal phases (Fig. 2.1a). Double emulsions can exist when all three of these fluid phases are immiscible, or if only the middle phase is immiscible with the other two phases. Typically, double emulsions are either of the form water-in-oil-water (W/O/W) or oil-in-water-in-oil (O/W/O) with the W/O/W variation being vastly more common in biological and medical research and industrial applications.
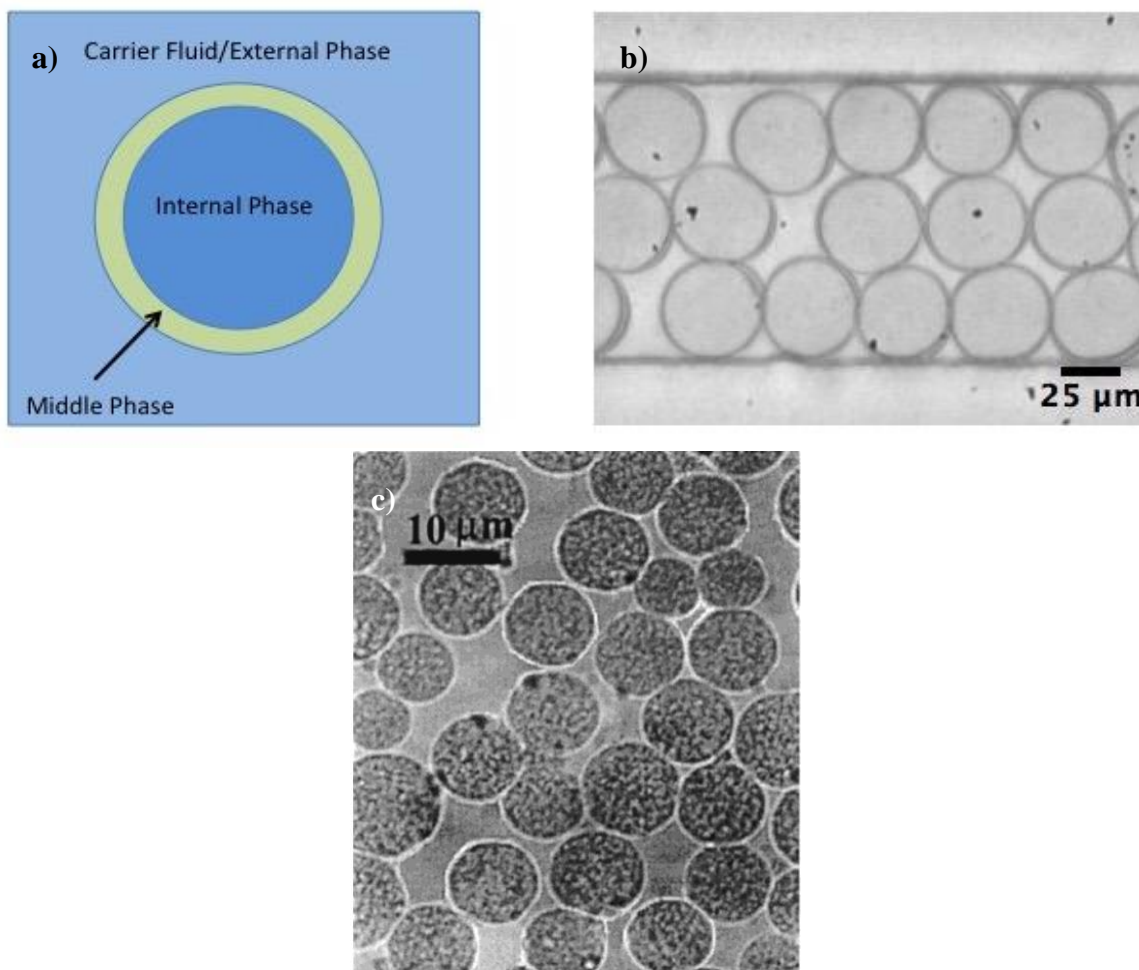
Figure 2.1. a) Illustration of a double emulsion. b) Brightfield image of W/O/W double emulsions in a microfluidic channel produced via microfluidic flow focusing. c) Image of double emulsions with multiple aqueous compartments produced by conventional two-step emulsification procedure. Reprinted (adapted) with permission from [146].

Double emulsions have attracted a lot of attention over the last two decades due to their ability to compartmentalize an aqueous phase within an aqueous solution. The pharmaceutical industry in particular has taken an interest in double emulsions as hydrophilic and hydrophobic dual drug carrier and delivery systems, as well as structures that could also be used to absorb active materials from the body for detoxification purposes. Building on the theme of detoxification, one can imagine double emulsions that could be applied to wastewater and oil spill cleanups.

Similar to what was touched upon for GUVs in section 1.3, the compartmentalized nature of double emulsions is reminiscent to the structure of a cell, whereby aqueous processes and components are isolated from an aqueous environment. Like a cell, the middle phase of a double emulsion is only partly restrictive, and the structure can be engineered such that activities in the environment can influence internal processes, paving the way for advanced structures that can be used for sensing, controlled content release or adsorption, cellular metabolic processes and protein synthesis, high throughput assays and screening, and the creation of artificial cells.

In general, the conventional method of producing double emulsions with fairly narrow size distributions involves a two-step procedure [146]. First, water is added via gentle stirring to an oil phase containing an oil soluble surfactant to create W/O single emulsions that are initially rather polydisperse, but larger in size than the intended final diameter. To achieve a greater degree of uniformity, the emulsions are placed in a Couette-type mixer [35] (Fig. 2.2) and exposed to high shear forces via rotation of a cylinder that can reach speeds up to 70 rad s^{-1}. The mean emulsion diameter (and uniformity) is dependent on the interfacial tension between the two fluid phases (i.e. surfactant type and
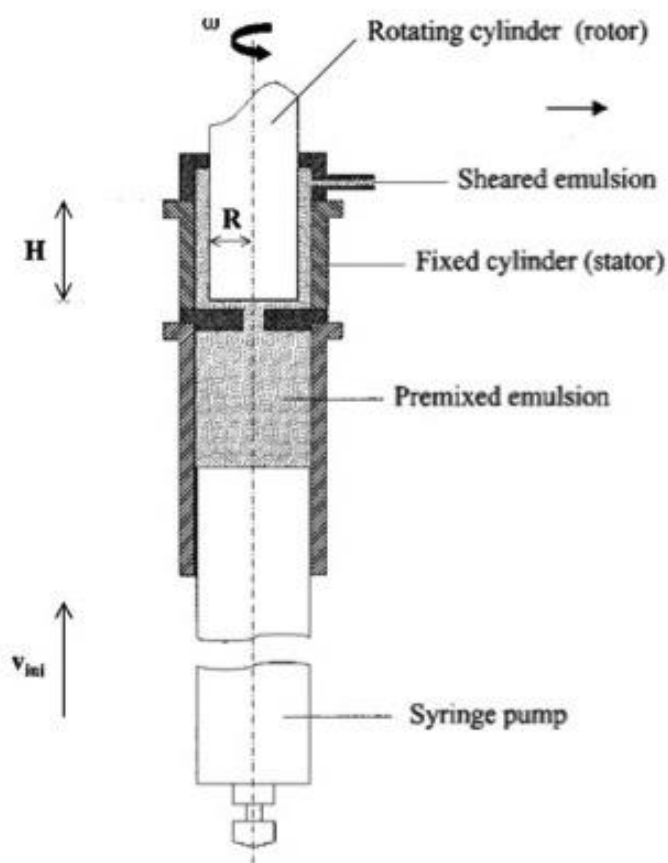
Figure 2.2. Illustration of a Couette mixer used to make quasi-monodisperse single W/O or O/W emulsions. The premixed polydisperse emulsion solution is contained within a syringe and pushed into the region with the rotating cylinder. The processed emulsion mixture is covered at the top. Reprinted (adapted) with permission from [35].

36

concentration) and the applied shear rate of the mixer. The system can achieve very high throughput (up to 1 L/hr) and the resultant mixture is very concentrated with emulsions (70 – 90% volume fraction). Though this method allows superior size homogeneity than traditional mixing or sonication, the degree of polydispersity is correlated to the intended size, and is considerably larger than what is achievable via microfluidics. After washing a resuspending the W/O emulsions to the desired concentration, there are then placed in an aqueous solution containing a low concentration of hydrophilic surfactant (typically 1% of the critical micelle concentration). With a high-pressure jet homogenizer, oil globules with encapsulated water drops can be obtained. Other than a lack of high uniformity, a major drawback to this method is that there is no control as to how many water droplets are encapsulated within each oil globule. An example of the resultant emulsion population can be seen in Fig. 2.1c.

With the advent of microfluidics, double and multiple emulsions can be produced with very fine control over size, inner droplet configuration, and the degree of emulsion multiplicity (Fig. 2.3) [147]. However, to achieve the level of throughput attainable by bulk means, various scale-up considerations have to be taken into account, which can result in additional device complexity. Coupled with the major economic hurdle of commercializing microfluidic devices, this presents a major limiting factor to the marketability of emulsions produced via microfluidic droplet production techniques. With further advancements to microfluidic technologies in terms of throughput, scale up, and mass production, it's only a matter of time before the incredible utility of microfluidically produced double and multiple emulsions are recognized outside the laboratory and put to use in medical and industrial applications.
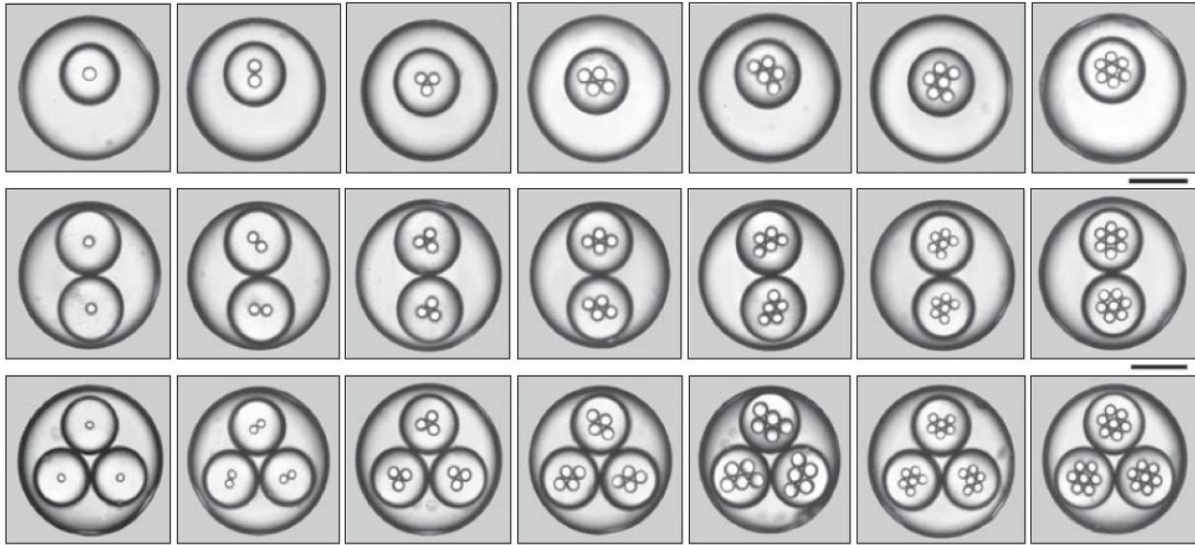
Figure 2.3. Examples of monodisperse triple emulsions produced from a microcapillary device. Both the size and number of each drop can be precisely controlled. Scale bars are 200μm. Reprinted (adapted) with permission from [147].

2.3 Previous Lab Work

2.3.1 Two-Step Generation

By utilizing a two-step droplet formation process Teh et al. [12] was able to produce monodisperse water-in-oil-water double emulsions at a rate of up to 200 droplets/sec ranging in size from 20-100μm in diameter. The double emulsions were composed of an aqueous core, surrounded by a shell made up of the phospholipid 1,2-dioleoyl-sn-glycero-3-phosphocholine (DOPC) dissolved in oleic acid. The ethanol present in the external solution would extract the oleic acid from the double emulsion over the course of approximately 15 hours, forming a lipid bilayer around the internal aqueous (Fig. 2.4). With a suitable lipid bilayer, Teh et al. demonstrated that the lipid vesicles could serve as a container for the cell-free synthesis of green fluorescent protein (GFP).

The devices used by Teh et al. to generate vesicles involved a two-step generation process. Aqueous droplets were produced first, and then encapsulated within oil-lipid droplets. The result was relatively low generation frequencies and double emulsions with relatively thick
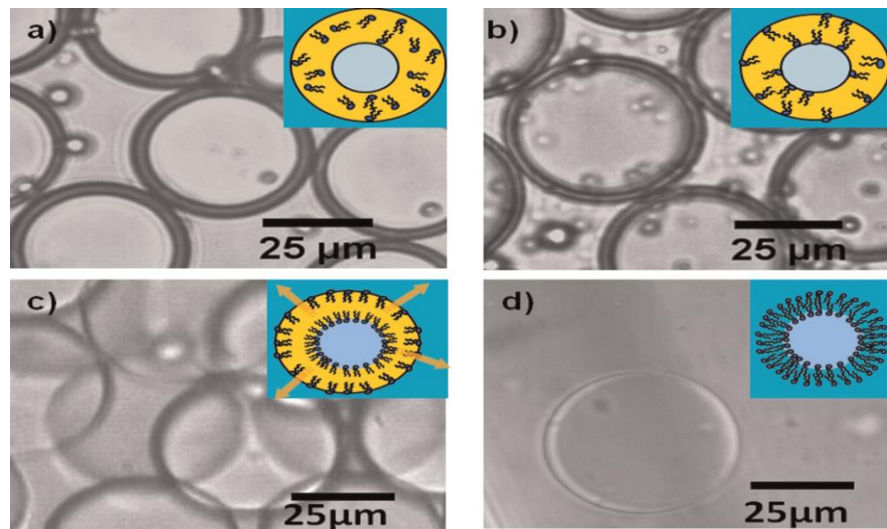
Figure 2.4. Time-lapse images of solvent extraction process at 0, 5, 10, and 15 hours (a-d) post-production. Solvent extraction is indicated by a reduction in thickness of the middle layer. As oil is removed, lipid molecules are forced to assemble into a bilayer at the water interface. Reprinted (adapted) with permission from [12].

oil shells. Considerable care also had be taken to control the spacing of the aqueous droplets in the first junction so that empty oil droplets were not produced in the second junction. To increase the generation rates beyond 1000 droplets/sec and decreasing the vesicle size below 15µm would require a substantial amount of timing and careful optimization of the external flow pressures with that system.

2.3.2 Single Step Generation

By modifying the device design to a one-step double emulsion generation setup (Fig. 2.5), Thege [148] was able to produced double emulsions at generation rates beyond 3000 droplets/sec and with diameters down to 6.3µm. However, the smaller
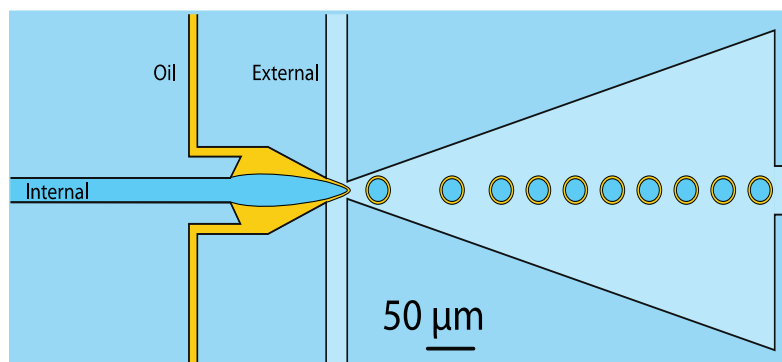
Figure 2.5. Schematic illustration of single-step double emulsion generation [148].

diameter vesicles retained larger oil shells relative to

39

larger vesicles, even after extended extraction time in a 14% ethanol solution. To compensate for this, isopropanol and ethyl acetate were added to the external phase solution with the intent to enhance extraction, limiting the possible encapsulation of biological reagents within these vesicles due to toxicity concerns. However, it is still uncertain whether there was still residual oil within the vesicles after extended extraction as the verification test performed was inconclusive.

2.4 Single Step Co-focusing Device

2.4.1 Design

The device (Fig. 2.6) is designed to produce W/O/W double emulsions at a single flow-focusing junction [18]. The external phase channel is rendered hydrophilic with a PVA surface treatment as described previously [12], while the oil and internal phase channels remain hydrophobic. The hydrophobic channel wall ensures that the oil phases sheaths the internal aqueous phase before reaching the "double emulsion generation zone". The hydrophilic external phase channel wall then allows sheathing of the oil phase by the external aqueous solution before droplet breakoff.
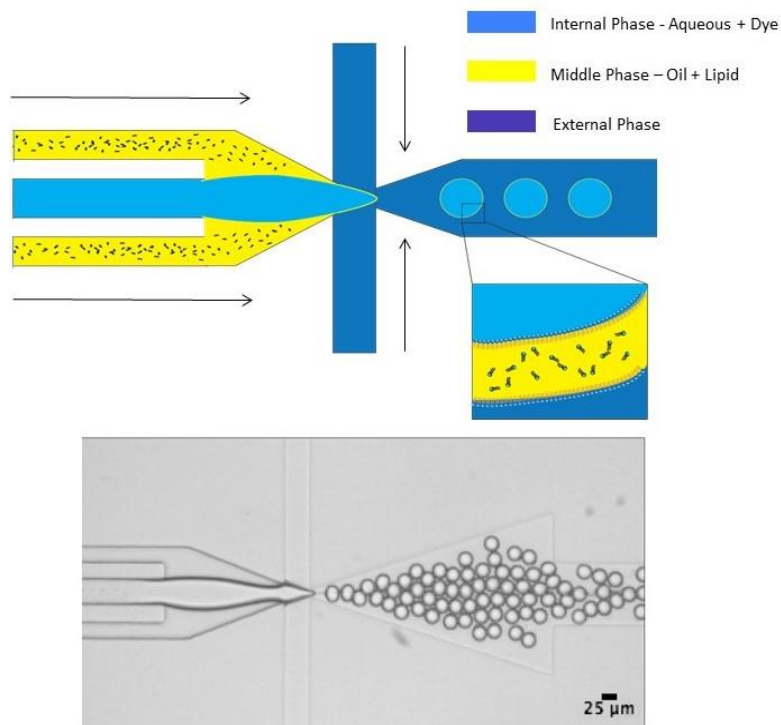
Figure 2.6. Schematic (top) and microscopic image (bottom) of single step production of double emulsions in a microfluidic device.

2.4.2 Fabrication

All devices were fabricated in poly(dimethyl) siloxane (PDMS) using standard soft lithography techniques [149] (Fig. 2.7). Briefly, channel geometries were designed in AutoCAD (Autodesk) and Adobe Illustrator (Adobe) and printed at 20,000 dpi onto a transparency mask by CAD/Art Services (Bandon, OR). In a class 10,000 cleanroom, a 3-inch silicon wafer was spin-coated with a 20μm thick layer of SU-8 (2050, MicroChem) photoresist, and patterned with the photomask through exposure to UV light. After post-exposure baking, the silicon wafer is submerged in SU-8 developer to remove the unexposed photoresist. The remaining SU-8 forms the positive
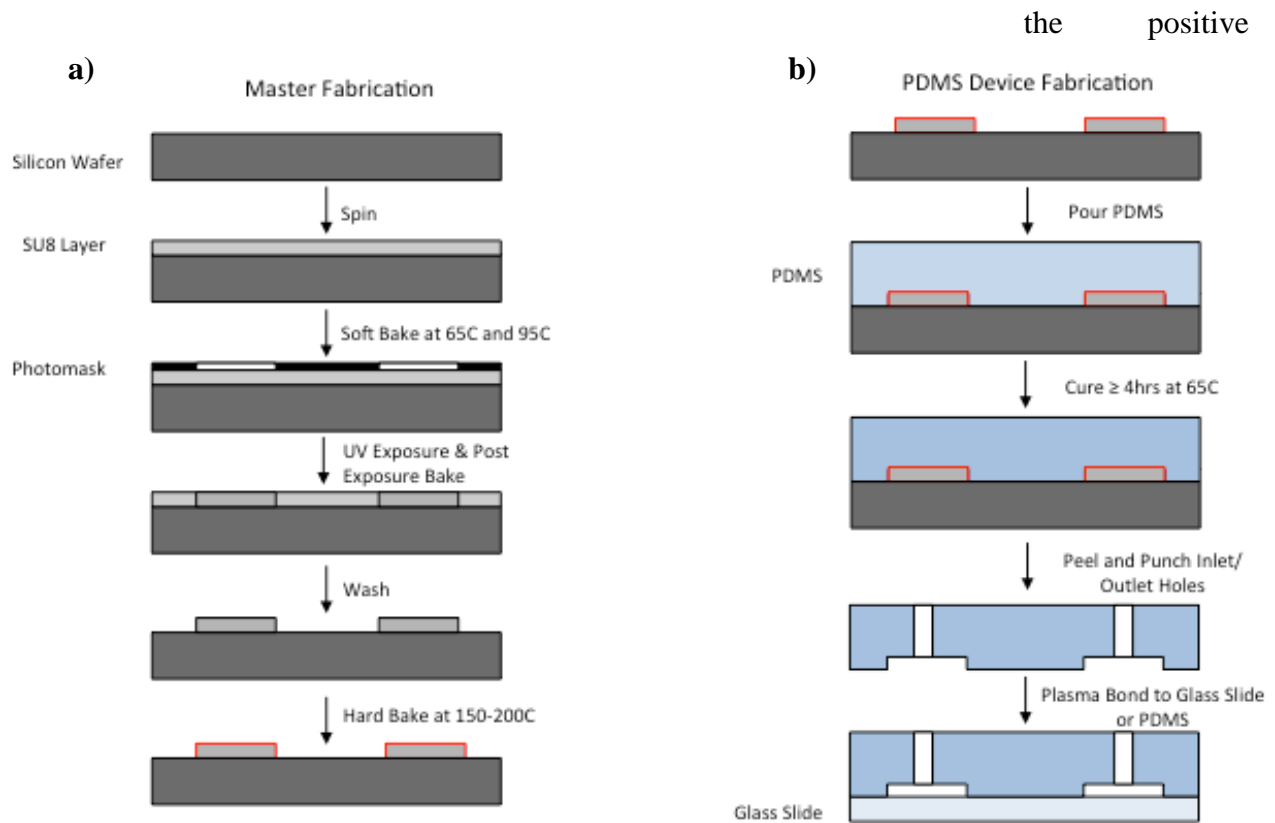
Figure 2.7. Schematic for the fabrication of a) SU-8 master mold b) PDMS device.

channel feature on the silicon wafer. Wafers were then hard-baked at 150°C for 5 minutes to harden and improve adhesion of the SU-8 to the wafer.

The wafers were spin-coated with 1% (v/v) Teflon® AF (DuPont™) in Fluorinert™ FC-43 (3M™) to reduce adhesion of PDMS to the wafer. PDMS (Sylgard 184, Dow Corning) was mixed at a ratio of 10:1 (w/w) pre-polymer base to curing agent, degassed for 30 minutes, and then poured onto the patterned silicon wafer. The polymer mixture was cured at 65°C overnight. After curing, devices were cut out and inlet/outlet tubing holes were punctured into the device using disposable biopsy punches (Integra™ Miltex®). The PDMS devices were then cleaned and treated with pure air plasma (Harrick Scientific, NY) for 90s at 300 mTorr to allow for irreversible bonding to a glass slide (Corning) (Fig. 2.8).
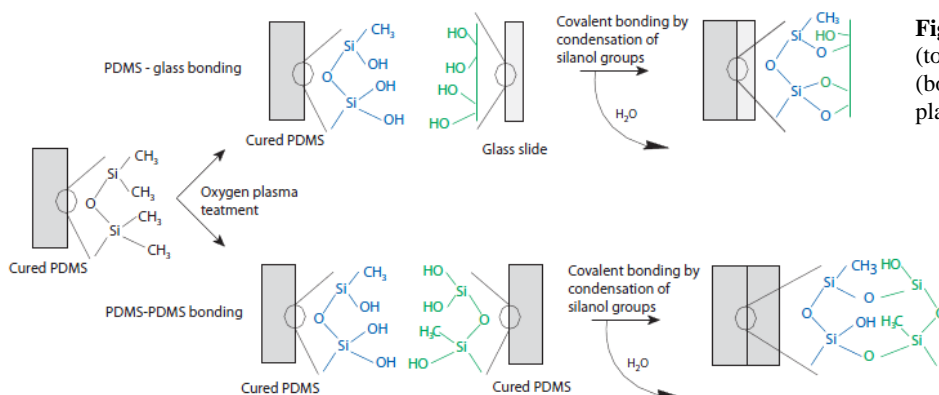
Figure 2.8. Covalent bnding of (top) PDMS-to-glass and (bottom) PDMS-to-PDMS via plasma surface activation [148].

2.4.3 Hydrophilic Surface Treatment

Due to the inherent hydrophobic nature of PDMS, a selective hydrophilic surface treatment was applied, immediately after bonding, to the external phase channel to render the channel permanently hydrophilic [12, 150]. The treatment promotes proper double emulsion production by ensuring that the external aqueous solution wets the walls of the microchannel at the droplet generation junction. Briefly, a vacuum was applied to the outlet of the device, and 5μL of a 0.4 wt. % PVA (polyvinyl alcohol, average MW 30,000-70,000, 87%-90% hydrolyzed, Sigma Aldrich) solution was passed through the external phase channels. Once the liquid cleared from the channels (within 30s), 5μL of a 0.1% PVA solution was passed through the external

phase channels to remove any PVA crystals that may have formed at the generation junction during the first application (Fig. 2.9). The vacuum was left on for 2 minutes afterwards to ensure complete removal of the PVA solution from the channels. The device was then cured overnight at 120°C.
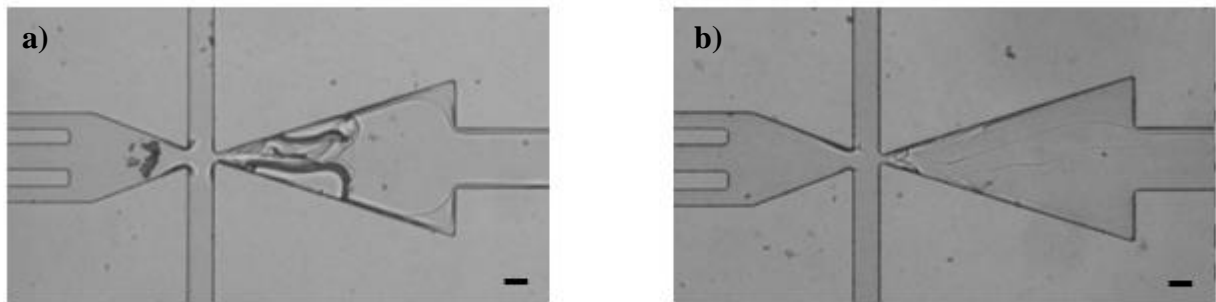
Figure 2.9. Image of droplet generation junction after PVA treatment a) without and b) with 0.1% PVA wash step.

2.4.4 Experimental Setup

Powdered lipid and cholesterol was dissolved oleic acid to a desired concentration (either 5-10 mg/ml), with the aid of a 10-minute sonication bath at 40°C. All solutions were sealed in 1.5mL plastic microtubes (Phenix Research Products) and controlled via a pump system similar to that utilized by Martz et al. [151]. Briefly, two lengths of Tygon tubing (Cole-Parmer) were inserted into holes drilled into the cap of the microtubes and glued into place to create an airtight seal. One length of tubing remained in the pressure headspace above the reagent and was connected at the other end to a SMC ITV0011-2UMS digital regulator (Automation Distribution) that was controlled via a custom LabView program. Another length of tubing was submerged in the reagent solution with the other end connected to the appropriate inlet of the microfluidic device. By manually applying a positive pressure head to the reagent vial via the SMC digital regulator, fluid was driven through the channels of the microfluidic device. A length of Tygon

tubing was also inserted in the outlet and placed in a microtube for collection of the double emulsions. A schematic of the experimental setup is shown in Fig. 2.10.
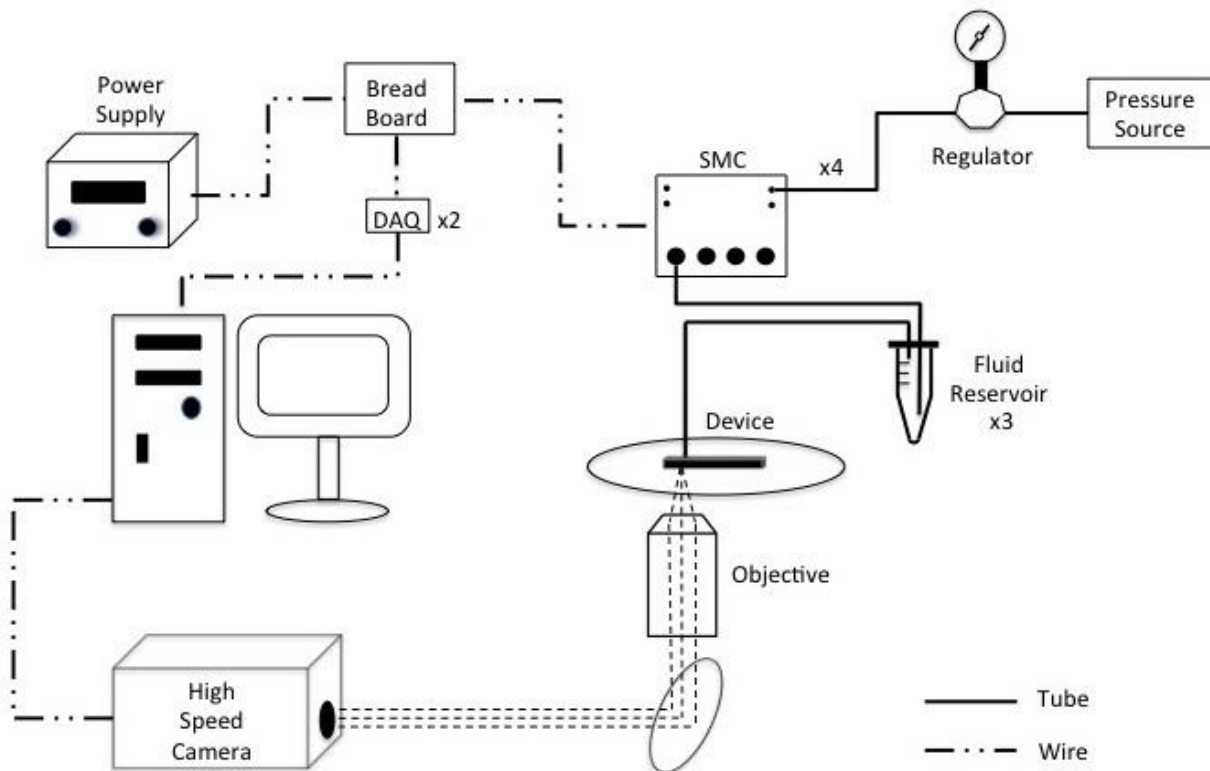
Figure 2.10. Schematic of experimental setup for double emulsion production.

2.4.5 Characterization

Production results are summarized in Fig. 2.11. As the double emulsions were being formed, the flow of the oil phase was maintained such that each water droplet was encased in a very thin (~1-3 μm thick) shell of oil. Fig. 25a plots double emulsion diameter (D), normalized to orifice width (D_0), as a function of the external phase flow-rate (Q_{Ext}) normalized to the sum of the oil and internal phase flow-rates (Q_{Disp}), simplifying the analysis to that of single emulsion production. The data is fitted to an inverse-power relation (Eq. 2.1) [16, 152], where $\sigma = Q_{Ext}/Q_{Disp.}$, and demonstrates reasonable agreement with the model ($r^2 = 0.701$). The production rate (Fig. 2B) demonstrates moderate dependence on the dimensionless parameter σ, and in

general, the production rate tends to increase as σ increases. Our double emulsions can be

produced with diameters ranging from 9-30 μm in a device with 20 μm tall channel features.

Double emulsions can still be produced with diameters ≤ 9 μm, with the sacrifice of some

monodispersity, since below 9μm, we could only achieve droplet formation in the jetting regime.

$$\frac{D}{D_0} = AS^C$$

Equation 2.1. Inverse power relation governing droplet diameter dependence on ratio of external and internal flowrates.

a)

b)

c)
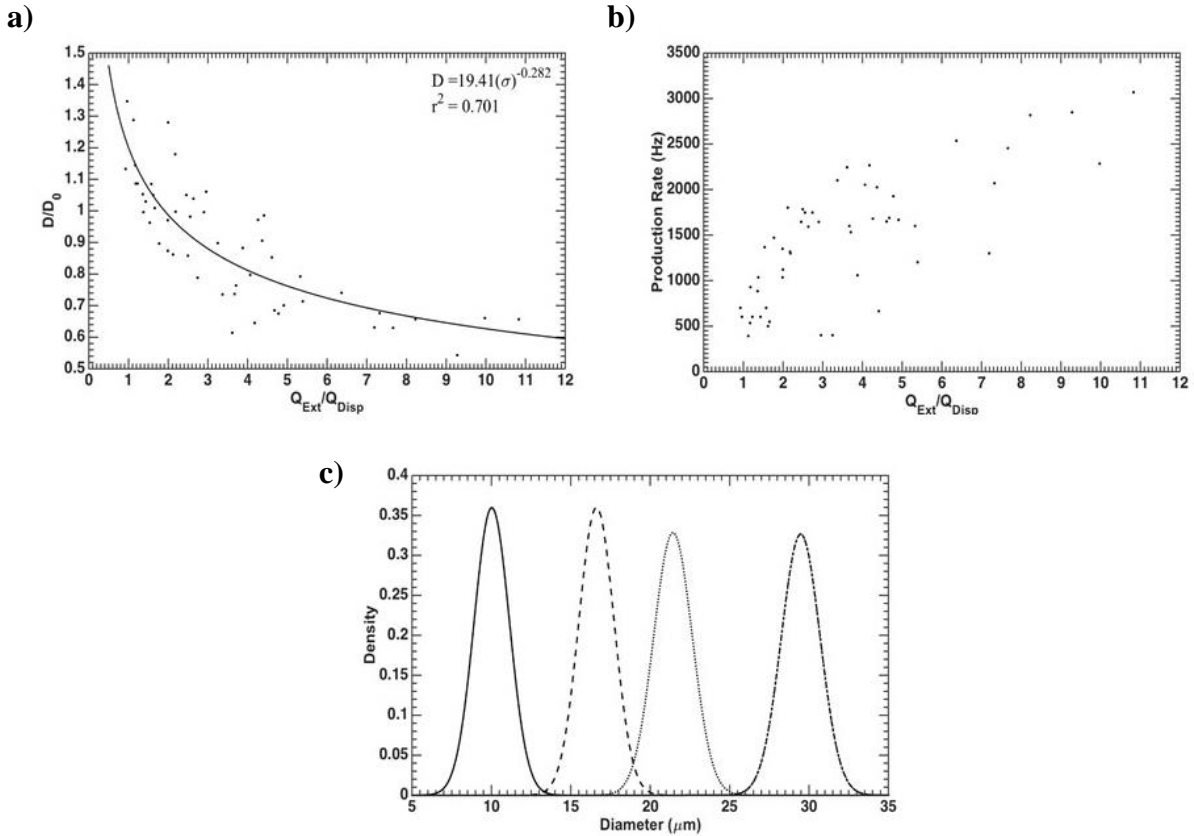
Figure 2.11 Production characteristics based on flow parameters. A) Droplet diameter normalized to orifice length (D/D₀) as a function of external phase flow (Q_Ext) normalized to the sum of the dispersed phase flow rates (Q_Disp). B) Droplet generation rate as a function of normalized flow rate. C) Population distribution of double emulsions at various diameters. From left-to-right: (Mean ± STD) 10.1±1.1 μm, 16.6±1.1 μm, 21.4±1.2 μm 28.5±1.5 μm.

2.5 Summary

Even though double emulsions can be reliably produced with diameters just below 10μm, future work will need to focus on producing monodisperse populations of double emulsions down to 5μm in diameter for in-vivo applications (immunotherapy, drug delivery, etc.) [82, 153], though larger structures may still be suitable given sufficient deformability. Given that double emulsion diameter demonstrates dependence on the channel geometry when droplet production occurs in the geometry controlled regime, a smaller droplet generation junction could be achieved via a chrome mask that can be printed with resolutions down to 3μm, though the relatively high viscosity of oleic acid may present an issue to droplet formation in a smaller orifice, and the PVA treatment protocol may also need to be altered as it will likely be fairly easy for crystal formation to occur in a smaller orifice. An introduction of an osmotic pressure difference post-production (via encapsulation of a lower concentration of solute relative to the final working solution) can also be used to promote double emulsions shrinkage as well.

Chapter 3 – Double Emulsion Stability and Morphological Changes

3.1 Interfacial Influence, Spreading Coefficient, and Dewetting

Through manipulation of the interfacial tensions between the fluid phases, the equilibrium morphology of the double emulsion can be controlled. The free energy of each interface can be summarized by a parameter known as the spreading coefficient (Eq. 3.1), which describes the tendency of a fluid phase to spontaneously spread on a solid surface (or fluid interface) [154]. Each fluid phase in the double emulsion has its own spreading coefficient that is calculated from Eq. 3.1, where γ_{ij} represents the interfacial tensions between fluids i and j. For a double emulsion with miscible inner and outer phases, three configurations are possible:

$$S_i = \gamma_{jk} - \gamma_{ik} - \gamma_{ij} \, , \{i, j, k\} = \{O, I, M\}$$

Equation 3.1. Spreading Coefficient
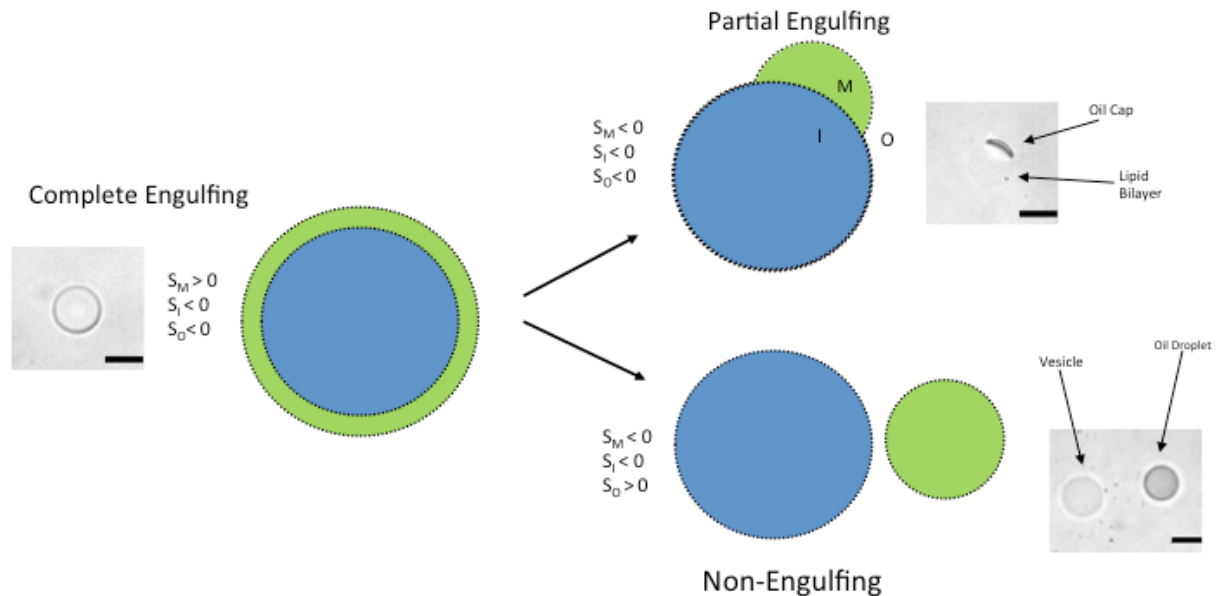
Figure 3.1. Illustration and phase contrast images of possible double emulsion equilibrium morphologies based on the values of the spreading coefficient for each fluid phase. Scale bar is 20μm.

complete engulfing (double emulsion), partial engulfing (SCM), and non-engulfing (GUV + Oil Drop), with the conditions for each morphology described by the spreading coefficient conditions given in Fig. 3.1.

Previous analysis of the influence of the spreading coefficient on droplet morphology typically utilizes double emulsions with three immiscible fluid phases (three-phase double emulsions). In a double emulsion system that has miscible inner and outer aqueous phases (two-phase double emulsions), an interface can only form between those two phases if amphiphilic molecules (lipids, polymers, etc.) are present at the inner and outer oil-water interfaces to form a membrane that can prevent mixing. Thus, for the system described herein, the value of γ_{IO} represents the tension in the resulting lipid bilayer [145]. According to Petelska et al. [155], the value of γ_{IO} for lipid bilayers can lie anywhere from 0.2-7 mN m^{-1}, contingent on the specific membrane composition, pH, and temperature. Given that the bilayer of the described system is composed of a 1:1 PC-lipid:cholesterol mixture, and potential residual oleic acid, an intermediate value of 3.5 mN m^{-1} was chosen for γ_{IO} in the following analysis, given that both cholesterol and fatty acids act to increase the interfacial tension relative to pure lipid bilayers. However, Petelska et al. only investigated the effect of cholesterol and fatty acids separately, so their effect on interfacial tension together in the same lipid bilayer was not explored. Interfacial tensions between fluid phases were measured via the pendant drop technique using the Attension Theta Lite Tensiometer (Biolin Scientific) and accompanied software.

3.2 Complete Engulfing – Double Emulsions

To ensure double emulsion stability, the spreading coefficient of the outer and inner phases (S_O and S_I) must be negative, while the spreading coefficient for the middle (oil) phase (S_M) must be positive [156]. When producing double emulsions for solvent extraction, Teh et al.

[12] used an internal phase that consisted of 5% Pluronic-F68, a biocompatible, non-ionic surfactant that is safe for cell cultures and has been shown to enhance cell robustness and survival [157]. Similarly, the external phase consisted of 6% Pluronic-F68, along with glycerol to increase viscosity and 14% ethanol for eventual solvent extraction to produce GUVs. The oil phase consisted of 5 mg ml^{-1} of DOPC in oleic acid. Collected double emulsions were placed in excess external phase solution and left overnight for extraction. No mention of any dewetting phenomenon was given in the manuscript [12] or in personal correspondence. Starting with the same fluid formulations (minus ethanol), double emulsion production was analyzed using a new single-step design (Chapter 2), with an interest to observe survival in cell culture media and PBS.

When placed in 1X PBS, the double emulsions did not survive long, with the majority popping in less than 5 minutes (Figure a). Addition of cholesterol to the oil phase caused the double emulsions to adopt the SCM morphology when transferred to 1x PBS (Figure b). A similar morphology was previous reported by Hayward et al. [158] during transformation of their double emulsions into polymersomes via solvent extraction. They suggested the driving force for transition into SCMs was a deletion effect, whereby excess copolymer in the middle organic phase repelled smaller solvent molecules, attracting the inner and outer water-oil interfaces to form a membrane and create an SCM. Given that such a membrane does not form in three-phase double emulsions, depletion effects must play an important role in the formation of the bilayer of
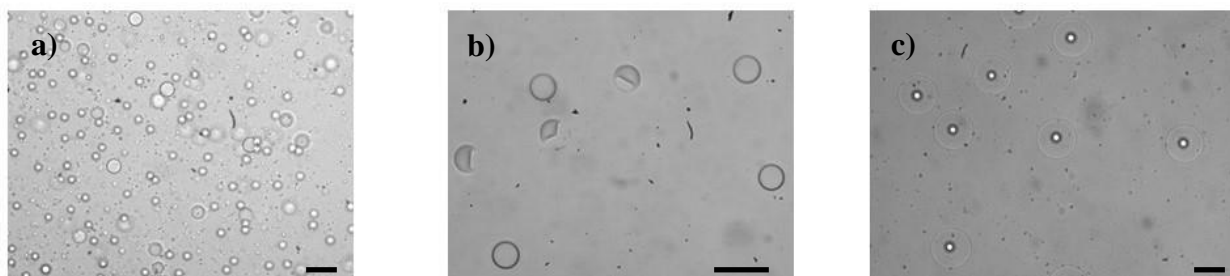
Figure 3.2. Phase contrast images demonstrating effect of lipid and cholesterol concentration on SCM formation in 1X PBS. A) 5 mg ml^{-1} DOPC in middle phase. B) 5 mg ml^{-1} DOPC + 2.5 mg ml^{-1} cholesterol in middle phase. C) 10 mg ml^{-1} DOPC + 5 mg ml^{-1} cholesterol in middle phase.

SCMs and GUVs from two-phase double emulsion templates. Upon increasing the concentration of DOPC to 10 mg ml^{-1} and maintaining a 1:1 molar ratio of cholesterol, SCMs like those seen in Figure c could be produced reliably and consistently upon transfer into 1X PBS. Since oleic acid is non-volatile and insoluble in water, the oil cap will remain permanently attached to these structures.

3.2.1 Double Emulsion Storage

The double emulsions themselves are very robust, and can survive at least 8 months (Figure a) when stored in 0.25% - 1% pluronic F68 with a 0.25 Osm NaCl or sucrose internal phase, for osmotic pressure balance. The presence of at least 0.25% of pluronic F68 in the storage solution is necessary for long-term survival to prevent fusion and droplet breakup, and to maintain low interfacial energy at the inner and outer water-oil interfaces. There was a slight increase in the diameter of the double emulsions over the course of eight months, most likely due to interfacial effects given the slight decrease in population size and possible lipid hydrolysis, but polydispersity remained unchanged (Figure b-c).

Given that the spreading coefficient plays a role in determining the final morphology of the double emulsions, it was essential to determine if the calculated spreading coefficients for the double emulsions in storage solution supported a complete engulfing morphology. As can be seen from Table 3.1, the storage solution promotes complete engulfing as the most energetically favorable morphology, in agreement with the results presented in Fig. 3.3.

Internal Phase: 0.25Osm Sucrose + 5% F68 Middle Phase: 10 mg ml^{-1} DOPC + 5 mg ml^{-1} Cholesterol in Oleic Acid	S_O	S_M	S_I
Storage Solution	-5.18	1.74	-1.82
0.25 Osm Sucrose	-6.58	0.34	-0.42
0.25 Osm Sucrose + 5% F68	-3.50	3.42	-3.50

Table 3.1. Spreading coefficients for double emulsions in external solution where double emulsion morphology is maintained.
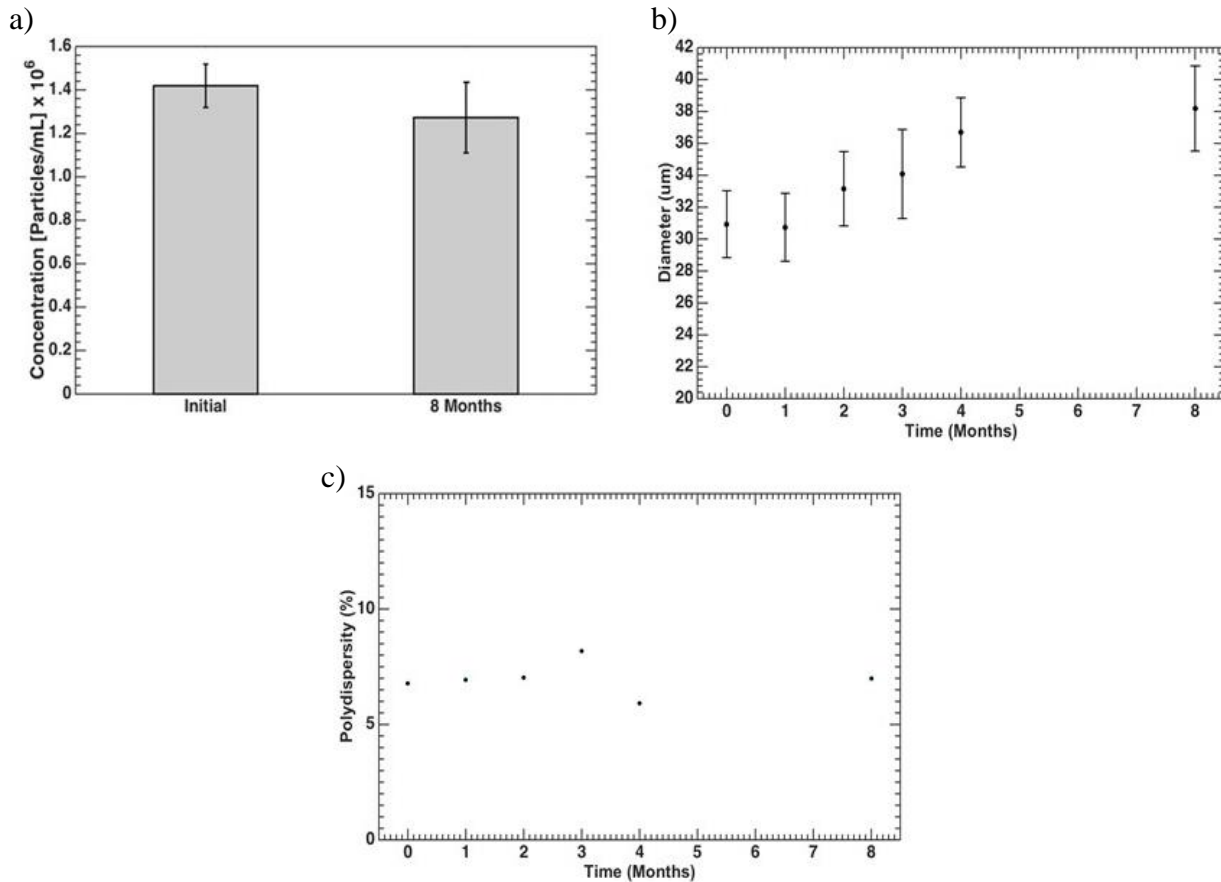
Figure 3.3. Measure of double emulsion a) survival, b) diameter, and c) polydispersity over the course of eight months.

3.3 Partial Engulfing – Single Compartment Multisomes (SCMs)

Multisomes are structures that consist of one or more aqueous droplets encapsulated within a drop of oil in the water. The encapsulated aqueous drops are connected via interface bilayers with at least one bilayer interface exposed to the external aqueous solution [145]. In contrast to traditional droplet interface bilayer (DIB) networks that are constrained to a bulk oil phase, multisomes can be placed in physiological, aqueous environments where they can be influenced by changes in pH, temperature, solutes, or cells to elicit a wide variety of functions similar to GUVs, or that can build upon applications previously demonstrated with DIBs, such as membrane protein and drug release studies [159], and functional networks that include battery

51

and light sensors [160]. Multisomes inherently combine the networking and compartmentalization capabilities of DIBs with the biosensing, drug delivery, and artificial cell functionalities of GUVs to create a particle that can be imbued with a wide range of functions suitable for applications in biosensing, therapeutics, and synthetic biology; but, their value and potential has been overlooked given the residual oil that is still present in their structure. Consequently, multisomes have not been widely studied and have only been produced via time-consuming, manual bulk methods [145], or microfluidically, using di-block copolymers rather than lipids [161].

The conversion of the double emulsion templates into SCMs or GUVs when placed in an electrolyte solution can be explained by an increase of the interfacial tension at the outer water-oil interface. Higher interfacial tensions tend to follow increased salt concentrations in the water phase at water-oil interfaces, a phenomenon known as the specific ion, or Hofmeister, effect [162-164]. The increased interfacial tension forces the oil phase to adopt a more energetically favorable morphology by reducing the surface area of the most energetically costly interface, whereby it accumulates at one region of the double emulsion to form an SCM (Figure). The high
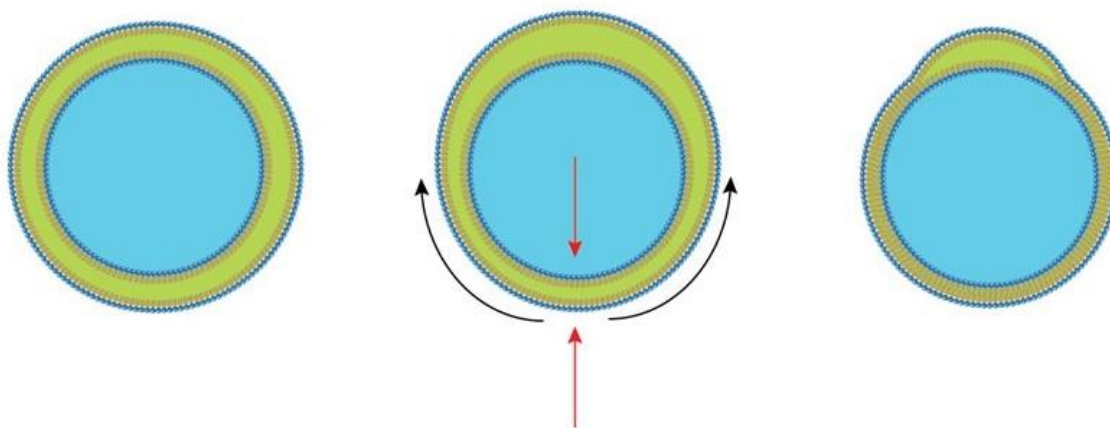
Figure 3.4. Illustration of the dewetting process to form SCMs. Process is from left-to-right. Upon exposure to increased interfacial tension from electrolytes, the oil in the double emulsion begins to accumulate to one side, causing a local thinning of the oil shell and an increase in the depletion force in that area. The lipid tails can then force out the excess oil to one side and form a bilayer.

local concentration of lipids in the thinning portion of the middle layer promotes bilayer formation via a depletion effect [158]. SCMs formed in different electrolyte solutions can be seen in Fig. 3.5, and the spreading coefficients are summarized in Table 3.2.
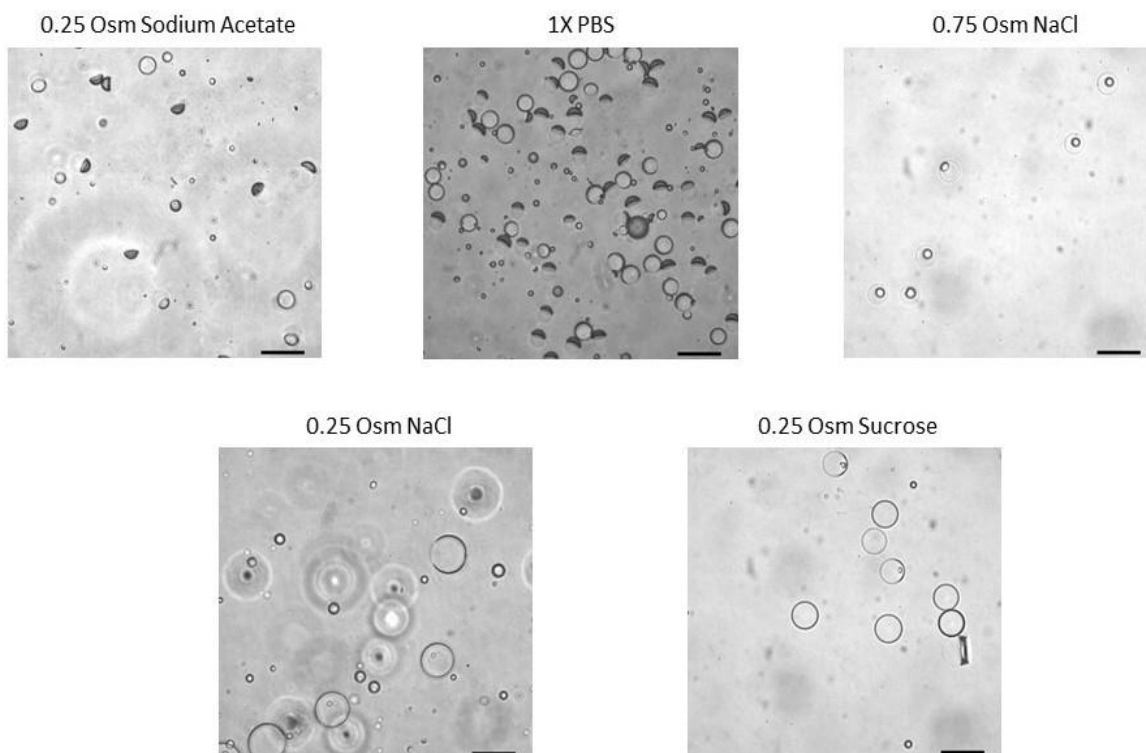
Figure 3.5. Morphological equilibrium of double emulsions when exposed to different solutions. Composition of internal and middle phase given in Table 3.2. Scale bar is 50μm.

Internal Phase: 0.25Osm Sucrose + 5% F68 Middle Phase: 10 mg ml^{-1} DOPC + 5 mg ml^{-1} Cholesterol in Oleic Acid	S_O	S_M	S_I
1x PBS	-7.86	-2.15	0.86
0.25 Osm Sodium Acetate	-7.69	-0.77	0.69
0.25 Osm NaCl	-5.65	1.28	-1.35

Table 3.1. Spreading coefficients for double emulsions in external solution where SCM morphology is promoted.

For the SCM morphology to be energetically favored, all three spreading coefficients should be negative according to the model in Fig. 3.1, yet this is not the case for the top two entries in Table 3.2. There are a few possible explanations for this discrepancy: 1) The value of γ_{IO} was chosen based what the authors believed would be a reasonable value given the possible

range of from 0.2-7 mN m^{-1} and the membrane components used. Furthermore, the value was assumed to be static, where in actuality it likely changes depending on pH and, potentially, solutes present in each phase. Presence of surfactant, pulling from the oil cap, and SCM diameter may also effect the true value. To increase the accuracy of the analysis, the membrane tension would have to be measured directly for each condition. 2) The depletion effect likely has an influence as the oil shell of the double emulsion thins, and could be enough to cause SCM formation in structures that are close to the transformation point based on the spreading coefficient alone. Reducing the amount of F68 surfactant in the internal phase brought values in line with what was seen experimentally (Table 3.3).

Internal Phase: 1x PBS + 1% F68 Middle Phase: 10 mg ml^{-1} DOPC + 5 mg ml^{-1} Cholesterol in Oleic Acid	S_O	S_M	S_I
Storage Solution	-2.50	-0.94	-4.50
1x PBS	-5.18	-3.62	-1.82
0.6 Osm KCl	-6.43	-4.77	-0.57

Table 3.2. Spreading coefficients for double emulsions in external solution where SCM morphology is promoted.

To test how the value of interfacial tension influenced the kinetics of dewetting and SCM formation, we placed the double emulsions in isotonic solutions of NaCl, NaI, NaC$_2$H$_3$O$_2$, and 1x PBS, each with F68 surfactant diluted to 0.10% (vol.), and counted the fraction of double emulsions that became SCMs within 10 minutes (Figure a). PBS was used in comparison to the other electrolytes because it is a very common biological buffer, though note that there is slight osmotic mismatch with PBS. Surprisingly, there is a correlation between ion placement in the Hofmeister series, and dewetting time. Within 10 minutes, all of the double emulsions in the solution of sodium acetate transitioned into SCMs, compared to less than 10% in the NaCl and NaI solutions. In PBS, approximately 50% of the double emulsions have transitioned into SCMs. We suspect that more SCMs were formed in PBS than in NaCl for two reasons: 1) although

approximately 90% of the anions in PBS are sodium and chloride ions, there is a small amount of hydrogen phosphate and potassium ions, which may be effecting the interfacial tension between 1X PBS and the middle phase due to direct interaction at the interface, or indirectly via pH. 2) The osmolarity of 1X PBS is slight greater than the other solutions, meaning a greater increase in interfacial tension relative to if it were isotonic with the double emulsion internal phase. The SCMs are also fairly stable, surviving long enough to allow experiments to be conducted. More than 90% of the SCMs survived after 24hrs in PBS, and 70% of the population was still present after 48 hours (Figure c), in agreement with survival rates reported by Villar et al. [145]. The fluorescent molecule FITC-Dextran was also included in the internal phase of the SCMs to

a)

b)

c)

$$SO_4^{2-} > HPO_4^{2-} > CH_3COO^- > F^- \;\vert\; Cl^- > Br^- > NO_3^- > I^- > ClO_4^- > SCN^-$$

Kosmotropes | Chaotropes
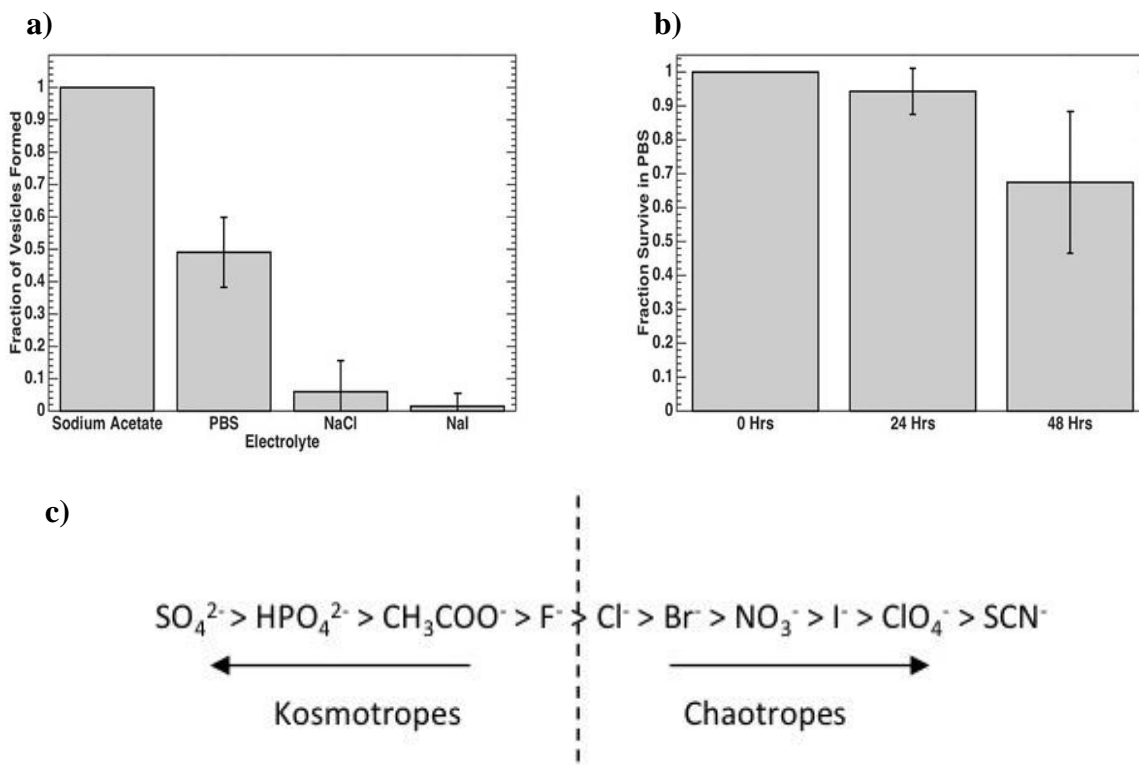
Figure 3.6. Dewetting Characteristics and SCM Survival. a) Fraction of SCMs seen after 10 minutes in various electrolytic solutions (N = 4). No dewetting was observed when double emulsion solution was diluted with deionized water. b) Survival characteristic of SCMs in PBS after dewetting (N = 9). c) Hofmeister series for anions.

demonstrate they can hold encapsulated material (Figure).

To confirm the presence of a unilamellar lipid bilayer in the SMC, as series of test were conducted on the SCMs: osmotic pressure shock to measure membrane permeability to water, insertion of a membrane protein, and fluorescent quenching assay using the fluorescent tagged lipid 2-dioleoyl-sn-glycero-3-phosphoethanolamine-N-(7-nitro-2-1,3-benzoxadiazol-4-yl) (NBD-PE).

3.3.1 Verification of Lipid Bilayer

Osmotic Shock Test

The lipid bilayer is a semipermeable membrane that allows passage of water and other small molecules, but restricts the passage of ions and large molecules. When placed in a hypertonic solution, the SCMs will shrink as water exits the membrane. By measuring the radius of the SCM over time, the permeability of the membrane can be calculated according to equation 8a [136, 165] if the SCM is modeled as a GUV, where r is the radius, V_w is the molar volume of water, Ω is the membrane permeability, and $\Delta c(t)$ is the difference in solute concentration between the interior of the SCM and the external solution. Since the volume of the external solution is much larger
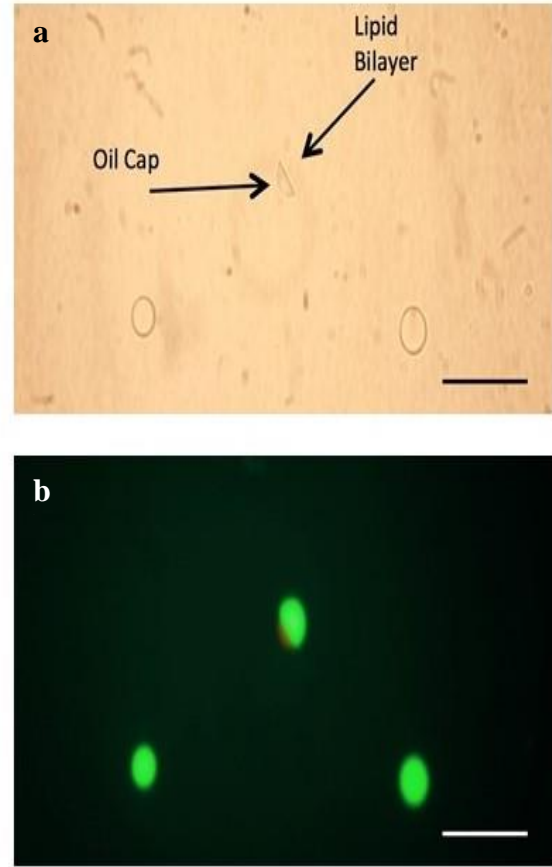
Figure 3.7 a) Bright field and b) Fluorescent image of SCM with FITC-Dextran in the internal phase. Scale bar is 50µm

a)
$$\frac{dr}{dt} = -V_w \Omega \Delta c(t)$$

b)
$$\frac{dr}{dt} = -V_w \Omega c_{ext}\left(1 - \left(\frac{r_{eq}}{r(t)}\right)^3\right)$$

Equation 3.2. Equation to calculate permeability of SCM membrane. Rate of radius change is measured when SCM is exposed to a known concentration gradient.

than the combined volume of vesicles, it's reasonable to assume that the external concentration of solute remains relatively constant. With this assumption, equation 3.2a can be rewritten as equation 3.2b, where c_{ext} is the solute concentration in the external solution, and r_{eq} is the radius of the SCM at equilibrium ($t = \infty$). By measuring the SCM radius over time, the membrane permeability to water was calculated to be 53.6 ± 3.4 μm s^{-1} (Fig. 3.8) well within the range of 25-150 μm s^{-1} reported in the literature for DOPC bilayers [165-167]. Since the surface area covered by the oil cap was not taken into account, this value could be underestimating the true permeability. A similar test conducted on double emulsions returned permeability values between 2-14 μm s^{-1} (data not shown), confirming that any passage of water through the oil cap due to reverse micelle formation is most likely minimal compared to the rate of passage through the membrane and shouldn't have a large effect on the measured membrane permeability value.
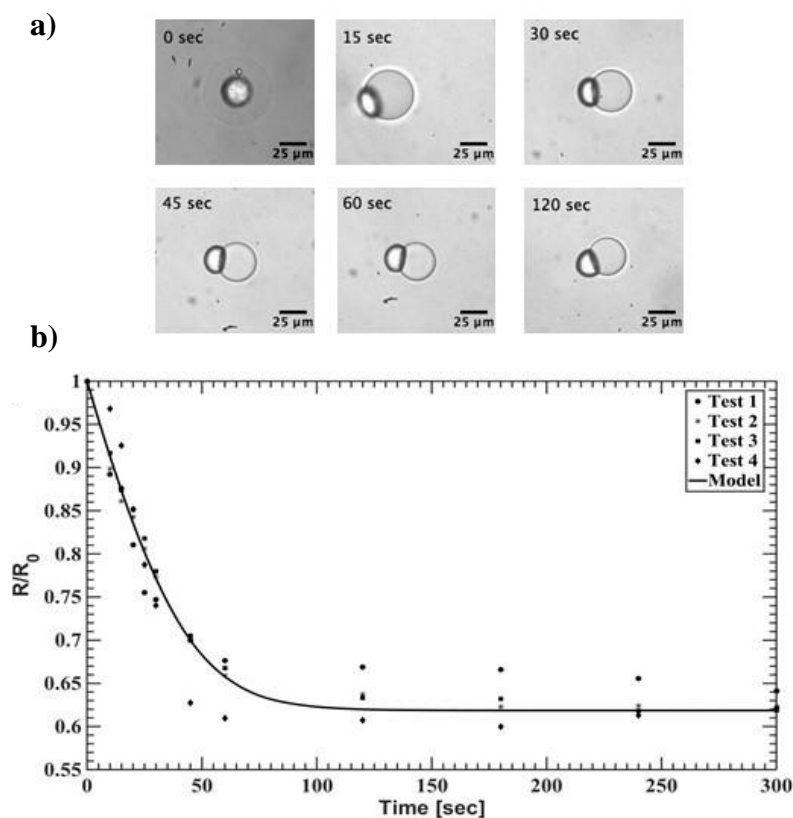
Figure 3.8 a) Bright field microscopic images of SCM shrinkage when exposed to osmotic pressure shock. b) SCM radius (normalized to the initial radius, R_0) plotted against time when subjected to hypertonic conditions ($\Delta c = 100$ mOsm).

Membrane Protein Incorporation

To further confirm the presence of a bilayer, the pore forming peptide melittin was tested for incorporation into the SCM bilayer. Melittin, the major toxin found in bee venom, is an
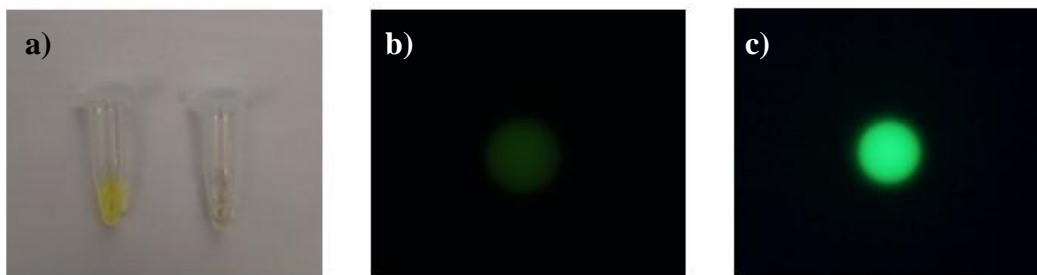
Figure 3.9 a) Comparison of FITC-Dextran solution color in neutral (left) and slighty acid (right, pH 4) solutions. b) Fluorescent image of double emulsion with encapsulated FITC-Dextran in NaCl solution (acidic) and c) in PBS (neutral).

antimicrobial peptide that forms non-specific pores in lipid bilayers [168]. To verify pore formation, we encapsulated 100μM of the pH sensitive dye fluorescein within the double emulsions during production. A 7:3 molar ratio of DOPC:DOPG (1,2-dioleoyl-sn-glycero-3-phospho-(1'-rac-glycerol), Avanti Polar Lipids) was used to improve melittin incorporation into the membrane [168]. Fluorescein shows weak fluorescence under acidic conditions, but will fluoresce brightly at neutral pH (Fig. 3.9). Since no buffer solution was incorporated into the interior SCMs for this test, they were slightly acidic and fluorescein only demonstrated weak fluorescence, as ions cannot penetrate the lipid bilayer.
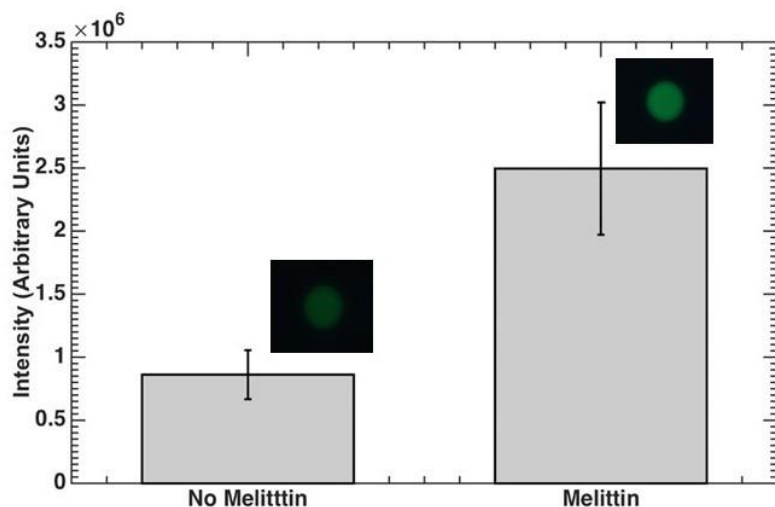
Figure 15. An increase in fluorescence intensity was observed for vesicles incubated with melittin for 30 minutes ($p < 0.01$, N = 16).

Following dewetting in PBS, the SCM solution was mixed with a solution of melittin in water to reach an effective melittin concentration of 4.5μM. The mixture was allowed to incubate

in PBS for 30 minutes before imaging. The group of SCMs incubated with melittin demonstrated a dramatic increase in fluorescence (Fig. 3.10). The pores created by melittin are large enough to allow ions to pass through [168, 169], such that the ions in PBS can enter the SCMs and raise the internal pH.

Unilamellarity Verification

To verify bilayer unilamellarity, a fluorescence-quenching assay was utilized to measure the fraction of lipids in the outer leaflet [170-172]. Double emulsions were prepared with a 20:1 molar ratio of DOPC:NBD-PE (Avanti Polar Lipids). Following dewetting, NBD-PE was verified to be present in the resulting membrane (Fig. 3.11b). 400μl of this solution containing the SCMs was placed in a cuvette, and the emission spectrum (480nm – 600nm) was measured using a SPEX Fluorolog 1680 0.22m Dual Spectrometer, with the excitation wavelength set to 465nm.

The fluorescent contribution of the outer leaflet was measured by inducing quenching of the NBD molecules with the addition of 4μl of 1M sodium dithionite in Tris buffer (pH 10, freshly prepared). Since sodium dithionite is membrane impermeable, it can only quench the outer leaflet and cannot penetrate further in a timely fashion. The decrease in fluorescence intensity during this step is labeled I_1 in Fig. 3.11c. The fluorescent contribution of the inner lipid layer(s) was measured with the addition of 5μl of 20% vol. Triton-X in water. Triton-X is a detergent that destroys the vesicles and exposes the inner leaflet lipids to the quencher in solution. For a unilamellar vesicle where NBD-PE is evenly distributed between the inner and outer leaflets, the contribution of the outer leaflet should be 50% of the fluorescence intensity of the GUV. The difference between the initial and final fluorescence intensity values is labeled as I_2 in Fig. 3.11c, and represents the fluorescent contribution of all the NBD-PE in the sample. The

index of unilamellarity (I_1/I_2) was used to determine the unilamellarity of the SCMs, and is equal to 0.5 if the bilayer is unilamellar [170-173]. For our SCMs, $I_1/I_2 = 0.46 \pm 0.06$, which is consistent with a unilamellar membrane with an equal distribution of NBD-PE in the inner and outer leaflets.
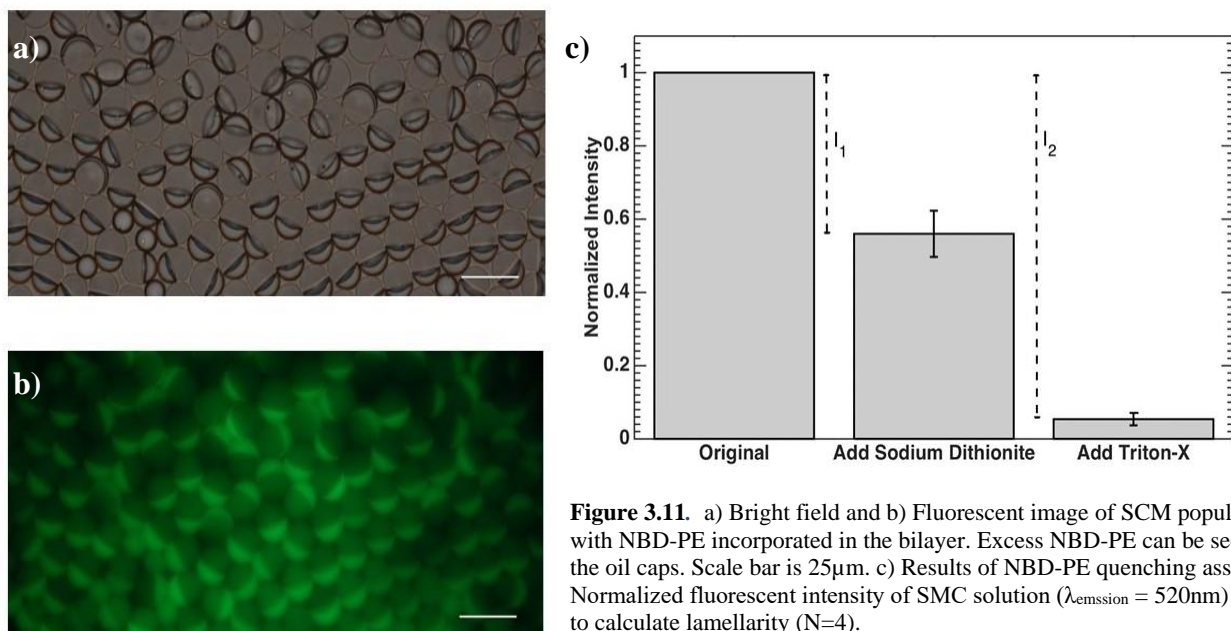
Figure 3.11. a) Bright field and b) Fluorescent image of SCM population with NBD-PE incorporated in the bilayer. Excess NBD-PE can be seen in the oil caps. Scale bar is 25µm. c) Results of NBD-PE quenching assay. Normalized fluorescent intensity of SMC solution ($\lambda_{emssion} = 520$nm) used to calculate lamellarity (N=4).

One interesting point of note is that it is well known that the emission spectrum of NBD-PE is environmentally sensitive [174-176]. When the emission spectrum was measured for SCMs, three peaks were present at 485nm, 500nm, and 520nm (Fig. 3.12a), which is likely due to the multitude of environments in which NBD-PE could reside within the sample. Since the sample inevitably contained oil drops from SCM/double emulsion popping, production artifacts, and the oil caps present after dewetting, there are three possible environments where the NBD-PE molecule can be found: inside an oil droplet, at the interface of an oil droplet, and within any lipid membranes present. With the addition of Triton-X, two peaks remained at 485nm and 500nm in the emission spectrum of the resulting solution (Fig. 3.12a). Since all the SCMs were destroyed at this point (confirmed via visual inspection), only oil droplets remained in solution.

The addition of excess Triton-X to the solution could not reduce the intensity of these peaks any further (data not shown). The two peaks at 485nm and 500nm were also clearly visible when measuring the emission spectrum for a solution of oil droplets in PBS made from the NBD-PE stock used to create the double emulsions templates (Fig. 3.12b), confirming that these two peaks are the result of NBD-PE in the oil droplets and at the oil-water interface, suggesting that the peak seen at 520nm was only due to the NBD-PE lipids in the SCM bilayer. Consequently, the fluorescence emission from the oil caps had no effect on our analysis of unilamellarity, as only the peak at 520nm was used for the intensity measurements.
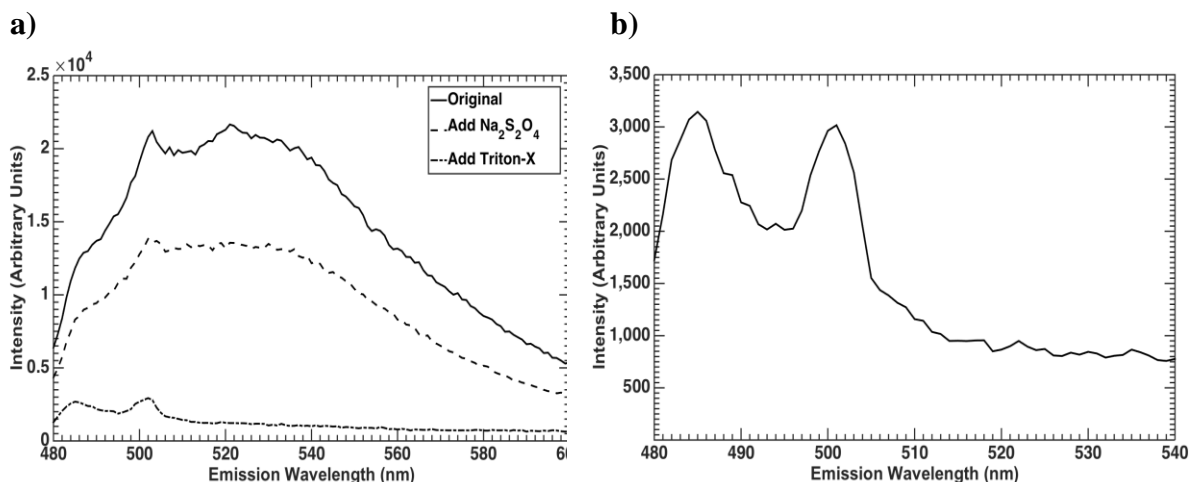
Figure 3.12. a) Emission spectrum of NBD-PE GUVs (solid), after quenching with sodium dithionite (dotted), and after the addition of Triton-X (dashed). b) Emission spectrum of a solution of single emulsion oil droplets in PBS that contain dissolved NBD-PE.

3.4 Non-Engulfing – GUVs

According to the spreading coefficient model, oil cap separation from the SCM can be achieved when $S_O>0$ and both $S_I<0$ and $S_M<0$. Essentially, this means that γ_{IM} becomes considerably larger than either γ_{IO} or γ_{MO} [$\gamma_{IM} > (\gamma_{IO} + \gamma_{MO})$, Eq. 3.3], so that the interface formed between the oil phase and the internal water phase becomes energetically too costly to maintain. To achieve this criterion, the amount of encapsulated surfactant was reduced to 1%, and sucrose

was replaced with 1X PBS. Furthermore, since a depletion effect drives bilayer formation, DPPC (1,2-dipalmitoyl-sn-glycero-3-phosphocholine, Avanti Polar Lipids) was included in the middle phase at a 25% molar ratio to DOPC. Since both DOPC and oleic have similar structures (each having 18-carbons in their tail(s), with a single double bond), it was theorized that adding a lipid with a more dissimilar structure may enhance depletion and bilayer formation. DPPC has a fully saturated 16-carbon chain in each tail, and has a higher phase transition temperature than DOPC. Furthermore, the solubility of DPPC in oleic acid was noticed to be lower compared to DOPC, suggesting DPPC may be more likely to dissociate from the oleic acid solvent and organize among itself during dewetting to form a bilayer. Since DPPC would be in the gel-crystalline phase when incorporated into lipid bilayers at room temperature, it could also act to enhance the robustness of SCMs and GUVs.

The collected double emulsions were placed in a variety of solutions ranging from 0.25 – 1.2 Osm, including NaCl, PBS, sodium acetate, sucrose, sodium iodide, and KCl. Osmotic pressure differences were introduced in some scenarios to cause the double emulsions to shrink and increase the internal PBS concentration so that the condition of in Eq. 3.3 could be realized; but most either became SCMs or remained double emulsions. Surprisingly though, it was noticed that after approximately 15 mins of placement in either 2x PBS or > 0.6 Osm KCl, the double
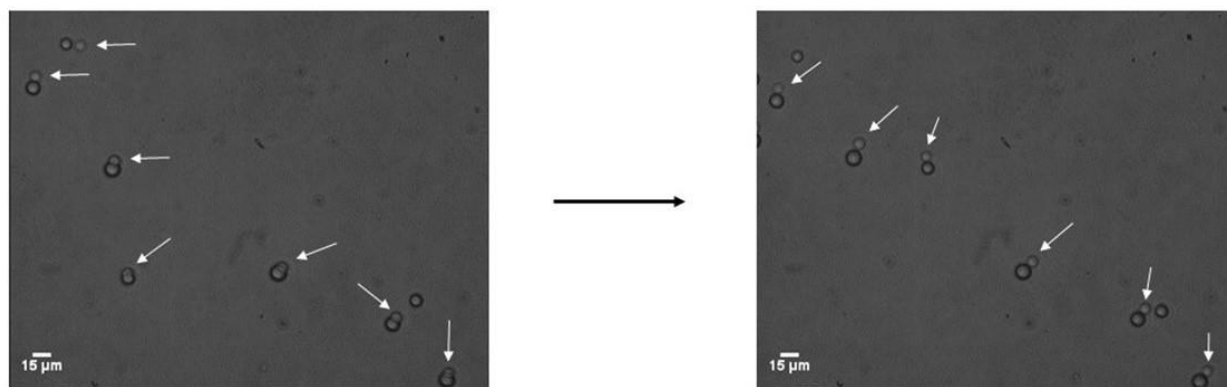
Figure 3.13. Formation of GUVs in concentrated solution of KCl. Arrows point to vesicles separating from the oil caps. Composition of internal and middle phase given in Table 4.

emulsions shrunk considerably, and began to transition into SMCs, and then GUVs (Fig. 3.13).

Since the solution used was only a few µL in volume, and was exposed to atmosphere on a glass

slide, it's possible that evaporation of the bulk solution lead to greater electrolyte concentrations

that promoted GUV formation.

The calculated spreading coefficients are listed in Table 3.4 for when the double emulsions were first introduced in the KCL solution and once they reached their equilibrium diameter. Notice that as the double emulsions shrink, S_O becomes more positive, while both S_M and S_I become more negative. Assuming the trend would continue, the conditions for the non-engulfing morphology in Fig. 3.1 would be
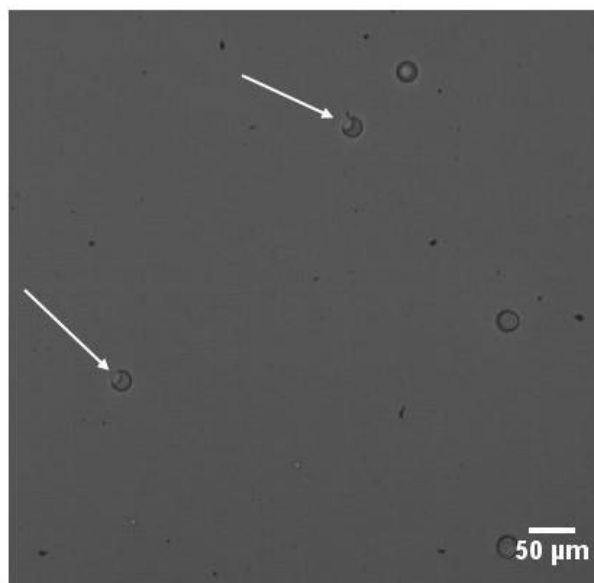
Figure 16. Beginning of SCM formation for double emulsions lacking DPPC placed in 0.6 Osm KCl solution. Composition of internal and middle phase is given in Table 3.3.

met. This is a probable scenario, as the external solution was likely evaporating and cap removal

occurred towards the edge of the solution where electrolyte concentration should be the highest.

It's also likely the enhancement to the depletion effect could play a role as repeating the

Internal Phase: 1x PBS + 1% F68 Middle Phase: 7.5 mg ml^{-1} DOPC + 2.5 mg ml^{-1} DPPC + 5 mg ml^{-1} Cholesterol in Oleic Acid	S_O	S_M	S_I
2x PBS - Initial	-7.21	-5.50	0.21
2x PBS - Equilibrium	-3.50	-9.21	-3.50
0.6 Osm KCl - Initial	-6.41	-4.70	-0.59
0.6 Osm KCl - Equilibrium	-2.70	-8.41	-4.30
0.25 Osm Sucrose + 5% F68	-0.89	0.82	-6.11

Table 3.4. Spreading coefficients for double emulsions in external solution where GUVs were formed, using a modified internal phase. Spreading coefficients are presented for both the 2X PBS and 0.6 Osm KCl conditions before (initial) and after (equilibrium) double emulsion/SCM shrinkage.

experiment without DPPC showed no cap removal in 0.6 Osm KCl. Even after 15 minutes, SCMs were only initially starting to form (Fig. 3.14).

Since the addition of DPPC helped to encourage oil cap removal, the molar ratio of DPPC to DOPC was increased even further to 1:1 (the 1:2 ratio of cholesterol to total lipid in the oil phase was maintained). These double emulsions were added to a solution of 0.5 Osm sucrose with 5% F68 to force γ_{MO} to approach 0 mN m^{-1}, reducing Eq. 3.3 to $\gamma_{IM} > \gamma_{IO}$ (Eq. 3.4). The spreading coefficient values for a 0.25 Osm sucrose solution with 5% F68 suggest that using an even higher sucrose concentration and causing double emulsion shrinkage could push the spreading coefficient values into the non-engulfing regime. As can be seen in Fig. 3.15a, the oil phase of the double emulsions immediately began to escape as small drops. It's probable that this observation is due to the formation of many small oil caps that are each then separating from the SCM individually. Since the interfacial tension at the outer water-oil interface is close to 0 mN m^{-1}, any small perturbations and shear forces could cause oil breakup due to an increase in the localized capillary number. Upon introducing shear forces to the system by washing with excess
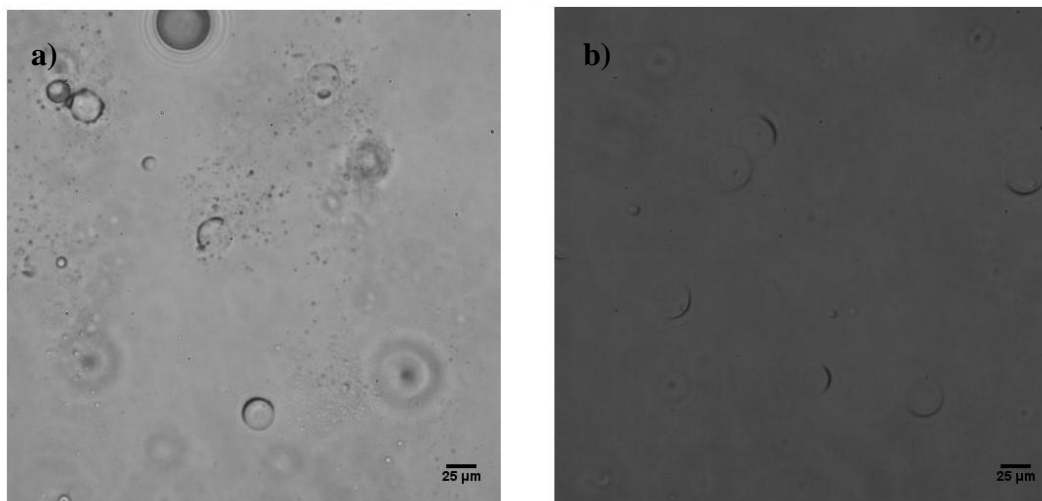
Figure 17. a) Breakup of oil phase from double emulsions introduced into a solution of 0.5 Osm Sucrose + 5% F68. Oil phase contained 5 mg ml^{-1} DOPC + 5 mg ml^{-1} DPPC + 5 mg ml^{-1} cholesterol in oleic acid. b) Washing with excess solution to introduce shear removes excess oil to create structures that resemble GUVs.

solution, possible GUVs could be seen (Fig. 3.15b). The small dark regions on the corner of some drops could be excess lipid or residual oil.

When cholesterol was completely removed from the 1:1 mixture of DOPC to DPPC, the double emulsions successfully underwent a transition from SMCs to GUVs via removal of the oil cap (Fig. 3.16) when exposed to a solution of 0.5 Osm sucrose with 5% F68. The results seen in Figs. 40 and 41 were not observed when the molar ratio of DOPC to DPPC was 3:1 (with and without cholesterol), as those double emulsions remained in a full-engulfing state under the same conditions. It is possible that at this higher ratio, the properties of DPPC began to dominate, enhancing the depletion effect and prompting superior bilayer formation than DOPC alone; nevertheless, the high percentage of cholesterol may have worked to weaken the interaction between opposing lipid tails that would form the bilayer, causing the results seen in Fig. 3.15. Unfortunately, GUVs were quick to collapse and fragment after separation from the oil.

Unexpectedly, upon introduction into a solution of 1x PBS with 50% glycerol, the SCMs

a)

b)
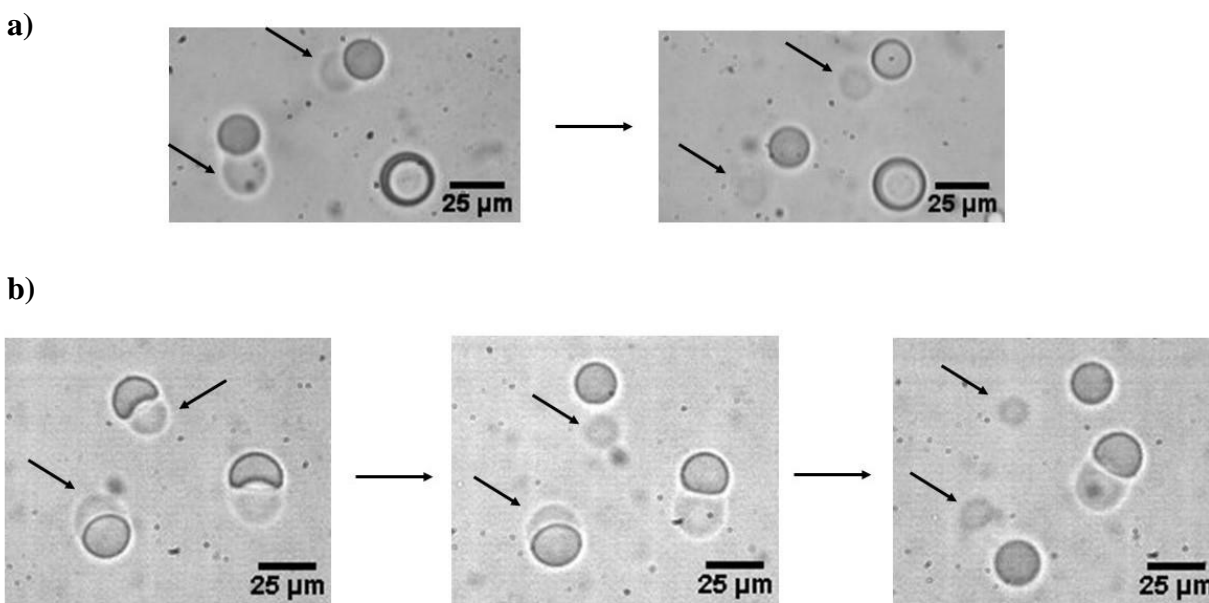
Figure 3.16. a) & b) Phase contrast images of GUVs separating from oil cap. Double emulsions introduced into a solution of 0.5 Osm Sucrose + 5% F68. Oil phase contained 5 mg ml^{-1} DOPC + 5 mg ml^{-1} DPPC in oleic acid. Cholesterol was not present.

underwent the same transition into GUVs (Fig. 3.17), but this time they did not fragment and remained stable under 1 hour of observation (data not shown). Further work is underway to elucidate more the specific affect glycerol had to cause complete dewetting, with interfacial effects, depletion effects, density, viscosity, and membrane integration (or some combination of) all possible factors to explain this observation.
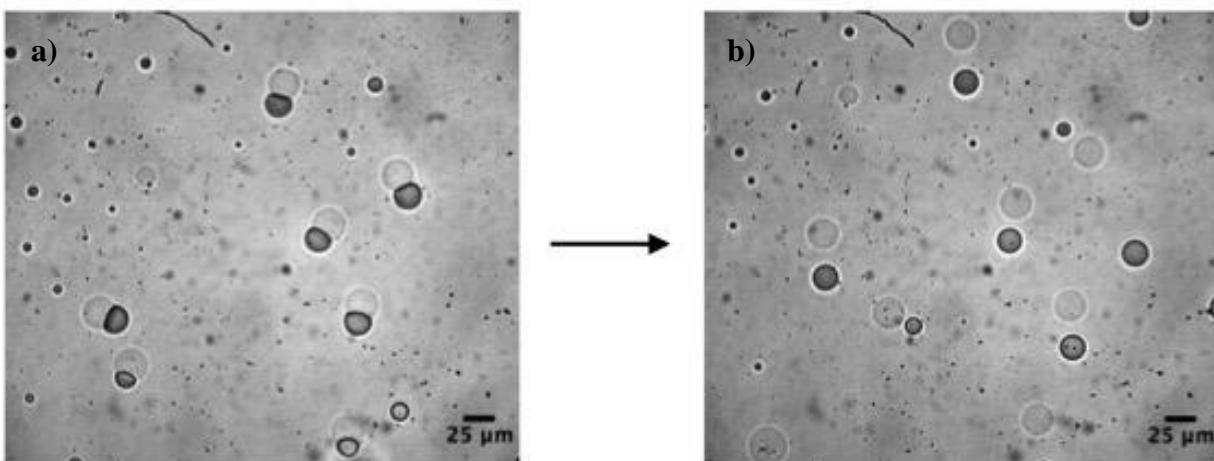
Figure 3.17 Phase contrast images SCMs shedding their oil caps to become GUVs.

3.3.4 Summary

We have presented a technique to convert microfluidically produced, cell-sized double emulsions suitable for long-term storage that can be converted into either SCMs or GUVs at any time post-production without the use of harmful, volatile solvents. The conversion is based on the "dewetting" mechanism by creating an interfacial tension imbalance on the two sides of the double emulsion oil-lipid shell layer, where the equilibrium morphology can be predicted by the spreading coefficients of each fluid phase.

The SCMs and GUVs both possess unilamellar lipid bilayer membranes and can be produced with a wide range of uniform sizes through control of the flow-rates/applied pressures of the various component phases. This method holds promise to provide a commercially viable

solution for the use as drug delivery vehicles, biosensors, and artificial cells, where pre-functionalized double emulsions can be stored for months at a time and converted into SCMs or GUVs at a moment's notice when ready for use. If necessary, fragile molecules and biological components can also be added to the surface for functionalization, or encapsulated into the SCMs/GUVs after the fact using standard nano-vesicle fusion techniques [177, 178]. By deliberately creating an osmotic imbalance with a known final solution, the SCMs or GUVs can be shrunk down to diameters smaller than what could be achievable with the current setup.

Currently, work is ongoing to optimize the process of GUV formation, although it may not be necessary for most applications, and the oil caps on the SCMs can become very small depending on the ions or the membrane lipid composition (≤10% total surface area, see Fig. 3.2c, section 3.2). Use of different lipids, cholesterol composition, and fatty acids will also be investigated for enhancements to GUV formation. Recently, Deshpande et al. [179] reported on a method to form GUVs on chip immediately following double emulsion template production, in a similar manner to that presented. The oil phase used for the double emulsions was 1-octanol, an 8-chain carbon molecule that is slightly soluble in water. It is probable that use of a small oil solvent molecule with a dissimilar structure to DOPC helped to enhance depletion and promote GUV formation in a way oleic acid cannot. However, given the slight solubility of 1-octanol in water, long-term double emulsion storage could be difficult, with the double emulsions spontaneously transitioning into SCMs or GUVs after a specific amount of time as the 1-octanol is slowly extracted from the middle phase. In addition to attempting to enhance the depletion effect, both Deshpande et al. [179] and Shum et al. [180] noted that shear forces may play a role in promtoing oil cap separation from the SCM. Introductions of shear force, either microfluidically or in bulk, will also be considered in future work investigating GUV formation.

Chapter 4 – Application: Artificial Cell Induced Ligand-Receptor Clustering

4.1 Introduction

Communication between cells is essential for many critical bodily functions and is mediated via a variety of methods, with varying degrees of distance. For example, the endocrine system involves the secretion of signals that are meant bind to distant target cells, while paracrine signaling makes use of secreted signals to reach local target cells, and autocrine signals are meant for the same cell that released them. Juxtacrine signaling involves direct cell-cell contact, and is vital for numerous important biological processes, from cell maturation and phenotypic development, metabolic and hormonal control, population control, and is fundamental component of communication in the immune system.

The cellular membrane itself plays a major role in juxtacrine signaling, as the lipid bilayer is complex and dynamic environment composed of various membrane proteins, lipids, and cholesterol whose spatial organization and structure can influence the biological functionality of membrane proteins and ensure correct confirmation configurations. To take advantage of the utility of lipid membranes, SCMs and GUVs can be functionalized to interact and provide instructions to a wide variety of different cells where the fluid bilayer can promote the biometric clustering effect that is seen in many cell-cell signal transduction mechanisms [181-185] (see aAPCs, section 1.3.3).

4.2 Background

The coordinated arrangement of ligand-receptor pairs into ordered spatial patterns on the cell surface has recently been recognized as a recurring theme that occurs in many, if not all, juxtacrine signaling pathways, and presents a paradigm shift from the concept of static cellular surface interactions [186, 187]. The importance of fluid micro-domains in cell-to-cell

communication came to light while investigating the use of aAPCs for immunotherapy. When antigen presenting cells present foreign peptide fragments to T-cells for targeting, the organization of ligands-receptors pairs that forms during contact between the two cells is known as the immune synapse, which consists of a cluster of T-cell receptors surrounded by adhesion and costimulatory molecules. Given the immense amount of literature available on this interaction, the immune synapse remains one of these most widely studied and referenced examples when discussing ligand-receptor clustering [188].

In addition to the immune synapse, another system that has been discovered to demonstrate ligand-receptor clustering is the neurexin-neuroligin signaling system. Neurexins are a widely recognized family of neuronal surface receptors that aid in synapse formation. In particular, β-neurexins are a class of receptors that bind to neuroligin-1, a postsynaptic cell surface protein [185]. Clustering of neuroligin-1 (or neuroligin-2) on the post-synaptic membrane induces clustering of presynaptic axonal neurexins, the result of which is the formation of presynaptic elements, synaptic maturation, and neurotransmitter secretion. Baksh et al. [183] demonstrated the significance of this clustering effect during this interaction by culturing neurons with both silica beads coated with neuroligin-1-containing lipid bilayers and naked polystyrene beads with covalently bonded neuroligin-1. Only the beads with neuroligin-1-containing lipid bilayers activated neurons in a manner similar to that seen in nature, while the beads lacking a membrane did not provide any activation.

Interestingly, pancreatic β-cells also utilize a neuroligin transcellular signaling system, expressing much of the same cellular components and proteins that are important for neurotransmitter secretion and repurposing them for the secretion of insulin [181, 189]. Specifically, pancreatic β-cells express neuroligin-2 (expressed in inhibitory synapses in the

nervous system), that binds with an unknown partner on neighboring β-cells, such that when one or a few β-cells detect elevated blood glucose levels, a signal can be sent to neighboring cells to also secrete insulin. This effect is apparently independent of interactions with neurexins that are also present on the β-cell surface [190]. Sure enough, it has been shown that expression of neuroligin-2 is directly related to quantity of insulin secretion [191] as well as INS-1 β-cell proliferation [181].

The mechanism of this process is nearly identical to that seen in the nervous system, namely that clustering of neuroligin-2 on the β-cell surface increases the insulin secretory capacity of neighboring β-cells during cell-to-cell contact [181]. Furthermore, as is the case with the membrane components that comprise the immune synapse, monomeric neuroligin-2 in solution will not have any effect and can actually hinder insulin secretion [181]. This presents an ideal therapeutic opportunity for the creation of GUV or SCM based artificial cells that can mimic the surface environment of β-cells to activate insulin secretion in diabetic patients.

4.3 Proof of Concept: Activation of Pancreatic Beta Cells to Secrete Insulin

To investigate the ability of lipid membrane particles to be utilized as artificial components in juxtacrine signaling for therapeutic purposes, SCMs were functionalized with a protein complex that consisted of the extracellular domain neuroligin-2 sandwiched between a Flag-tag and Fc domain at each end. The SCMs were co-cultured with pancreatic β-cells to examine whether they could promote insulin secretion for therapeutic benefit.

4.3.1 Methods: Multisome Surface Functionalization

Proteins can be covalently coupled to vesicles or SCMs via the inclusion of lipids containing amine-reactive cyanur-groups (cyanur-DSPE or cyanur-PEG$_{2000}$-PE(Cyanur 1,2-distearoyl-sn-glycero-3-phosphoethanolamine-N-[cyanur(polyethylene glycol)-2000] (ammonium salt)) [192,

193]. Cyanuric chloride at the PEG terminus functions to link peptides, antibodies and other amine-containing biomolecules or nanoparticles via a nucleophilic substitution reaction under basic conditions. Antibodies or other proteins can be conjugated without any previous derivatization.

Depending on the application, the protein or antibody orientation can also be of critical importance. Since the N-terminus of the protein contained the binding site [183], Protein A (Sigma-Aldrich) was used to ensure proper orientation, as it specifically binds with the Fc domain tagged to one en of the protein, leaving the binding region exposed and facing away from the vesicle surface for optimal antigen capture [119]. Fluorescent IgG-FITC

Figure 4.1. Fluorescent image demonstrating successful conjugation of IgG-FITC to SCM surface.

(Jackson ImmunoResearch) was used as a model protein to ensure successful conjugation (Figure 4.1).

To create the functionalized SCMs, double emulsions were first prepared using a 10% molar ratio of DSPE-PEG(2000) Cyanur (Avanti Polar Lipids) to DOPC in oleic acid with 5mg/ml of cholesterol. After placement in phosphate buffer (40mM, pH 8.3), the double emulsions subsequently converted into SCMs upon which 0.2M of protein A was added to the solution followed by 0.2M of the neuroligin-2 protein complex after 2 hours. The mixture was then left to incubate overnight. Afterwards, the SCMs were washed three times in PBS to remove excess protein.

4.3.2 Results

SMCs were cultured for 24 hours with rat INS-1 832 cells on 24-well plates. The two control groups consisted of blank SCMs (Control 1) and SCMs coated with only protein A (Control 2). The two experimental groups included one group with neurologin-2 coated SCMs (Experimental 2) and a second group with a 10x dilution of the same SCMs (Experimental 1). The results are displayed in Fig. 4.2, where it can be seen that protein coated SCMs promoted approximately a 20% increase in insulin secretion compared to blank controls. It

Figure 18. a) Total and b) normalized insulin secretion after incubation with functionalized SCMs.

should be noted that upon running a one-way ANOVA test of variance, the results were not deemed statistically significant (p-value just above 0.05), though it is still interesting that both experimental groups did show a biological response. Given that both experimental groups promoted similar intensities of insulin secretion, it's likely that above a certain SCM concentration, secretion reaches a plateau as negative feedback loops are initiated.

4.4 Summary

As a proof-of-concept, the SCMs demonstrated the capability to initiate a biological response in a cell line that could be useful for future therapeutic endeavors, though SCM fragility

could still be hindering performance. Further work will be undertaken to improve the insulin response by increasing the robustness of the SCMs with the addition of DPPC to the membrane, as it is possible many did not survive the full 24 hours in culture. SCMs will also be functionalized with components of the immune synapse to activate naive T-cells to investigate there utility as aAPCs (section 5.2.1).

Chapter 5 – Future Work

5.1 Artificial Antigen Presenting Cells

5.1.1 Aim

Physiological antigen presenting cells include dendritic cells, macrophages, and B cells. Dendritic cells, in particular, have the unique ability to activate naïve T-cells within the body. These cells take up antigens and process them into peptides that are presented to $CD4^+$ T-cells through the major histocompatibility complex (MHC) class II molecules present on the cell membrane [194]. Once activated, the T-cells can go on to specifically kill target pathogens. The ultimate goal of this work is to lead to the formation of artificial antigen presenting cells (aAPCs) made from SCMs or GUVs that can be introduced *in vivo* into a patient's blood stream or lymphatic system and activate the immune system (specifically T-cells) to effectively target and destroy pathogens (i.e., cancer cells, circulating tumor cells, malaria, various bacteria, viruses, etc.).

5.1.2 Proposal

Formation of aAPC

In order to attach MHC-II-peptide molecules to the membrane of SCMs or GUVs, 1,2-dioleoyl-sn-glycero-3-phosphoethanolamine-N-(cap biotinyl) (Biotinyl-Cap-PE) (Avanti) will be included in the lipid mixture along with DOPC, DPPC, and cholesterol. The final molar ratio of DOPC:DPPC:Cholesterol:DOPE will be 30:10:12:1 respectively. In an 11μm diameter GUV/SCM, assuming an initial 1μm thick oil shell in the double emulsion, this will correspond to a binding site density of no more than $3.48e16/m^2$, once the dewetting is complete. This number is of the same order of magnitude seen on the a-APCs utilized by Koffeman et al. [195].

After bilayer formation, the GUVs/SCMS will be washed and transferred to a solution containing excess streptavidin. Following incubation and another wash, they will be transferred to another solution containing biotinylated MHC-II-peptide complexes (NIH Tetramer Core Facility), biotinylated anti-LFA-1 (Biodesign), and biotinylated anti-CD28 (BD Biosciences) in equal molar ratios. Biotinyl-cap-PE will provide an anchoring point for streptavidin. Ideally, the investigators would wish to use a naturally occurring dimeric streptavidin produced by the bacterium *Rhizobium etli* CFN42 known as rhizavidin [196], but if unable to obtain, streptavidin will be used instead. Using rhizavidin, rather than streptavidin, would allow there to be one component of the immune synapse per lipid head, instead of having to pack all three components on a single avidin molecule, where it would be difficult to ensure that each avidin molecule
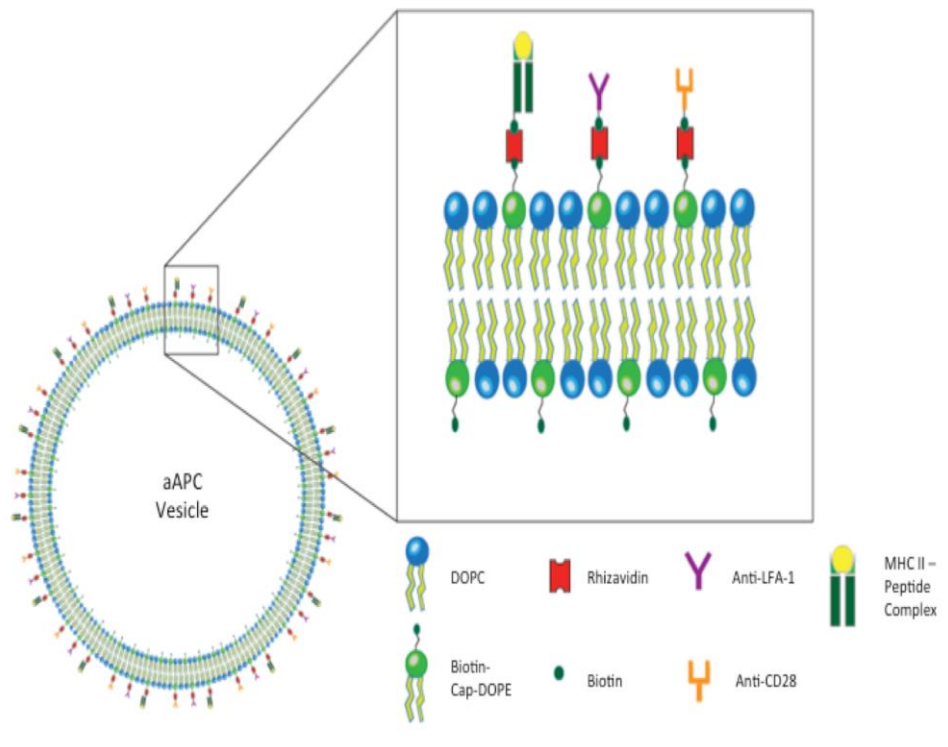
Figure 5.1 Structure of proposed aAPC GUV. Rhizavidin is a naturally occurring dimeric avidin that the investigators would ideally use in the creation of the aAPCs. Without access to rhizavidin, streptavidin will be used in its place.

contained one of each component of the immune synapse and steric effects could hinder binding (Fig. 5.1).

The number of binding sites can be optimized to determine if there is a range to allow for optimal T-cell activation. This can be accomplished using microfluidic techniques because the size of the SCMs/GUVs can be easily controlled and the resulting populations are monodisperse. Thus, changing the inlet flow rates to produce different diameter vesicles can easily alter binding site density. Since previous studies have only produced polydisperse vesicle populations [57, 195], binding site density was not maintained as a constant within the population. Our ability to finely control this parameter, as well as SCM/GUV diameter, can lead to further optimization of the a-APCs. Studies will also be done using DSPE-PEG(2000) Biotin, which contains a long hydrocarbon chain between the lipid head and biotin. The presence of this chain may play a role in how effective the a-APCs are at activating T-cells.

Approach to Measure T-Cell Stimulation and Expansion

Immunotherapeutic approaches to expand tumor T-cells (in vitro or in vivo) are secondary T-cell responses since they cause the expansion of already primed T-cells. For the present proposed experiments, NY-ESO-1 will be used, which is an antigen found in normal testis that is overexpressed in many cancer types [197]. Furthermore, NY-ESO-1 spontaneously elicits humoral and cellular responses in many patients with cancer [198]. It is one of the most promising tumor antigen for immunotherapy [199], and different vaccines using NY-ESO-1 peptides, protein, DNA are currently being evaluated in phase 2 clinical trials. Furthermore, the MHC-II tetramers for the NY-ESO-1 are available.

Generation and Expansion of NY-ESO-1 Specific T-Cells

The NY-ESO-1–specific CD4 T-cell will be generated by adapting previously described method for generating tumor specific T-cells [200]. Briefly, PBMCs will be stimulated with NY-ESO-1 antigen for one week. Expanded CD4 T-cells will be negatively purified and stimulated again with autologous DCs pulsed with NY-ESO-1 to further expand the antigen-specific T-cells. The presence of NY-ESO-1 will be determined by specific tetramer staining. Cells will be maintained in the presence of IL-2 and used for the T-cell assays described below.

Antigen Presentation Assays for CD4 T-Cells

CD4 T-cells obtained as above will be loaded will the fluorescent dye, carboxyfluorescein succinimidyl ester (CFSE). aAPCs prepared with NY-ESO-1 specific MHC-II will be cultured with isolated CD4 T-cells at various ratios ranging from T-cell:aAPC ratios of 10:1, 5:1 to 1:1 for 6-10 days. AIM V medium containing 3% human serum in the presence of IL-1 β (2 IU/mL), IL-2 (0.2 IU/mL), and IL-4 (50 IU/mL) will be used. Proliferation of CD4 T-cells will be measured by measuring the dilution of CFSE dye by flow cytometry. Supernatants collected will be assayed for IFN-γ. IFN-γ production by specific NY-ESO-1 CD4 T-cells will be determined via intracellular cytokine staining and flow cytometry.

5.1.3 Summary

An issue that may arise is that detectable levels of T-cell proliferation may not be observed because of the low frequency of antigen-specific CD4 T-cells. To overcome this limitation, various approaches will be explored- 1) antigen specific CD4 T-cells will be enriched by staining the T-cells with phycoerythin (PE)- or allophycocyanin-labeled tetramers for 30 min at 4°C, followed by magnetic bead isolation using fluorochrome-specific magnetic beads and

then determine the proliferation. 2) CD4 T-cells will be stimulated multiple times to expand the antigen specific T-cells to detectable levels.

Given the initial success that the SCMs demonstrated in promoting insulin secretion of pancreatic β-cells, we are confident that we can achieve similar or improved success utilizing SCM or GUV aAPCs. We hope that one day it may be possible that these aAPCs can be introduced within a cancer patient's bloodstream in large numbers and stimulate T-cells to differentiate and more effectively destroy malignant tumor cells, negating the need for ex-vivo expansion.

References

[1]   G. M. Whitesides, "The origins and the future of microfluidics," *Nature,* vol. 442, pp. 368-373, Jul 27 2006.

[2]   A. Gaspar, M. Salgado, S. Stevens, and F. A. Gomez, "Microfluidic "thin chips" for chemical separations," *Electrophoresis,* vol. 31, pp. 2520-2525, 2010.

[3]   A. C. Hatch, J. S. Fisher, S. L. Pentoney, D. L. Yang, and A. P. Lee, "Tunable 3D droplet self-assembly for ultra-high-density digital micro-reactor arrays," *Lab on a Chip,* vol. 11, pp. 2509-2517, 2011.

[4]   R. Booth and H. Kim, "Characterization of a microfluidic in vitro model of the blood-brain barrier ([small mu]BBB)," *Lab on a Chip,* 2012.

[5]   H. J. Kim, D. Huh, G. Hamilton, and D. E. Ingber, "Human gut-on-a-chip inhabited by microbial flora that experiences intestinal peristalsis-like motions and flow," *Lab on a Chip,* 2012.

[6]   Y.-H. H. M. L. Moya, C. C. Hughes, A. P. Lee, and S. C. George, "3D In Vitro Microenvironment Containing Perfused Human Capillaries," presented at the Biomedical Engineering Society (BMES) 2011 Annual meeting., Hartford, CT, 2011.

[7]   P. Garstecki, H. A. Stone, and G. M. Whitesides, "Mechanism for flow-rate controlled breakup in confined geometries: A route to monodisperse emulsions," *Physical Review Letters,* vol. 94, Apr 29 2005.

[8]   S. L. Anna and H. C. Mayer, "Microscale tipstreaming in a microfluidic flow focusing device," *Physics of Fluids,* vol. 18, pp. 121512-13, 2006.

[9]   A. S. Utada, E. Lorenceau, D. R. Link, P. D. Kaplan, H. A. Stone, and D. A. Weitz, "Monodisperse double emulsions generated from a microcapillary device," *Science,* vol. 308, pp. 537-541, Apr 22 2005.

[10]   S. Y. Teh, R. Lin, L. H. Hung, and A. P. Lee, "Droplet microfluidics," *Lab on a Chip,* vol. 8, pp. 198-220, 2008.

[11]   K. L. Lao, J. H. Wang, and G. B. Lee, "A microfluidic platform for formation of double-emulsion droplets," *Microfluidics and Nanofluidics,* vol. 7, pp. 709-719, Nov 2009.

[12]   S.-Y. Teh, R. Khnouf, H. Fan, and A. P. Lee, "Stable, biocompatible lipid vesicle generation by solvent extraction-based droplet microfluidics," *Biomicrofluidics,* vol. 5, p. 044113, 2011.

[13]   Y. Hennequin, N. Pannacci, C. P. de Torres, G. Tetradis-Meris, S. Chapuliot, E. Bouchaud*, et al.*, "Synthesizing Microcapsules with Controlled Geometrical and Mechanical Properties with Microfluidic Double Emulsion Technology," *Langmuir,* vol. 25, pp. 7857-7861, Jul 21 2009.

[14]   A. Kumachev, J. Greener, E. Tumarkin, E. Eiser, P. W. Zandstra, and E. Kumacheva, "High-throughput generation of hydrogel microbeads with varying elasticity for cell encapsulation," *Biomaterials,* vol. 32, pp. 1477-1483, Feb 2011.

[15]   E. Kemna, R. Schoeman, F. Wolbers, I. Vermes, D. A. Weitz, and A. van den Berg, "High-yield cell ordering and deterministic cell-in-droplet encapsulation using Dean flow in a curved microchannel," *Lab on a Chip,* 2012.

[16]   D. Bardin, T. D. Martz, P. S. Sheeran, R. Shih, P. A. Dayton, and A. P. Lee, "High-speed, clinical-scale microfluidic generation of stable phase-change droplets for gas embolotherapy," *Lab on a Chip,* vol. 11, pp. 3990-3998, 2011.

[17]   A. C. Larsen, M. R. Dunn, A. Hatch, S. P. Sau, C. Youngbull, and J. C. Chaput, "A general strategy for expanding polymerase function by droplet microfluidics," *Nature Communications,* vol. 7, Apr 2016.

[18]   K. Hettiarachchi, A. P. Lee, S. Zhang, S. Feingold, and P. A. Dayton, "Controllable Microfluidic Synthesis of Multiphase Drug-Carrying Liposphere for Site-Targeted Therapy," *Biotechnology Progress,* vol. 25, pp. 938-945, Jul-Aug 2009.

[19]   K. Hettiarachchi, E. Talu, M. L. Longo, P. A. Dayton, and A. P. Lee, "On-chip generation of microbubbles as a practical technology for manufacturing contrast agents for ultrasonic imaging," *Lab on a Chip,* vol. 7, pp. 463-468, 2007.

[20]   M. Takinoue and S. Takeuchi, "Droplet microfluidics for the study of artificial cells," *Analytical and Bioanalytical Chemistry,* vol. 400, pp. 1705-1716, Jun 2011.

[21]   A. Akbarzadeh, R. Rezaei-Sadabady, S. Davaran, S. W. Joo, N. Zarghami, Y. Hanifehpour, *et al.*, "Liposome: classification, preparation, and applications," *Nanoscale Research Letters,* vol. 8, Feb 22 2013.

[22]   D. van Swaay and A. deMello, "Microfluidic methods for forming liposomes," *Lab on a Chip,* vol. 13, pp. 752-767, 2013.

[23]   J. P. Reeves and R. M. Dowben, "Formation and Properties of Thin-Walled Phospholipid Vesicles," *Journal of Cellular Physiology,* vol. 73, pp. 49-&, 1969.

[24]   K. Akashi, H. Miyata, H. Itoh, and K. Kinosita, "Preparation of giant liposomes in physiological conditions and their characterization under an optical microscope," *Biophysical Journal,* vol. 71, pp. 3242-3250, Dec 1996.

[25]   M. Hishida, H. Seto, and K. Yoshikawa, "Smooth/rough layering in liquid-crystalline/gel state of dry phospholipid film, in relation to its ability to generate giant vesicles," *Chemical Physics Letters,* vol. 411, pp. 267-272, Aug 5 2005.

[26]   M. I. Angelova and D. S. Dimitrov, "Liposome Electroformation," *Faraday Discussions,* vol. 81, pp. 303-+, 1986.

[27]   T. Shimanouchi, H. Umakoshi, and R. Kuboi, "Kinetic Study on Giant Vesicle Formation with Electroformation Method," *Langmuir,* vol. 25, pp. 4835-4840, May 5 2009.

[28]   T. Pott, H. Bouvrais, and P. Meleard, "Giant unilamellar vesicle formation under physiologically relevant conditions," *Chemistry and Physics of Lipids,* vol. 154, pp. 115-119, Aug 2008.

[29]   O. Mertins, N. P. da Silveira, A. R. Pohlmann, A. P. Schroder, and C. M. Marques, "Electroformation of Giant Vesicles from an Inverse Phase Precursor," *Biophysical Journal,* vol. 96, pp. 2719-2726, Apr 8 2009.

[30]   Y. Okumura, H. Zhang, T. Sugiyama, and Y. Iwata, "Electroformation of giant vesicles on a non-electroconductive substrate," *Journal of the American Chemical Society,* vol. 129, pp. 1490-+, Feb 14 2007.

[31]   P. Taylor, C. Xu, P. D. I. Fletcher, and V. N. Paunov, "A novel technique for preparation of monodisperse giant liposomes," *Chemical Communications,* pp. 1732-1733, 2003.

[32]   S. Pautot, B. J. Frisken, and D. A. Weitz, "Production of unilamellar vesicles using an inverted emulsion," *Langmuir,* vol. 19, pp. 2870-2879, Apr 1 2003.

[33]   S. Pautot, B. J. Frisken, and D. A. Weitz, "Engineering asymmetric vesicles," *Proceedings of the National Academy of Sciences of the United States of America,* vol. 100, pp. 10718-10721, Sep 16 2003.

[34]   S. Sugiura, T. Kuroiwa, T. Kagota, M. Nakajima, S. Sato, S. Mukataka, *et al.*, "Novel method for obtaining homogeneous giant vesicles from a monodisperse water-in-oil

emulsion prepared with a microfluidic device," *Langmuir,* vol. 24, pp. 4581-4588, May 6 2008.

[35]   C. Mabille, V. Schmitt, P. Gorria, F. L. Calderon, V. Faye, B. Deminiere*, et al.*, "Rheological and shearing conditions for the preparation of monodisperse emulsions," *Langmuir,* vol. 16, pp. 422-429, Jan 25 2000.

[36]   J. C. Stachowiak, D. L. Richmond, T. H. Li, A. P. Liu, S. H. Parekh, and D. A. Fletcher, "Unilamellar vesicle formation and encapsulation by microfluidic jetting," *Proceedings of the National Academy of Sciences of the United States of America,* vol. 105, pp. 4697-4702, Mar 25 2008.

[37]   S. Ota, S. Yoshizawa, and S. Takeuchi, "Microfluidic Formation of Monodisperse, Cell-Sized, and Unilamellar Vesicles," *Angewandte Chemie-International Edition,* vol. 48, pp. 6533-6537, 2009.

[38]   J. C. Stachowiak, D. L. Richmond, T. H. Li, F. Brochard-Wyart, and D. A. Fletcher, "Inkjet formation of unilamellar lipid vesicles for cell-like encapsulation," *Lab on a Chip,* vol. 9, pp. 2003-2009, 2009.

[39]   H. C. Shum, D. Lee, I. Yoon, T. Kodger, and D. A. Weitz, "Double emulsion templated monodisperse phospholipid vesicles," *Langmuir,* vol. 24, pp. 7651-7653, Aug 5 2008.

[40]   L. R. Arriaga, S. S. Datta, S.-H. Kim, E. Amstad, T. E. Kodger, F. Monroy*, et al.*, "Ultrathin Shell Double Emulsion Templated Giant Unilamellar Lipid Vesicles with Controlled Microdomain Formation," *Small,* pp. 950-956, 2013.

[41]   S. H. Kim, H. C. Shum, J. W. Kim, J. C. Cho, and D. A. Weitz, "Multiple Polymersomes for Programmed Release of Multiple Components," *Journal of the American Chemical Society,* vol. 133, pp. 15165-15171, Sep 28 2011.

[42]   H. C. Shum, Y. J. Zhao, S. H. Kim, and D. A. Weitz, "Multicompartment Polymersomes from Double Emulsions," *Angewandte Chemie-International Edition,* vol. 50, pp. 1648-1651, 2011.

[43]   H. Bouvrais, T. Pott, L. A. Bagatolli, J. H. Ipsen, and P. Meleard, "Impact of membrane-anchored fluorescent probes on the mechanical properties of lipid bilayers," *Biochimica Et Biophysica Acta-Biomembranes,* vol. 1798, pp. 1333-1337, Jul 2010.

[44]   D. J. Busch, J. R. Houser, C. C. Hayden, M. B. Sherman, E. M. Lafer, and J. C. Stachowiak, "Intrinsically disordered proteins drive membrane curvature," *Nature Communications,* vol. 6, Jul 2015.

[45]   L. Parolini, B. M. Mognetti, J. Kotar, E. Eiser, P. Cicuta, and L. Di Michele, "Volume and porosity thermal regulation in lipid mesophases by coupling mobile ligands to soft membranes," *Nature Communications,* vol. 6, Jan 2015.

[46]   K. Karamdad, R. V. Law, J. M. Seddon, N. J. Brooks, and O. Ces, "Preparation and mechanical characterisation of giant unilamellar vesicles by a microfluidic method," *Lab on a Chip,* vol. 15, pp. 557-562, 2015.

[47]   F. J. Zendejas, R. J. Meagher, J. C. Stachowiak, C. C. Hayden, and D. Y. Sasaki, "Orienting lipid domains in giant vesicles using an electric field," *Chemical Communications,* vol. 47, pp. 7320-7322, 2011.

[48]   M. S. Long, A. S. Cans, and C. D. Keating, "Budding and asymmetric protein microcompartmentation in giant vesicles containing two aqueous phases," *Journal of the American Chemical Society,* vol. 130, pp. 756-762, Jan 16 2008.

[49]   M. Andes-Koback and C. D. Keating, "Complete Budding and Asymmetric Division of Primitive Model Cells To Produce Daughter Vesicles with Different Interior and

Membrane Compositions," *Journal of the American Chemical Society,* vol. 133, pp. 9545-9555, Jun 22 2011.

[50] M. E. Haque, T. J. McIntosh, and B. R. Lentz, "Influence of Lipid Composition on Physical Properties and PEG-Mediated Fusion of Curved and Uncurved Model Membrane Vesicles: "Nature's Own" Fusogenic Lipid Bilayer†," *Biochemistry,* vol. 40, pp. 4340-4348, 2001/04/01 2001.

[51] N. Kahya, E. I. Pecheur, W. P. de Boeij, D. A. Wiersma, and D. Hoekstra, "Reconstitution of membrane proteins into giant unilamellar vesicles via peptide-induced fusion," *Biophysical Journal,* vol. 81, pp. 1464-1474, Sep 2001.

[52] K. Tsumoto, Y. Yamazaki, K. Kamiya, and T. Yoshimura, "Reconstitution and Microscopic Observation of G Protein Subunits on Giant Liposomes: Attempt to Construct a Cell Model with Functional Membrane Protein Components," in *Micro-NanoMechatronics and Human Science, 2008. MHS 2008. International Symposium on*, 2008, pp. 145-150.

[53] H. Yasuga, R. Kawano, M. Takinoue, Y. Tsuji, T. Osaki, K. Kamiya*, et al.*, "Logic Gate Using Artificial Cell-Membrane: Nand Operation by Transmembrane DNA Via a Biological Nanopore," *26th Ieee International Conference on Micro Electro Mechanical Systems (Mems 2013),* pp. 1005-1006, 2013.

[54] D. Paterson, J. Reboud, R. Wilson, M. Tassieri, and J. M. Cooper, "Integrating microfluidic generation, handling and analysis of biomimetic giant unilamellar vesicles," *Lab on a Chip,* 2014.

[55] H. Valkenier, N. López Mora, A. Kros, and A. P. Davis, "Visualization and Quantification of Transmembrane Ion Transport into Giant Unilamellar Vesicles," *Angewandte Chemie International Edition,* vol. 54, pp. 2137-2141, 2015.

[56] O. P. Medina, Y. Zhu, and K. Kairemo, "Targeted liposomal drug delivery in cancer," *Curr Pharm Des,* vol. 10, pp. 2981-9, 2004.

[57] R. Zappasodi, M. Di Nicola, C. Carlo-Stella, R. Mortarini, A. Molla, C. Vegetti*, et al.*, "The effect of artificial antigen-presenting cells with preclustered anti-CD28/-CD3/-LFA-1 monoclonal antibodies on the induction of ex vivo expansion of functional human antitumor T cells," *Haematologica-the Hematology Journal,* vol. 93, pp. 1523-1534, Oct 2008.

[58] V. Noireaux and A. Libchaber, "A vesicle bioreactor as a step toward an artificial cell assembly," *Proceedings of the National Academy of Sciences of the United States of America,* vol. 101, pp. 17669-17674, December 21, 2004 2004.

[59] G. Murtas, Y. Kuruma, P. Bianchini, A. Diaspro, and P. L. Luisi, "Protein synthesis in liposomes with a minimal set of enzymes," *Biochemical and Biophysical Research Communications,* vol. 363, pp. 12-17, 2007.

[60] T. Pereira de Souza, P. Stano, and P. L. Luisi, "The Minimal Size of Liposome-Based Model Cells Brings about a Remarkably Enhanced Entrapment and Protein Synthesis," *Chembiochem,* vol. 10, pp. 1056-1063, 2009.

[61] D. A. Hammer and N. P. Kamat, "Towards an artificial cell," *Febs Letters,* vol. 586, pp. 2882-2890, Aug 31 2012.

[62] P. Walde, "Building artificial cells and protocell models: Experimental approaches with lipid vesicles," *Bioessays,* vol. 32, pp. 296-303, Apr 2010.

[63] N. P. Kamat, J. S. Katz, and D. A. Hammer, "Engineering Polymersome Protocells," *Journal of Physical Chemistry Letters,* vol. 2, pp. 1612-1623, Jul 7 2011.

[64]	S. F. Fenz and K. Sengupta, "Giant vesicles as cell models," *Integrative Biology,* vol. 4, pp. 982-995, 2012.

[65]	S. Razin, H. J. Morowitz, and T. M. Terry, "Membrane Subunits of Mycoplasma Laidlawii and Their Assembly to Membranelike Structures," *Proceedings of the National Academy of Sciences of the United States of America,* vol. 54, pp. 219-&, 1965.

[66]	T. M. Chang and M. J. Poznansky, "Semipermeable aqueous microscapsules. Artificial cells. V. Permeability characteristics," *J Biomed Mater Res,* vol. 2, pp. 187-99, Jun 1968.

[67]	D. G. Gibson, J. I. Glass, C. Lartigue, V. N. Noskov, R. Y. Chuang, M. A. Algire, *et al.*, "Creation of a Bacterial Cell Controlled by a Chemically Synthesized Genome," *Science,* vol. 329, pp. 52-56, Jul 2 2010.

[68]	I. Dunham, A. Kundaje, S. F. Aldred, P. J. Collins, C. Davis, F. Doyle, *et al.*, "An integrated encyclopedia of DNA elements in the human genome," *Nature,* vol. 489, pp. 57-74, Sep 6 2012.

[69]	E. Yus, T. Maier, K. Michalodimitrakis, V. van Noort, T. Yamada, W. H. Chen, *et al.*, "Impact of Genome Reduction on Bacterial Metabolism and Its Regulation," *Science,* vol. 326, pp. 1263-1268, Nov 27 2009.

[70]	P. Graves and H. Gelband, "Vaccines for preventing malaria (SPf66)," *Cochrane Database of Systematic Reviews,* 2006.

[71]	A. M. Stern and H. Markel, "The history of vaccines and immunization: Familiar patterns, new challenges," *Health Affairs,* vol. 24, pp. 611-621, May-Jun 2005.

[72]	C. Yee, "Adoptive T cell therapy: Addressing challenges in cancer immunotherapy," *Journal of Translational Medicine,* vol. 3, Apr 28 2005.

[73]	V. F. Surmont, E. R. van Thiel, K. Vermaelen, and J. P. van Meerbeeck, "Investigational approaches for mesothelioma," *Front Oncol,* vol. 1, p. 22, 2011.

[74]	M. Oelke, C. Krueger, R. L. Giuntoli Ii, and J. P. Schneck, "Artificial antigen-presenting cells: artificial solutions for real diseases," *Trends in Molecular Medicine,* vol. 11, pp. 412-420, 2005.

[75]	L. E. M. Oosten, E. Blokland, A. G. S. van Halteren, J. Curtsinger, M. F. Mescher, J. H. F. Falkenburg, *et al.*, "Artificial antigen-presenting constructs efficiently stimulate minor histocompatibility antigen-specific cytotoxic T lymphocytes," *Blood,* vol. 104, pp. 224-226, Jul 1 2004.

[76]	M. Oelke and J. P. Schneck, "HLA-Ig-based artificial antigen-presenting cells: setting the terms of engagement," *Clinical Immunology,* vol. 110, pp. 243-51, Mar 2004.

[77]	M. Oelke, M. V. Maus, D. Didiano, C. H. June, A. Mackensen, and J. P. Schneck, "Ex vivo induction and expansion of antigen-specific cytotoxic T cells by HLA-Ig-coated artificial antigen-presenting cells," *Nature Medicine,* vol. 9, pp. 619-24, May 2003.

[78]	M. L. Dustin, "Stop and go traffic to tune T cell responses," *Immunity,* vol. 21, pp. 305-314, Sep 2004.

[79]	S. Valitutti and A. Lanzavecchia, "Serial triggering of TCRs: a basis for the sensitivity and specificity of antigen recognition," *Immunology Today,* vol. 18, pp. 299-304, 1997.

[80]	A. Grakoui, S. K. Bromley, C. Sumen, M. M. Davis, A. S. Shaw, P. M. Allen, *et al.*, "The immunological synapse: A molecular machine controlling T cell activation," *Science,* vol. 285, pp. 221-227, Jul 9 1999.

[81]	B. Prakken, M. Wauben, D. Genini, R. Samodal, J. Barnett, A. Mendivil, *et al.*, "Artificial antigen-presenting cells as a tool to exploit the immune 'synapse'," *Nature Medicine,* vol. 6, pp. 1406-1410, Dec 2000.

[82] F. Giannoni, J. Barnett, K. Bi, R. Samodal, P. Lanza, P. Marchese, *et al.*, "Clustering of T cell Ligands on artificial APC membranes influences T cell activation and protein kinase C theta translocation to the T cell plasma membrane," *Journal of Immunology,* vol. 174, pp. 3204-3211, Mar 15 2005.

[83] T. Pentcheva-Hoang, J. G. Egen, K. Wojnoonski, and J. P. Allison, "B7-1 and B7-2 selectively recruit CTLA-4 and CD28 to the immunological synapse," *Immunity,* vol. 21, pp. 401-413, Sep 2004.

[84] A. J. M. L. van Rensen, M. H. M. Wauben, M. C. Grosfeld-Stulemeyer, W. van Eden, and D. J. A. Crommelin, "Liposomes with incorporated MHC class II peptide complexes as antigen presenting vesicles for specific T cell activation," *Pharmaceutical Research,* vol. 16, pp. 198-204, Feb 1999.

[85] V. Vamvakaki and N. A. Chaniotakis, "Pesticide detection with a liposome-based nano-biosensor," *Biosensors & Bioelectronics,* vol. 22, pp. 2848-2853, Jun 15 2007.

[86] R. D. Peterson, W. L. Chen, B. T. Cunningham, and J. E. Andrade, "Enhanced sandwich immunoassay using antibody-functionalized magnetic iron-oxide nanoparticles for extraction and detection of soluble transferrin receptor on a photonic crystal biosensor," *Biosensors & Bioelectronics,* vol. 74, pp. 815-822, Dec 15 2015.

[87] M. Bhuvana, J. S. Narayanan, V. Dharuman, W. Teng, J. H. Hahn, and K. Jayakumar, "Gold surface supported spherical liposome-gold nano-particle nano-composite for label free DNA sensing," *Biosensors & Bioelectronics,* vol. 41, pp. 802-808, Mar 15 2013.

[88] L. Zou, Q. Wang, M. M. Tong, H. B. Li, J. Wang, N. Hu, *et al.*, "Detection of diarrhetic shellfish poisoning toxins using high-sensitivity human cancer cell-based impedance biosensor," *Sensors and Actuators B-Chemical,* vol. 222, pp. 205-212, Jan 2016.

[89] A. Solovyev, G. Kuncova, and K. Demnerova, "Whole-cell optical biosensor for mercury - operational conditions in saline water," *Chemical Papers,* vol. 69, pp. 183-191, Jan 2015.

[90] S. T. Girousi, A. A. Pantazaki, and A. N. Voulgaropoulos, "Mitochondria-based amperometric biosensor for the determination of L-glutamic acid," *Electroanalysis,* vol. 13, pp. 243-245, Mar 2001.

[91] R. Carpentier, C. Loranger, J. Chartrand, and M. Purcell, "Photoelectrochemical Cell Containing Chloroplast Membranes as a Biosensor for Phytotoxicity Measurements," *Analytica Chimica Acta,* vol. 249, pp. 55-60, Aug 15 1991.

[92] Y. H. Yun, E. Eteshola, A. Bhattacharya, Z. Y. Dong, J. S. Shim, L. Conforti, *et al.*, "Tiny Medicine: Nanomaterial-Based Biosensors," *Sensors,* vol. 9, pp. 9275-9299, Nov 2009.

[93] H. J. Kim, H. P. Bennetto, and M. A. Halablab, "A Novel Liposome-Based Electrochemical Biosensor for the Detection of Hemolytic Microorganisms," *Biotechnology Techniques,* vol. 9, pp. 389-394, Jun 1995.

[94] N. Zehani, P. Fortgang, M. S. Lachgar, A. Baraket, M. Arab, S. V. Dzyadevych, *et al.*, "Highly sensitive electrochemical biosensor for bisphenol A detection based on a diazonium-functionalized boron-doped diamond electrode modified with a multi-walled carbon nanotube-tyrosinase hybrid film," *Biosensors & Bioelectronics,* vol. 74, pp. 830-835, Dec 15 2015.

[95] D. D. Li, W. Cheng, Y. R. Yan, Y. Zhang, Y. B. Yin, H. X. Ju, *et al.*, "A colorimetric biosensor for detection of attomolar microRNA with a functional nucleic acid-based amplification machine," *Talanta,* vol. 146, pp. 470-476, Jan 1 2016.

[96] S. G. Bhand, S. Soundararajan, I. Surugiu-Warnmark, J. S. Milea, E. S. Dey, M. Yakovleva, *et al.*, "Fructose-selective calorimetric biosensor in flow injection analysis," *Analytica Chimica Acta,* vol. 668, pp. 13-18, May 23 2010.

[97] S. C. Park, E. J. Cho, S. Y. Moon, S. I. Yoon, Y. J. Kim, D. H. Kim, *et al.*, "A calorimetric biosensor and its application for detecting a cancer cell with optical imaging," *World Congress on Medical Physics and Biomedical Engineering 2006, Vol 14, Pts 1-6,* vol. 14, pp. 637-640, 2007.

[98] H. Jang, S. Jung, K. S. Shin, S. M. Kim, and T. J. Jeon, "Polydiacetylene (PDA) Vesicle Based Colorimetric Biosensor for Detection of Genetically Modified (GM) Crops," *Biophysical Journal,* vol. 106, pp. 417a-417a, Jan 28 2014.

[99] N. Giamblanco, S. Conoci, D. Russo, and G. Marletta, "Single-step label-free hepatitis B virus detection by a piezoelectric biosensor," *Rsc Advances,* vol. 5, pp. 38152-38158, 2015.

[100] S. Kim and S. J. Choi, "A lipid-based method for the preparation of a piezoelectric DNA biosensor," *Analytical Biochemistry,* vol. 458, pp. 1-3, Aug 1 2014.

[101] E. B. Bahadir and M. K. Sezginturk, "Applications of commercial biosensors in clinical, food, environmental, and biothreat/biowarfare analyses," *Analytical Biochemistry,* vol. 478, pp. 107-120, Jun 1 2015.

[102] C. I. L. Justino, A. C. Freitas, R. Pereira, A. C. Duarte, and T. A. P. R. Santos, "Recent developments in recognition elements for chemical sensors and biosensors," *Trac-Trends in Analytical Chemistry,* vol. 68, pp. 2-17, May 2015.

[103] V. Vamakaki and N. A. Chaniotakis, "Carbon nanostructures as transducers in biosensors," *Sensors and Actuators B-Chemical,* vol. 126, pp. 193-197, Sep 20 2007.

[104] S. Frey, T. Millat, S. Hohmann, and O. Wolkenhauer, "How quantitative measures unravel design principles in multi-stage phosphorylation cascades," *Journal of Theoretical Biology,* vol. 254, pp. 27-36, Sep 7 2008.

[105] E. Eriksson and A. Aspan, "Comparison of culture, ELISA and PCR techniques for salmonella detection in faecal samples for cattle, pig and poultry," *BMC Vet Res,* vol. 3, p. 21, 2007.

[106] L. D. Mello and L. T. Kubota, "Review of the use of biosensors as analytical tools in the food and drink industries," *Food Chemistry,* vol. 77, pp. 237-256, May 2002.

[107] R. van den Hurk and S. Evoy, "A Review of Membrane-Based Biosensors for Pathogen Detection," *Sensors,* vol. 15, pp. 14045-14078, Jun 2015.

[108] L. Y. Jin, Y. M. Dong, X. M. Wu, G. X. Cao, and G. L. Wang, "Versatile and Amplified Biosensing through Enzymatic Cascade Reaction by Coupling Alkaline Phosphatase in Situ Generation of Photoresponsive Nanozyme," *Analytical Chemistry,* vol. 87, pp. 10429-10436, Oct 20 2015.

[109] X. Zhu, L. Sun, Y. Y. Chen, Z. H. Ye, Z. M. Shen, and G. X. Li, "Combination of cascade chemical reactions with graphene-DNA interaction to develop new strategy for biosensor fabrication," *Biosensors & Bioelectronics,* vol. 47, pp. 32-37, Sep 15 2013.

[110] S. M. Kuiper, M. Nallani, D. M. Vriezema, J. J. L. M. Cornelissen, J. C. M. van Hest, R. J. M. Nolte, *et al.*, "Enzymes containing porous polymersomes as nano reaction vessels for cascade reactions," *Organic & Biomolecular Chemistry,* vol. 6, pp. 4315-4318, 2008.

[111] S. F. M. van Dongen, M. Nallani, J. L. L. M. Cornelissen, R. J. M. Nolte, and J. C. M. van Hest, "A Three-Enzyme Cascade Reaction through Positional Assembly of Enzymes

in a Polymersome Nanoreactor," *Chemistry-a European Journal,* vol. 15, pp. 1107-1114, 2009.

[112] P. Tanner, V. Balasubramanian, and C. G. Palivan, "Aiding Nature's Organelles: Artificial Peroxisomes Play Their Role," *Nano Letters,* vol. 13, pp. 2875-2883, Jun 2013.

[113] N. Ben-Haim, P. Broz, S. Marsch, W. Meier, and P. Hunziker, "Cell-specific integration of artificial organelles based on functionalized polymer vesicles," *Nano Letters,* vol. 8, pp. 1368-1373, May 2008.

[114] L. Steller, M. Kreir, and R. Salzer, "Natural and artificial ion channels for biosensing platforms," *Analytical and Bioanalytical Chemistry,* vol. 402, pp. 209-230, Jan 2012.

[115] M. A. Reppy and B. A. Pindzola, "Biosensing with polydiacetylene materials: structures, optical properties and applications," *Chemical Communications,* pp. 4317-4338, 2007.

[116] L. Silbert, I. Ben Shlush, E. Israel, A. Porgador, S. Kolusheva, and R. Jelinek, "Rapid chromatic detection of bacteria by use of a new biomimetic polymer sensor," *Applied and Environmental Microbiology,* vol. 72, pp. 7339-7344, Nov 2006.

[117] Y. L. Su, J. R. Li, and L. Jiang, "A study on the interactions of surfactants with phospholipid/polydiacetylene vesicles in aqueous solutions," *Colloids and Surfaces a-Physicochemical and Engineering Aspects,* vol. 257-58, pp. 25-30, May 5 2005.

[118] M. Bally, K. Bailey, K. Sugihara, D. Grieshaber, J. Voros, and B. Stadler, "Liposome and Lipid Bilayer Arrays Towards Biosensing Applications," *Small,* vol. 6, pp. 2481-2497, Nov 22 2010.

[119] G. L. Damhorst, C. E. Smith, E. M. Salm, M. M. Sobieraj, H. K. Ni, H. Kong*, et al.*, "A liposome-based ion release impedance sensor for biological detection," *Biomedical Microdevices,* vol. 15, pp. 895-905, Oct 2013.

[120] J. A. A. Ho and R. D. Wauchope, "A strip liposome immunoassay for aflatoxin B-1," *Analytical Chemistry,* vol. 74, pp. 1493-1496, Apr 1 2002.

[121] S. Ahn-Yoon, T. R. DeCory, and R. A. Durst, "Ganglioside-liposome immunoassay for the detection of botulinum toxin," *Analytical and Bioanalytical Chemistry,* vol. 378, pp. 68-75, Jan 2004.

[122] J. A. A. Ho, S. C. Zeng, W. H. Tseng, Y. J. Lin, and C. H. Chen, "Liposome-based immunostrip for the rapid detection of Salmonella," *Analytical and Bioanalytical Chemistry,* vol. 391, pp. 479-485, May 2008.

[123] H. A. H. Rongen, H. M. Vanderhorst, G. W. K. Hugenholtz, A. Bult, W. P. Vanbennekom, and P. H. Vandermeide, "Development of a Liposome Immunosorbent-Assay for Human Interferon-Gamma," *Analytica Chimica Acta,* vol. 287, pp. 191-199, Mar 21 1994.

[124] L. J. Ou, S. J. Liu, X. Chu, G. L. Shen, and R. Q. Yu, "DNA Encapsulating Liposome Based Rolling Circle Amplification Immunoassay as a Versatile Platform for Ultrasensitive Detection of Protein," *Analytical Chemistry,* vol. 81, pp. 9664-9673, Dec 1 2009.

[125] H. Chen, Y. Zheng, J. H. Jiang, H. L. Wu, G. L. Shen, and R. Q. Yu, "An ultrasensitive chemiluminescence biosensor for cholera toxin based on ganglioside-functionalized supported lipid membrane and liposome," *Biosensors & Bioelectronics,* vol. 24, pp. 684-689, Dec 1 2008.

[126] M. A. Cooper, A. Hansson, S. Lofas, and D. H. Williams, "A vesicle capture sensor chip for kinetic analysis of interactions with membrane-bound receptors," *Analytical Biochemistry,* vol. 277, pp. 196-205, Jan 15 2000.

[127] F. Patolsky, A. Lichtenstein, and I. Willner, "Amplified microgravimetric quartz-crystal-microbalance assay of DNA using oligonucleotide-functionalized liposomes or biotinylated liposomes," *Journal of the American Chemical Society,* vol. 122, pp. 418-419, Jan 19 2000.

[128] D. Grieshaber, V. de Lange, T. Hirt, Z. Lu, and J. Voros, "Vesicles for Signal Amplification in a Biosensor for the Detection of Low Antigen Concentrations," *Sensors,* vol. 8, pp. 7894-7903, Dec 2008.

[129] C. Qi, Y. J. Zhu, Y. G. Zhang, Y. Y. Jiang, J. Wu, and F. Chen, "Vesicle-like nanospheres of amorphous calcium phosphate: sonochemical synthesis using the adenosine 5 '-triphosphate disodium salt and their application in pH-responsive drug delivery," *Journal of Materials Chemistry B,* vol. 3, pp. 7347-7354, 2015.

[130] L. Xiao, P. Rasouli, and D. M. Ruden, "Possible effects of early treatments of Hsp90 inhibitors on preventing the evolution of drug resistance to other anti-cancer drugs," *Current Medicinal Chemistry,* vol. 14, pp. 223-232, 2007.

[131] Y. Chen, Y. Gao, H. R. Chen, D. P. Zeng, Y. P. Li, Y. Y. Zheng*, et al.*, "Engineering Inorganic Nanoemulsions/Nanoliposomes by Fluoride-Silica Chemistry for Efficient Delivery/Co-Delivery of Hydrophobic Agents," *Advanced Functional Materials,* vol. 22, pp. 1586-1597, Apr 24 2012.

[132] F. Kong, X. Zhang, and M. T. Hai, "Microfluidics Fabrication of Monodisperse Biocompatible Phospholipid Vesicles for Encapsulation and Delivery of Hydrophilic Drug or Active Compound," *Langmuir,* vol. 30, pp. 3905-3912, Apr 8 2014.

[133] F. Danhier, O. Feron, and V. Preat, "To exploit the tumor microenvironment: Passive and active tumor targeting of nanocarriers for anti-cancer drug delivery," *Journal of Controlled Release,* vol. 148, pp. 135-146, Dec 1 2010.

[134] B. Yang, S. Y. Geng, X. M. Liu, J. T. Wang, Y. K. Chen, Y. L. Wang*, et al.*, "Positively charged cholesterol derivative combined with liposomes as an efficient drug delivery system, in vitro and in vivo study," *Soft Matter,* vol. 8, pp. 518-525, 2012.

[135] K. Takiguchi and M. Hayashi, "Construction of artificial motile cell model," in *Micro-NanoMechatronics and Human Science (MHS), 2013 International Symposium on*, 2013, pp. 1-6.

[136] E. Lorenceau, A. S. Utada, D. R. Link, G. Cristobal, M. Joanicot, and D. A. Weitz, "Generation of polymerosomes from double-emulsions," *Langmuir,* vol. 21, pp. 9183-9186, Sep 27 2005.

[137] S. S. Lee, A. Abbaspourrad, and S. H. Kim, "Nonspherical Double Emulsions with Multiple Distinct Cores Enveloped by Ultrathin Shells," *Acs Applied Materials & Interfaces,* vol. 6, pp. 1294-1300, Jan 22 2014.

[138] E. T. Kisak, B. Coldren, and J. A. Zasadzinski, "Nanocompartments enclosing vesicles, colloids, and macromolecules via interdigitated lipid bilayers," *Langmuir,* vol. 18, pp. 284-288, Jan 8 2002.

[139] Y. Elani, A. Gee, R. V. Law, and O. Ces, "Engineering multi-compartment vesicle networks," *Chemical Science,* vol. 4, pp. 3332-3338, 2013.

[140] Q. T. Liu and B. J. Boyd, "Liposomes in biosensors," *Analyst,* vol. 138, pp. 391-409, 2013.

[141] Y. Tamba, T. Tanaka, T. Yahagi, Y. Yamashita, and M. Yamazaki, "Stability of giant unilamellar vesicles and large unilamellar vesicles of liquid-ordered phase membranes in

the presence of Triton X-100," *Biochimica Et Biophysica Acta-Biomembranes,* vol. 1667, pp. 1-6, Nov 17 2004.

[142] B. Stark, G. Pabst, and R. Prassl, "Long-term stability of sterically stabilized liposomes by freezing and freeze-drying: Effects of cryoprotectants on structure," *Eur J Pharm Sci,* vol. 41, pp. 546-55, Nov 20 2010.

[143] W. Seifriz, "Studies in emulsions," *Journal of Physical Chemistry,* vol. 29, pp. 834-841, Jul-Dec 1925.

[144] Z. H. Nie, W. Li, M. Seo, S. Q. Xu, and E. Kumacheva, "Janus and ternary particles generated by microfluidic synthesis: Design, synthesis, and self-assembly," *Journal of the American Chemical Society,* vol. 128, pp. 9408-9412, Jul 26 2006.

[145] G. Villar, A. J. Heron, and H. Bayley, "Formation of droplet networks that function in aqueous environments," *Nature Nanotechnology,* vol. 6, pp. 803-808, Dec 2011.

[146] K. Pays, J. Giermanska-Kahn, B. Pouligny, J. Bibette, and F. Leal-Calderon, "Coalescence in surfactant-stabilized double emulsions," *Langmuir,* vol. 17, pp. 7758-7769, Dec 11 2001.

[147] A. S. Utada, L. Y. Chu, A. Fernandez-Nieves, D. R. Link, C. Holtze, and D. A. Weitz, "Dripping, jetting, drops, and wetting: The magic of microfluidics," *Mrs Bulletin,* vol. 32, pp. 702-708, Sep 2007.

[148] F. Thege, "Single-step microfuidic generation of cell-sized giant unilamellar vesicles: Characterization and dielectrophoretic patterning and sorting," Masters Masters, Department of Electrical Measurements, Lund University, Lund, 2011.

[149] Y. N. Xia and G. M. Whitesides, "Soft lithography," *Angewandte Chemie-International Edition,* vol. 37, pp. 551-575, Mar 16 1998.

[150] M. Kozlov, M. Quarmyne, W. Chen, and T. J. McCarthy, "Adsorption of poly(vinyl alcohol) onto hydrophobic substrates. A general approach for hydrophilizing and chemically activating surfaces," *Macromolecules,* vol. 36, pp. 6054-6059, Aug 12 2003.

[151] T. D. Martz, D. Bardin, P. S. Sheeran, A. P. Lee, and P. A. Dayton, "Microfluidic Generation of Acoustically Active Nanodroplets," *Small,* vol. 8, pp. 1876-1879, 2012.

[152] T. Ward, M. Faivre, M. Abkarian, and H. A. Stone, "Microfluidic flow focusing: Drop size and scaling in pressure versus flow-rate-driven pumping," *ELECTROPHORESIS,* vol. 26, pp. 3716-3724, Oct 2005.

[153] S. Ugel, A. Zoso, C. De Santo, Y. Li, I. Marigo, P. Zanovello*, et al.*, "In vivo Administration of Artificial Antigen-Presenting Cells Activates Low-Avidity T Cells for Treatment of Cancer," *Cancer Research,* vol. 69, pp. 9376-9384, Dec 15 2009.

[154] J. Guzowski, P. M. Korczyk, S. Jakiela, and P. Garstecki, "The structure and stability of multiple micro-droplets," *Soft Matter,* vol. 8, pp. 7269-7278, 2012.

[155] A. D. Petelska, "Interfacial tension of bilayer lipid membranes," *Central European Journal of Chemistry,* vol. 10, pp. 16-26, Feb 2012.

[156] S. Torza and S. G. Mason, "3-Phase Interactions in Shear and Electrical Fields," *Journal of Colloid and Interface Science,* vol. 33, pp. 67-&, 1970.

[157] T. Tharmalingam, H. Ghebeh, T. Wuerz, and M. Butler, "Pluronic enhances the robustness and reduces the cell attachment of mammalian cells," *Molecular Biotechnology,* vol. 39, pp. 167-177, Jun 2008.

[158] R. C. Hayward, A. S. Utada, N. Dan, and D. A. Weitz, "Dewetting instability during the formation of polymersomes from block-copolymer-stabilized double emulsions," *Langmuir,* vol. 22, pp. 4457-4461, May 9 2006.

[159] S. Punnamaraju, H. You, and A. J. Steckl, "Triggered Release of Molecules across Droplet Interface Bilayer Lipid Membranes Using Photopolymerizable Lipids," *Langmuir,* vol. 28, pp. 7657-7664, May 22 2012.

[160] M. A. Holden, D. Needham, and H. Bayley, "Functional bionetworks from nanoliter water droplets," *Journal of the American Chemical Society,* vol. 129, pp. 8650-8655, Jul 11 2007.

[161] S. Okushima, T. Nisisako, T. Torii, and T. Higuchi, "Controlled production of monodisperse double emulsions by two-step droplet breakup in microfluidic devices," *Langmuir,* vol. 20, pp. 9905-9908, Nov 9 2004.

[162] A. P. dos Santos, A. Diehl, and Y. Levin, "Surface Tensions, Surface Potentials, and the Hofmeister Series of Electrolyte Solutions," *Langmuir,* vol. 26, pp. 10778-10783, Jul 6 2010.

[163] E. R. A. Lima, B. M. de Melo, L. T. Baptista, and M. L. L. Paredes, "Specific Ion Effects on the Interfacial Tension of Water/Hydrocarbon Systems," *Brazilian Journal of Chemical Engineering,* vol. 30, pp. 55-62, Jan-Mar 2013.

[164] A. P. dos Santos and Y. Levin, "Surface and interfacial tensions of Hofmeister electrolytes," *Faraday Discussions,* vol. 160, pp. 75-87, 2013.

[165] T. Yoshitani and M. Yamazaki, "Water permeability of lipid membranes of GUVs and its dependence on actin cytoskeletons inside the GUVs," in *Micro-NanoMechatronics and Human Science, 2008. MHS 2008. International Symposium on*, 2008, pp. 130-134.

[166] M. Bloom, E. Evans, and O. G. Mouritsen, "Physical-Properties of the Fluid Lipid-Bilayer Component of Cell-Membranes - a Perspective," *Quarterly Reviews of Biophysics,* vol. 24, pp. 293-397, Aug 1991.

[167] B. M. Discher, Y. Y. Won, D. S. Ege, J. C. M. Lee, F. S. Bates, D. E. Discher*, et al.*, "Polymersomes: Tough vesicles made from diblock copolymers," *Science,* vol. 284, pp. 1143-1146, May 14 1999.

[168] M. T. Lee, T. L. Sun, W. C. Hung, and H. W. Huang, "Process of inducing pores in membranes by melittin," *Proceedings of the National Academy of Sciences of the United States of America,* vol. 110, pp. 14243-14248, Aug 27 2013.

[169] G. van den Bogaart, J. V. Guzman, J. T. Mika, and B. Poolman, "On the Mechanism of Pore Formation by Melittin," *Journal of Biological Chemistry,* vol. 283, pp. 33854-33857, Dec 5 2008.

[170] J. C. Mcintyre and R. G. Sleight, "Fluorescence Assay for Phospholipid Membrane Asymmetry," *Biochemistry,* vol. 30, pp. 11819-11827, Dec 24 1991.

[171] H. J. Gruber and H. Schindler, "External Surface and Lamellarity of Lipid Vesicles - a Practice-Oriented Set of Assay-Methods," *Biochimica Et Biophysica Acta-Biomembranes,* vol. 1189, pp. 212-224, Jan 19 1994.

[172] K. Matsuzaki, O. Murase, K. Sugishita, S. Yoneyama, K. Akada, M. Ueha*, et al.*, "Optical characterization of liposomes by right angle light scattering and turbidity measurement," *Biochimica Et Biophysica Acta-Biomembranes,* vol. 1467, pp. 219-226, Jul 31 2000.

[173] P. Girard, J. Pecreaux, G. Lenoir, P. Falson, J. L. Rigaud, and P. Bassereau, "A new method for the reconstitution of membrane proteins into giant unilamellar vesicles. (vol 87, pg 419, yr 2004)," *Biophysical Journal,* vol. 87, pp. 2098-2098, Sep 2004.

[174] S. Feryforgues, J. P. Fayet, and A. Lopez, "Drastic Changes in the Fluorescence Properties of Nbd Probes with the Polarity of the Medium - Involvement of a Tict State,"

Journal of Photochemistry and Photobiology a-Chemistry, vol. 70, pp. 229-243, Mar 1 1993.

[175] A. Chattopadhyay and S. Mukherjee, "Fluorophore Environments in Membrane-Bound Probes - a Red Edge Excitation Shift Study," *Biochemistry,* vol. 32, pp. 3804-3811, Apr 13 1993.

[176] A. Chattopadhyay, S. Mukherjee, and H. Raghuraman, "Reverse micellar organization and dynamics: A wavelength-selective fluorescence approach," *Journal of Physical Chemistry B,* vol. 106, pp. 13002-13009, Dec 19 2002.

[177] K. Tsumoto, K. Kamiya, S. Kitaoka, S. Ogata, M. Tomita, and T. Yoshimura, "G protein coupled receptors (GPCRs) reconstituted on recombinant proteoliposomes using baculovirus-liposome membrane fusion," in *Micro-NanoMechatronics and Human Science, 2009. MHS 2009. International Symposium on*, 2009, pp. 202-207.

[178] A. Csiszár, N. Hersch, S. Dieluweit, R. Biehl, R. Merkel, and B. Hoffmann, "Novel Fusogenic Liposomes for Fluorescent Cell Labeling and Membrane Modification," *Bioconjugate Chemistry,* vol. 21, pp. 537-543, 2010/03/17 2010.

[179] S. Deshpande, Y. Caspi, A. E. Meijering, and C. Dekker, "Octanol-assisted liposome assembly on chip," *Nat Commun,* vol. 7, p. 10447, 2016.

[180] H. C. Shum, E. Santanach-Carreras, J. W. Kim, A. Ehrlicher, J. Bibette, and D. A. Weitz, "Dewetting-Induced Membrane Formation by Adhesion of Amphiphile-Laden Interfaces," *Journal of the American Chemical Society,* vol. 133, pp. 4420-4426, Mar 30 2011.

[181] A. T. Suckow, C. Zhang, S. Egodage, D. Comoletti, P. Taylor, M. T. Miller*, et al.*, "Transcellular Neuroligin-2 Interactions Enhance Insulin Secretion and Are Integral to Pancreatic beta Cell Function," *Journal of Biological Chemistry,* vol. 287, pp. 19816-19826, Jun 8 2012.

[182] S. Pautot, H. Lee, E. Y. Isacoff, and J. T. Groves, "Neuronal synapse interaction reconstituted between live cells and supported lipid bilayers," *Nature Chemical Biology,* vol. 1, pp. 283-289, Oct 2005.

[183] M. M. Baksh, C. Dean, S. Pautot, S. DeMaria, E. Isacoff, and J. T. Groves, "Neuronal activation by GPI-linked neuroligin-1 displayed in synthetic lipid bilayer membranes," *Langmuir,* vol. 21, pp. 10693-10698, Nov 8 2005.

[184] E. Stein, A. A. Lane, D. P. Cerretti, H. O. Schoecklmann, A. D. Schroff, R. L. Van Etten*, et al.*, "Eph receptors discriminate specific ligand oligomers to determine alternative signaling complexes, attachment, and assembly responses," *Genes & Development,* vol. 12, pp. 667-678, Mar 1 1998.

[185] C. Dean, F. G. Scholl, J. Choih, S. DeMaria, J. Berger, E. Isacoff*, et al.*, "Neurexin mediates the assembly of presynaptic terminals," *Nat Neurosci,* vol. 6, pp. 708-16, Jul 2003.

[186] J. T. Groves, "Molecular organization and signal transduction at intermembrane junctions," *Angewandte Chemie-International Edition,* vol. 44, pp. 3524-3538, 2005.

[187] M. M. Davis, M. Krogsgaard, J. B. Huppa, C. Sumen, M. A. Purbhoo, D. J. Irvine*, et al.*, "Dynamics of cell surface molecules during T cell recognition," *Annual Review of Biochemistry,* vol. 72, pp. 717-742, 2003.

[188] B. N. Manz and J. T. Groves, "Spatial organization and signal transduction at intercellular junctions," *Nature Reviews Molecular Cell Biology,* vol. 11, pp. 342-352, May 2010.

[189] R. A. Easom, "beta-granule transport and exocytosis," *Seminars in Cell & Developmental Biology,* vol. 11, pp. 253-266, Aug 2000.

[190] M. Mosedale, S. Egodage, R. C. Calma, N. W. Chi, and S. D. Chessler, "Neurexin-1 alpha Contributes to Insulin-containing Secretory Granule Docking," *Journal of Biological Chemistry,* vol. 287, pp. 6350-6361, Feb 24 2012.

[191] A. T. Suckow, D. Comoletti, M. A. Waldrop, M. Mosedale, S. Egodage, P. Taylor*, et al.*, "Expression of Neurexin, Neuroligin, and Their Cytoplasmic Binding Partners in the Pancreatic beta-Cells and the Involvement of Neuroligin in Insulin Secretion," *Endocrinology,* vol. 149, pp. 6006-6017, Dec 2008.

[192] H. Bakowsky, T. Richter, C. Kneuer, D. Hoekstra, U. Rothe, G. Bendas*, et al.*, "Adhesion characteristics and stability assessment of lectin-modified liposomes for site-specific drug delivery," *Biochimica Et Biophysica Acta-Biomembranes,* vol. 1778, pp. 242-249, Jan 2008.

[193] G. Bendas, A. Krause, U. Bakowsky, J. Vogel, and U. Rothe, "Targetability of novel immunoliposomes prepared by a new antibody conjugation technique," *International Journal of Pharmaceutics,* vol. 181, pp. 79-93, Apr 20 1999.

[194] J. Banchereau and R. M. Steinman, "Dendritic cells and the control of immunity," *Nature,* vol. 392, pp. 245-252, Mar 19 1998.

[195] E. Koffeman, E. Keogh, M. Klein, B. Prakken, and S. Albani, "Identification and manipulation of antigen specific T-cells with artificial antigen presenting cells," *Methods Mol Med,* vol. 136, pp. 69-86, 2007.

[196] S. H. Helppolainen, K. P. Nurminen, J. A. Maatta, K. K. Halling, J. P. Slotte, T. Huhtala*, et al.*, "Rhizavidin from Rhizobium etli: the first natural dimer in the avidin protein family," *Biochem J,* vol. 405, pp. 397-405, Aug 1 2007.

[197] O. L. Caballero and Y. T. Chen, "Cancer/testis (CT) antigens: potential targets for immunotherapy," *Cancer Sci,* vol. 100, pp. 2014-21, Nov 2009.

[198] M. Mandic, F. Castelli, B. Janjic, C. Almunia, P. Andrade, D. Gillet*, et al.*, "One NY-ESO-1-derived epitope that promiscuously binds to multiple HLA-DR and HLA-DP4 molecules and stimulates autologous CD4+ T cells from patients with NY-ESO-1-expressing melanoma," *J Immunol,* vol. 174, pp. 1751-9, Feb 1 2005.

[199] J. F. Fonteneau, F. Brilot, C. Munz, and M. Gannage, "The Tumor Antigen NY-ESO-1 Mediates Direct Recognition of Melanoma Cells by CD4+ T Cells after Intercellular Antigen Transfer," *J Immunol,* vol. 196, pp. 64-71, Jan 1 2016.

[200] S. Agrawal, S. Gupta, and A. Agrawal, "Human dendritic cells activated via dectin-1 are efficient at priming Th17, cytotoxic CD8 T and B cell responses," *PLoS One,* vol. 5, p. e13418, 2010.